Docket No. SA-538

Exhibit No. 13-A

NATIONAL TRANSPORTATION SAFETY BOARD

Washington, D.C.

Aircraft Performance Study

(72 Pages)

NATIONAL TRANSPORTATION SAFETY BOARD

Office of Research and Engineering
Washington, D.C. 20594

February 11, 2014

Aircraft Performance Study

by John O'Callaghan

ACCIDENT:

Location:	Birmingham, AL
Date:	August 14, 2013
Time:	04:47 Central Daylight Time (CDT) 09:47 Universal Coordinated Time (UTC)
Aircraft:	Airbus A300 F4-622R, registration N155UP
NTSB#:	DCA13MA133

TABLE OF CONTENTS

NATIONAL TRANSPORTATION SAFETY BOARD

Office of Research and Engineering
Washington, D.C. 20594

February 11, 2014

Aircraft Performance Study

by John O'Callaghan

A. ACCIDENT

Location: Birmingham, AL
Date: August 14, 2013
Time: 04:47 Central Daylight Time (CDT)
09:47 Universal Coordinated Time (UTC)[1]
Aircraft: Airbus A300 F4-622R, registration N155UP
NTSB#: DCA13MA133

B. GROUP

Chairman: John O'Callaghan
National Resource Specialist - Aircraft Performance
National Transportation Safety Board (NTSB)
490 L'Enfant Plaza E, SW
Washington, DC 20594

Members: Nicolas Bardou
Director of Flight Safety / Accident Investigator
Airbus S.A.S.
1 Rond-point Maurice Bellonte
31707 Blagnac cedex
France

Joe Jacobsen
Performance & Flight Test, ANM-111
Federal Aviation Administration (FAA), Transport Airplane Directorate
1601 Lind Ave. S.W.
Renton, WA 98057-3356

Martin McKinney
Aircraft Performance Engineering Manager
United Parcel Service (UPS)
825 Lotus Ave
Louisville, KY 40213

[1] CDT = UTC - 5 hours. Times in this *Performance Study* are based on the BHM ASR-9 time in CDT unless otherwise noted.

Stéphane Pion
Safety Investigator - Engineering Department
Bureau d'Enquêtes et d'Analyses pour la Sécurité de l'Aviation civile (BEA)
Zone Sud - Bâtiment 153
200 rue de Paris
Aéroport du Bourget
F – 93352 Le Bourget Cedex
France

C. HISTORY OF FLIGHT

On August, 14, 2013, at about 04:47 Central Daylight Time (CDT), United Parcel Service flight 1354, an Airbus A300 F4-622R, N155UP, crashed short of runway 18 while on approach to Birmingham-Shuttlesworth International Airport (KBHM), Birmingham, Alabama. The two flight crew members were fatally injured and the airplane was destroyed. The scheduled cargo flight was operating under the provisions of 14 Code of Federal Regulations (CFR) Part 121 and originated from Louisville International – Standiford Field Airport (KSDF), Louisville, Kentucky.

The objective of this *Aircraft Performance Study* is to determine and analyze the motion of the airplane and the physical forces that produce that motion. In particular, the *Study* attempts to define the airplane's position and orientation throughout the flight, and determine the airplane's response to control inputs, external disturbances, and other factors that could affect its trajectory.

The data the *Study* uses to determine and analyze the airplane motion includes but is not limited to the following:

- Wreckage location and condition.
- Ground scars / markings and damage to ground structures.
- Airport Surveillance Radar (ASR) data.
- Flight Data Recorder (FDR) data.
- Cockpit Voice Recorder (CVR) information.
- Enhanced Ground Proximity Warning System (EGPWS) data.
- Weather information.
- Airport navigational aids and surveillance / security videos.
- Output from computer programs and simulations that calculate aircraft performance.

This *Study* describes the results of using the data listed above in defining the position of flight 1354 relative to the KBHM runway 18 threshold throughout the final approach, and in particular during the descent from the BASKN final approach fix (FAF) to impact with trees. The *Study* introduces the airplane motion data collected during the investigation, describes the methods used to extract additional airplane motion information from the recorded data, and presents the results of these calculations. The *Study* also presents an estimate of the height of the cloud bases on the final approach, based on an analysis of video images from a security camera attached to a hangar on the airport, that captured the airplane's emergence from the clouds and final descent into terrain. Finally, the *Study* presents the results of simulation work performed to determine the minimum altitude at which the crew could have taken action to avoid a collision with the trees.

D. DETAILS OF THE INVESTIGATION

I. The Airbus A300 F4-622R Airplane

Figure 1 shows a 3-view image of the Airbus A300 F4-622R. Table 1 provides some dimensions of the airplane, as well as relevant mass properties for flight 1354.

Item	Value
Reference dimensions:[2]	
Wing area	260 m^2 (2800 ft^2)
Wing span	44.8 m (147 ft)
Mean Aerodynamic Chord (MAC)	6.61 m (21.7 ft)
Mass properties for UPS flight 1354:[3]	
Estimated landing weight	291,577 pounds
FDR gross weight at 04:46:46 CDT	291,160 pounds
Estimated landing center of gravity (CG) position	28.0% MAC
FDR CG position at 04:46:42 CDT	29.7% MAC

Table 1. Dimensions of A300 F4-622R airplane, and relevant mass properties for flight 1354.

II. Ground scars and markings

Surveys of the accident scene and survey coordinate systems

The recorded data described in Section D-III, and ground scars and damage to trees and other structures north of the KBHM runway 18 threshold, indicate that after passing BASKN, flight 1354 descended along the KBHM runway 18 localizer centerline at a nearly constant 1500 ft./min. until a few seconds before impacting trees located 6400 ft. north of the threshold. The end of recorded data on the flight data recorder (FDR) occurs about 1 second after the CVR recorded the first sounds of impact with the trees. Five (5) seconds before the sounds of first impact, the rate of descent decreased from 1500 ft./min. to about 530 ft./min.. Accident scene evidence, and surveillance video footage from a hangar on the airport, indicate that after the first impact with trees, flight 1354 clipped a power pole about 5490 ft. north of the threshold, before descending to impact with terrain 5017 ft. north of the threshold.

The tree strikes, ground scars, and debris items of interest surveyed by the Aircraft Performance Group (ACPG) on-scene are listed in Table 2 and presented in Figure 2.[4] The coordinate system used in this *Study* to locate items in the wreckage field is centered at the KBHM runway 18 threshold, with axes extending east, north, and up from the center of the Earth.

[2] From Reference 1.
[3] Estimated weight and CG are from email from NTSB Operations Group Chairman to Aircraft Performance Group Chairman, dated 9/16/2013.
[4] Several Figures in this *Study* have an “a” and a “b” version, which present the same information but at different scales, or with different background images. When the *Study* refers to a Figure with two or more versions without specifying the version, all versions are meant to be included in the reference.

Point #	Name	Height, ft.	Elevation, ft.	Altitude, ft.	N Latitude	W Longitude	North, ft.	East, ft.
1	Tree M2	73.7	748	821.7	33° 35' 26.88"	086° 44' 49.20"	6400	58
2	Tree M1	76.6	754	830.6	33° 35' 26.16"	086° 44' 49.20"	6327	58
3	Tree 0	69.1	753	822.1	33° 35' 26.12"	086° 44' 49.31"	6323	49
4	Tree 1	53.0	753	806.0	33° 35' 25.44"	086° 44' 49.92"	6254	-3
5	Tree 2	78.0	753	831.0	33° 35' 25.48"	086° 44' 49.88"	6258	0
6	Tree 3	65.6	765	830.6	33° 35' 23.68"	086° 44' 49.93"	6076	-4
7	Tree 4	39.8	773	812.8	33° 35' 21.84"	086° 44' 49.92"	5890	-3
8	Tree 5	50.4	773	823.4	33° 35' 21.67"	086° 44' 49.82"	5873	5
9	Tree 6	35.6	774	809.6	33° 35' 21.51"	086° 44' 49.92"	5857	-3
10	Tree 7	41.8	777	818.8	33° 35' 21.46"	086° 44' 50.20"	5852	-27
11	Tree 8	65.7	754	819.7	33° 35' 19.68"	086° 44' 49.20"	5672	58
12	Tree 9 - top	69.7	750	819.7	33° 35' 19.68"	086° 44' 48.84"	5672	88
13	Tree 9 - break	64.8	751	815.8	33° 35' 19.66"	086° 44' 48.86"	5670	86
14	Tree 10 (unbroken)	53.7	802	855.7	33° 35' 17.88"	086° 44' 48.84"	5490	88
15	Tree 11	30.4	800	830.4	33° 35' 17.88"	086° 44' 49.20"	5490	58
16	Tree 12	31.0	797	828.0	33° 35' 17.93"	086° 44' 49.35"	5495	46
17	Tree 13	20.6	795	815.6	33° 35' 17.88"	086° 44' 49.56"	5490	27
18	Tree 14	43.1	786	829.1	33° 35' 18.31"	086° 44' 50.07"	5533	-16
19	Tree 15W	17.8	797	814.8	33° 35' 17.53"	086° 44' 49.67"	5455	18
20	Tree 15E	14.4	797	811.4	33° 35' 17.53"	086° 44' 49.63"	5454	21
21	TP1 (unbroken)	35.3	783	818.3	33° 35' 18.24"	086° 44' 50.64"	5526	-64
22	TP2 (unbroken)	35.2	790	825.2	33° 35' 17.70"	086° 44' 50.29"	5472	-34

Notes:

1. Altitude = Elevation + Height
2. North and East coordinates are relative to the KBHM runway 18 threshold (N 33° 34' 23.5702" / W 086° 44' 49.8841" / 644.3 ft. elevation)
3. The “image filename” refers to digital photos taken of the items in question.
4. These items are also contained in the DCA13MA133.kmz *Google Earth* file, for display in that application.
5. The elevation of Point 40 is the elevation reported by the GPS; the *Google Earth* elevation for this point is observably incorrect relative to the elevations of surrounding points.
6. No attempt is made here to identify the engines or main landing gear as to which is right and which is left. Hence, individual engines and main gear are labeled as either “A” or “B”.

Table 2. Items surveyed by the ACPG (page 1 of 2).

Point #	Name	Height, ft.	Elevation, ft.	Altitude, ft.	Latitude	Longitude	North, ft.	East, ft.
23	Start of ground scar	0.0	768	768.0	33° 35' 13.20"	086° 44' 49.20"	5017	58
24	Scar width 18 ft	0.0	754	754.0	33° 35' 11.40"	086° 44' 49.20"	4835	58
25	Furrow 1	0.0	752	752.0	33° 35' 10.68"	086° 44' 49.20"	4762	58
26	Burn Line	0.0	754	754.0	33° 35' 09.60"	086° 44' 48.84"	4653	88
27	Furrow 2	0.0	755	755.0	33° 35' 09.24"	086° 44' 48.84"	4617	88
28	Furrow 3	0.0	757	757.0	33° 35' 08.88"	086° 44' 48.84"	4580	88
29	Furrow 4	0.0	760	760.0	33° 35' 08.16"	086° 44' 48.48"	4507	119
30	Furrow 5	0.0	763	763.0	33° 35' 07.80"	086° 44' 48.48"	4471	119
31	Tire	0.0	766	766.0	33° 35' 07.44"	086° 44' 48.12"	4435	149
32	Cowl	0.0	776	776.0	33° 35' 06.72"	086° 44' 47.40"	4362	210
33	Engine A (see note 6)	0.0	792	792.0	33° 35' 04.92"	086° 44' 47.04"	4180	241
34	Engine B (see note 6)	0.0	798	798.0	33° 35' 04.20"	086° 44' 47.04"	4107	241
35	Back of nose section	0.0	791	791.0	33° 35' 04.20"	086° 44' 45.90"	4107	337
36	Front of nose section	0.0	787	787.0	33° 35' 03.80"	086° 44' 44.80"	4067	430
37	Main gear A (see note 6)	0.0	759	759.0	33° 34' 59.70"	086° 44' 45.60"	3652	362
38	Empennage	0.0	745	745.0	33° 34' 59.50"	086° 44' 46.30"	3632	303
39	Main gear B (see note 6)	0.0	749	749.0	33° 34' 59.30"	086° 44' 45.20"	3612	396
40	Right wingtip (see note 5)	0.0	715	715.0	33° 34' 59.30"	086° 44' 44.10"	3612	489

Notes:

1. Altitude = Elevation + Height.
2. North and East coordinates are relative to the KBHM runway 18 threshold (N 33° 34' 23.5702" / W 086° 44' 49.8841" / 644.3 ft. elevation).
3. The “image filename” refers to digital photos taken of the items in question.
4. These items are also contained in the DCA13MA133.kmz *Google Earth* file, for display in that application.
5. The elevation of Point 40 is the elevation reported by the GPS; the *Google Earth* elevation for this point is observably incorrect relative to the elevations of surrounding points.
6. No attempt is made here to identify the engines or main landing gear as to which is right and which is left. Hence, individual engines and main gear are labeled as either “A” or “B”.

Table 2. Items surveyed by the ACPG (page 2 of 2).

The wreckage field starts 6400 ft. north of the threshold of KBHM runway 18, at a tree that was struck by the airplane. The top of the tree was snapped off at a height of 73.7 ft. above the base of the tree. The terrain elevation at the base of the tree is 748 ft., so the MSL altitude of the break in the tree is 821.7 ft.. Pieces of the airplane (wing, flap, and engine parts) were found on the ground a few feet south of this tree, and extending all the way to the ground impact in the main debris field.

The first evidence of the airplane's contact with the ground is a ground scar that starts 5017 ft. (0.83 nmi) north of the runway threshold, on the downward slope of a hill at an elevation of 768 ft.. About 360 ft. further south, at the bottom of a local valley in the terrain (elevation 754), the ground and grass show evidence of fuel spillage and fire. Just south of this point, the terrain rises again and there are deep furrows and scars in the ground, consistent with heavy parts of the airplane (such as the landing gear and engines) contacting the ground.

The left wing disintegrated during the impact sequence, and the forward fuselage, engines, and right wing / aft fuselage / empennage separated and came to rest in different locations (see Figure 2). The right wing / aft fuselage / empennage section travelled the furthest south, coming to rest about 3630 ft. (0.60 nmi) north of the runway threshold.

The locations of the significant tree strikes, ground scars, and resting points of the large sections of the airplane were surveyed by the ACPG using a hand-held Global Positioning System (GPS) unit. The heights of the breaks in the trees were measured using an inclinometer and tape measure. The results of this survey are shown in Table 2, and plotted in Figure 2.

The survey items listed in Table 2 were also surveyed using a Total Station system by the Federal Bureau of Investigation (FBI) Evidence Recovery Team (ERT). The FBI survey included elevation measurements at various points along the wreckage path and in the debris field. This elevation data is used along with other information to estimate how terrain may have obstructed the line of sight of a security camera that recorded the descent of the airplane into the trees, as described in Section D-VI.

III. Radar data

Radar returns from UPS flight 1354 were recorded by the Birmingham (BHM) Airport Surveillance Radar (ASR) during its approach to runway 18.

Description of Airport Surveillance Radar data

Airport Surveillance Radars (ASRs) are short range (60 NM) radars used to provide air traffic control services in terminal areas. ASR antennas rotate at 13 to 14 RPM, resulting in a radar return every 4.3 to 4.6 seconds. In addition to detecting radar energy reflected from aircraft surfaces (primary returns), the radars also emit transponder interrogations and detect the corresponding transponder replies from aircraft (secondary returns), which contain identifying beacon code (Mode A) and altitude (Mode C) information. Secondary radar returns from UPS flight 1354 were recorded by the Birmingham (BHM) ASR-9 during its approach to runway 18. In addition, three primary returns that are consistent with the extended flight path of the airplane were recorded after secondary returns were no longer received.

Recorded radar data

Recorded data from the BHM ASR-9 were obtained from the Air Traffic Control (ATC) Group Chairman, who received them from the FAA. The data include the following parameters:

- UTC time of the radar return, in hours, minutes, and seconds.
- Transponder beacon code associated with the return (secondary returns only). The transponder code for UPS 1354 is 4016.
- Transponder reported altitude in hundreds of feet MSL (secondary returns only). This altitude is pressure altitude, and must be corrected for the local altimeter setting (29.97 "Hg) to obtain true altitude.[5] The resolution of the altitude data is ± 50 ft..
- Slant Range from the radar antenna to the return, in nautical miles (nmi). The accuracy of this data is ± 1/16 nmi or about ± 380 ft..
- Azimuth relative to Magnetic North from the radar antenna to the return[6]. The azimuth is reported in Azimuth Change Pulses (ACPs), which range from 0 to 4096, where 0 = 0° magnetic and 4096 = 360° magnetic. Thus, the azimuth to the target in degrees is:

  (Azimuth in degrees) = (360/4096) x (Azimuth in ACPs) = (0.08789) x (Azimuth in ACPs)

  The accuracy of azimuth data is ± 2 ACP or ± 0.176°.

The geographic location of the radar antenna must be known to determine the latitude and longitude of radar returns from the range and azimuth data recorded by the radar. The BHM ASR-9 antenna coordinates are:

Latitude:	N 33° 34' 25.6120"
Longitude:	W 086° 45' 24.1850"
Elevation:	772.9 ft.

To calculate an airplane's performance parameters (such as groundspeeds, airspeeds, rates of climb, etc.) from the radar data, it is convenient to express the position of the airplane in rectangular Cartesian coordinates. As mentioned above, the Cartesian coordinate system used in this *Study* is centered at the KBHM runway 18 threshold, with axes extending east, north, and up from the center of the Earth. The data from the BHM ASR-9 are converted into this coordinate system for plotting and performance calculations. Latitude and longitude coordinates are transformed into this coordinate system using the WGS84 ellipsoid model of the Earth. The coordinates of the runway 18 threshold are:

Latitude:	N 33° 34' 23.5702"
Longitude:	W 086° 44' 49.8841"
Elevation:	644.3 ft.

The BHM ASR-9 data for UPS 1354 during its final approach are presented in Figures 4-9. Figure 3 is the approach plate for the KBHM LOC Rwy 18 approach used by the flight crew, presented here for reference (see Ref. 2 for more information about this approach plate and its use for approaches at night). Figures 4-7 depict the approach of UPS 1354 to KBHM runway 18 from about 18 nmi north of the runway threshold, as it was descending through 9500 ft. MSL. Figure 4 is a plan view of the approach, and shows UPS 1354 joining the

[5] An altimeter setting of 29.97 "Hg will result in a true altitude about 46 ft. higher than the pressure altitude.
[6] The magnetic variation used by the BHM ASR-9 radar to determine magnetic azimuth is 1° W.

runway 18 localizer about 12 nmi north of the threshold. The COLIG, BASKN, and IMTOY approach fixes are also shown in the Figure, along with selected, paraphrased comments from the CVR transcript, shown at the points along the flight path at which they occurred. The ASR-9 radar returns are labeled with the time of the return (in HH:MM:SS CDT), and the FDR pressure altitude, corrected for the altimeter setting of 29.97 “Hg, and for time lags in the FDR altitude data (see Section D-V for more information about this correction). The actual CVR transcript text corresponding to the paraphrased comments shown in Figure 4 (and other Figures throughout this *Study*) are shown in Table 3. Figure 5 shows altitude vs. time during the approach, and Figure 7 shows a profile view (altitude vs. distance north of the threshold). More detailed plots of the final approach, from about 5 nmi north of the threshold, are shown in Figures 6-9.

IV. Recorded flight data

FDR and CVR Data Description

The aircraft cockpit voice recorder (CVR) and flight data recorder (FDR) were recovered from the aircraft and sent to Washington, DC for readout.

Descriptions of the FDR and CVR and the recorder readout processes can be found in Refs. 3 and 4, respectively. The FDR readout results in tabulated and plotted values of the recorded flight parameters versus time. The CVR readout results in a transcript of the CVR events, a partial list of which is shown in Table 3. The paraphrased version of the selected CVR events listed in Table 3 are also presented along with other information in various Figures throughout this *Study*. For the complete list of CVR events, see Ref. 4.

BHM ASR Time	Full CVR transcript text	Paraphrased text on plots
04:43:24.3	**TWRBHM1**: UPS thirteen fifty four heavy is one one miles from BASKIN maintain two thousand five hundred till established on localizer. cleared localizer one eight approach.	[ATC clears for LOC 18 appr, maintain 2,500]
04:43:53.5	**HOT-2**: there's loc star.	[crew notes loc star/loc alive]
04:44:13.1	**HOT-1**: ...activate that final if you haven't already.	[crew activates final]
04:46:17.4	**HOT-2**: landing checklist complete.	[F/O landing checklist complete]
04:46:27.0	**HOT-1**: ...yeah I'm gonna do vertical speed. yeah he kept us high.	[crew comments will do vertical speed mode]
04:46:29.6	**HOT-2**: kept ya high. could never get it over to profile (we didn't) do it like that.	[f/o comments not in profile mode]
04:46:53.7	**HOT-1**: and we're like way high...	[crew comments high on approach]
04:46:56.8	**HOT-1**: ...or higher [chuckle].	-
04:47:02.9	**HOT-2**: there's a thousand feet instruments cross checked no flags.	[F/O 1,000 feet no flags]
04:47:05.4	**HOT-1**: alright ah DA is twelve ah hundred.	[CA comments DA is 1,200 feet]
04:47:10.9	**HOT-1**: two miles.	[CA comments "two miles"]
04:47:24.5	**EGPWS**: sink rate.	EGPWS - "sink rate"
04:47:27.9	**HOT-1**: oh I got the runway out there twelve o'clock.	[crew comments about runway]
04:47:31.5	**CAM**: [sound of click, similar to autopilot paddle switch]	[autopilot disconnect click]
04:47:32.5	**CAM**: [sound of rustling, similar to impact, volume increases for about 5.4 seconds]	[first sound of impact]
04:47:33.5	**EGPWS**: too low terrain [recorded on CAM]	EPGWS - "too low terrain"
04:47:41.3	**CAM**: [end of loudest noise]	[end of loudest noise on CVR]

Table 3. Full CVR transcript text corresponding to paraphrased text on plots in this *Study*.

Correlation of Radar, FDR, and CVR Times

The ASR-9 radar, the FDR, and the CVR record their information with respect to time, but these recorded times are not synchronized. To use these data sources together, their times must be synchronized to a single reference time. This reference time is the BHM ASR CDT time introduced in Section D-III and used throughout this *Study*.

Time on the FDR is measured in terms of the Subframe Reference Number (SRN), with one SRN equivalent to one second of time.

The relationship between the time recorded by the BHM ASR-9 radar and the FDR SRN is established by comparing the altitude recorded by the FDR with the Mode C altitude recorded by the radar (uncorrected for altimeter setting). Both altitudes are based on the static pressure sensed at the airplane's static pressure ports, and on a sea level pressure of 29.92 "Hg (i.e., both altitudes are pressure altitude). By adjusting the FDR times so that the FDR altitude falls within the ±50 ft. uncertainty band of the EWR Mode C altitude throughout the flight, the offset between the FDR SRN and radar time can be determined.

In this case, this alignment process was complicated by lags in the FDR pressure altitude and GPS latitude & longitude data. These lags become apparent when one compares the FDR radio altitude to the height above terrain computed by subtracting the elevation of the terrain under the FDR latitude and longitude data from the MSL altitude computed from the FDR pressure altitude data. These lags, and their corrections, are described further below. In what follows, references to the FDR pressure altitude and latitude / longitude data refer to these data *corrected* to account for the lags, unless noted otherwise.

The alignment of the Mode C altitude data from the BHM ASR-9 with the FDR pressure altitude (corrected for time lags) yields the following relationship:

$$04{:}30{:}00\ (\text{CDT})\ \text{BHM ASR-9 Radar Time} = 252285.480\ \text{FDR SRN} \qquad [1]$$

The relationship between the times of events recorded on the CVR and the BHM ASR-9 reference time is established by first establishing the conversion from CVR to FDR time, and then using the FDR to EWR ASR-9 time conversion defined by Equation [1]. The correlation between the FDR and CVR times is described in Ref. 4. The CVR transcript provided in Ref. 4 uses the BHM ASR-9 times.

Many of the plots in this *Study* portray selected CVR content at positions corresponding to the occurrence of the content on the CVR. For example, plots of data vs. time include CVR content overlaid on vertical lines that intersect the x axis of the plot at the times that the CVR content was recorded. The CVR content portrayed on the plots is not the verbatim CVR transcript text, but rather a paraphrase or short-hand code for this text. The full CVR transcript text associated with each paraphrase or code is shown in Table 3.

V. Additional performance parameters computed using recorded data

Overview

The FDR records many, but not all, performance parameters of interest. Many additional parameters can be derived from the FDR parameters; however, the FDR parameters themselves can suffer from inherent measurement errors[7] and must be corrected before being used in these calculations.

This section describes the corrections applied to the FDR data, and the calculations used to derive additional performance parameters from the corrected data. The airplane weight used in these calculations is 291,160 lb.[8] Further details on the derivation of the equations and calculation methods used in this *Study* can be found in Appendix A of Ref. 5.

The FDR corrections discussed in this Study attempt to remove the following errors:

- Altitude error associated with non-standard day conditions (pressure altitude to actual altitude estimate)
- Altitude and GPS position time lags relative to other FDR parameters
- Accelerometer bias errors
- Errors in recorded groundspeed and drift angle that result in a ground track that differs slightly from the recorded GPS-based track

The performance parameters derived from the corrected FDR data include:

- True airspeed
- True altitude and density altitude
- Static temperature
- Groundspeed and drift angle "calibrated" to match GPS track
- Airplane positions and velocities from accelerometer integration
- Flight path angle (γ)
- Angle of attack (α)
- Wind speed and direction

The results of these corrections and derivations for the last 92 seconds of recorded data (corresponding to the airplane's descent from the BASKN FAF) are presented in Figures 4-13.

True airspeed calculation

True airspeed equals the Mach number multiplied by the speed of sound; the speed of sound is a function of the static temperature. Static temperature is obtained from total temperature and Mach number.

[7] "Measurement error" in this context means the difference between the actual true value of the quantity being measured and the measured or recorded value. It does not necessarily imply defects or malfunctions in the measurement and recording equipment itself. This difference can result from, among other things, limitations in the sensor accuracy and / or resolution.

[8] This is the gross weight recorded on the FDR at 04:46:46 CDT; see Table 1.

Mach number can be computed from calibrated airspeed and static pressure. Total temperature and calibrated airspeed are recorded directly by the FDR, and the static pressure can be determined from the pressure altitude recorded by the FDR (which is based on the standard sea-level pressure of 29.92 “Hg).

Figure 12 shows the results of the true airspeed calculation, compared with the indicated (calibrated) airspeed recorded by the FDR. Figure 12 also shows the groundspeed recorded by the FDR, and the groundspeed obtained from integration of the accelerometer data (this calculation is described below).

Pressure-based true altitude and density altitude calculations

The altitude recorded in the FDR parameter *AltitudePress*[9] is pressure altitude (i.e., the altitude in the standard atmosphere corresponding to the static pressure sensed at the airplane’s static port). The altimeter setting at the time of the accident was 29.97 “Hg,[10] and so actual MSL altitude is about 46 ft. higher than pressure altitude. However, the pressure altitude adjusted for altimeter setting alone may not necessarily match the true MSL altitude throughout the flight because, in general, the lapse rate of pressure with altitude does not match the lapse rate in the standard atmosphere.

To estimate the actual altitude of UPS flight 1354, the change in altitude corresponding to a change in static pressure is calculated by solving the hydrostatic equation continuously (the hydrostatic equation describes the pressure increment across a differential element of air required to balance the weight of the element; see Appendix A of Ref. 5). With static pressure and the static temperature values from the speed calculations, the density and weight of the air elements at each point in time can be calculated, as well as the corresponding change in altitude. The resulting altitude vs. time calculation is then shifted so that the altitude intersects the altitude of tree “M2” at the time of the “first sound of impact” recorded on the CVR.

The results of this calculation are shown in Figures 8 and 9 as the lines labeled “FDR altitude corrected for non-standard temperature & pressure.” The density altitude is the altitude in the standard atmosphere corresponding to the actual air density at each point in the flight. Because of the warmer-than-standard day, the density altitude during the final approach was about 1100 ft. higher than the true MSL altitude at 2600 ft. MSL, and about 1000 ft. higher than true MSL at 800 ft. MSL.

The calculated static temperature is shown in the bottom graph of Figure 13, along with the total temperature recorded by the FDR.

Correction of apparent time lags in the FDR pressure altitude and GPS position data

As mentioned above, time lags in the FDR pressure altitude and GPS latitude & longitude data relative to other FDR parameters become apparent when one compares the FDR radio altitude to the height above terrain computed by subtracting the elevation of the terrain under the FDR latitude and longitude data from the MSL altitude computed from the FDR pressure altitude data. The lag appears as a shift, or time offset, between these two measures of the airplane’s altitude above the terrain. The lag also becomes apparent by time-aligning several FDR and EGPWS parameters (normal load factor, airspeed, radio altitude, rate of climb, pitch

[9] As named in Ref. 3.
[10] From the KBHM 5-minute ASOS observation closest to the time of the accident (03:45:31 CDT); see Table 5.

angle), and then observing the resulting mismatch between the FDR and EGPWS latitude and pressure altitude parameters. These observations are most easily understood by considering the comparison of the FDR and EGPWS data first.

Figures 14a and 14b compare several FDR and EGPWS parameters. The times associated with the EGPWS parameters are from the EGPWS download, documented in Ref. 6; these times are shown on the separate x-axis at the bottom of the Figures. The times associated with the FDR parameters are the FDR Subframe Reference Numbers (SRNs) generated during the FDR readout, as documented in Ref. 3, and are shown on the x-axis of each plot within the Figures. In Figures 14a and 14b, the relationship between the EGPWS and FDR times has been determined by aligning the EGPWS and FDR radio altitude parameters (see the second plot of Figure 14b). This alignment also produces good agreement between the EGPWS and FDR rate of climb, calibrated airspeed, pitch angle, and normal load factor parameters (though it appears in Figure 14a that the match of the pitch angle and normal load factor parameters could be improved with a slightly different alignment; but in that case, the radio altitude match would not be as good). The relationship between the EGPWS elapsed time and FDR SRN based on the radio altitude alignment is:

$$\text{(FDR SRN)} = \text{(EGPWS elapsed time)} + 253282.181 \text{ seconds} \qquad [2]$$

Observe that in Figure 14b, the time alignment given by Equation [2] results in a significant mismatch between the EGPWS and FDR pressure altitude and latitude parameters, even though the match of the other parameters is much better. This indicates that the time relationship between the pressure altitude parameter and other parameters is different on the EGPWS and on the FDR (the same is true for the latitude parameter). There are three mutually-exclusive explanations for this discrepancy:

- Only the time relationships on the EGPWS are correct;
- Only the time relationships on the FDR are correct;
- Neither the time relationships on the EGPWS or on the FDR are correct.

As will be seen below, assuming that the time relationships on the EGPWS are correct (and correcting the FDR pressure altitude and latitude parameters to match the EGPWS data) results in consistency between the FDR, EGPWS, radar data, and known terrain elevation north of the KBHM runway 18 threshold. Accordingly, in this *Study* the FDR pressure altitude and latitude sample times are corrected as follows:

$$\text{(Corrected FDR SRN)} = \text{(Uncorrected FDR SRN)} - 1.727 \text{ seconds} \qquad [3]$$

Equation [3] indicates that the correct times associated with the FDR pressure altitude and latitude data occur 1.727 seconds *earlier* than the recorded times. Hence, the recorded data “lags” the truth by 1.727 seconds.

The FDR pressure altitude and latitude data plotted with the FDR SRNs are shown in Figure 14b as the data with a “-1.727 sec. time shift” label. Note that the shifted data matches the corresponding EGPWS data well, as designed. See also Figures 6a-6c, which present the airplane’s distance north of the KBHM runway threshold at various scales; the good agreement between the radar, EGPWS, and time-shifted FDR data is evident in these plots.

As mentioned above, when the airplane's height above the terrain is computed using FDR based on the pressure altitude and latitude[11] parameters corrected with the time shift given by Equation [3], the result matches the FDR radio altitude well, as shown in Figure 15. The red line in this figure is the height above the ground obtained by subtracting the terrain elevation from the airplane's MSL altitude. The MSL altitude is computed from an integration of the FDR accelerometer data (described below), and the terrain elevation is obtained from Shuttle Radio Topography Mission (SRTM) data[12] corresponding to the airplane's latitude and longitude. The airplane's latitude and longitude is also computed by integrating the FDR accelerometer data. The accelerometer integration calculations rely on the FDR pressure altitude and GPS latitude / longitude data, with sample times corrected per Equation [3]. The times plotted in Figure 15 are the BHM ASR times, converted from the FDR SRN times using Equation [1].

Note that the red line in Figure 15 matches the FDR and EGPWS radio altitude data well. In particular, the drop in radio altitude between 04:47:11 and 04:47:15 is duplicated. The black line in Figure 15 is identical to the red line, but with the times increased by 1.727 seconds; this is what the computed radio altitude would be *without* the corrections to the sample times of the FDR pressure altitude and latitude data given by Equation [3]. Clearly, the drop in radio altitude indicated by the black line lags the drop indicated by the EGPWS and FDR data.

Additional plots of the FDR and computed radio altitude are presented in Figure 10 (vs. time), and in Figure 11 (vs. distance north of the threshold). The CVR comments from Table 3 are overlaid on these Figures.

Flight path angle (γ), angle of attack (α), and sideslip angle (β) calculations

The flight path angle is defined by

$$\gamma = \sin^{-1}\left(\frac{\dot{h}}{V}\right) \qquad [4]$$

where γ is the flight path angle, $\dot{h}$ is the rate of climb, and V is speed. The γ relative to the airmass resulting from using $\dot{h}$ and V from the true altitude[13] and true airspeed calculations described above in Equation [4] is shown in Figure 16 as the cyan line. The γ relative to the Earth resulting from using $\dot{h}$ and V from integrated accelerometer data is shown in Figure16 as the blue line (the accelerometer integration method is described below). The γ relative to the airmass resulting from using $\dot{h}$ and V from integrated accelerometer data and smoothed winds during the approach is shown in Figure16 as the green line (the wind calculations are also described below).

---

[11] The FDR longitude data does not change while the airplane is centered on the localizer, and so the sample times of the longitude do not need to be shifted for the time segment examined in this *Study.*

[12] The SRTM elevation database is maintained by the United States Geological Survey (USGS). The USGS provides SRTM digital elevation data with a resolution of 1 arc-second (about 100 ft.) for the United States and 3 arc-seconds (300 ft.) for global coverage See https://lta.cr.usgs.gov/SRTM2. The SRTM data for the KBHM runway 18 threshold elevation was not in as good agreement with official FAA data as data from *Google Earth*; consequently, the elevations along the runway depicted in the Figures in this *Study* are from *Google Earth*.

[13] In this context, "true altitude" refers to the "FDR altitude corrected for non-standard temperature & pressure" altitude shown in Figures 8 and 9.

The sideslip angle (β) is the angle that the velocity vector of the airplane relative to the airmass makes with the airplane's plane of symmetry (see Figure 17). This angle is required to resolve the airspeed of the airplane into components along each of the airplanes axes, which in turn is required to estimate the atmospheric wind from the FDR data.

β is not sensed or recorded by the FDR, and so must be calculated from other parameters. An estimate of β can be made if the side force (Y) characteristics of the airplane are known and if the side force generated during the flight can be calculated. The most significant contributors to the side force are β and rudder deflection (δr):

$$C_Y = \frac{Y}{\frac{1}{2}\rho V^2 S} = \frac{\partial C_Y}{\partial \beta}\beta + \frac{\partial C_Y}{\partial \delta r}\delta r + \{\text{smaller terms}\} \quad [5]$$

Where C_Y is the side force coefficient, ρ is the air density, V is true airspeed, and S is the wing reference area. Ignoring the smaller terms, Equation [5] can be solved for an estimate of β:

$$\beta \cong \frac{C_Y - \frac{\partial C_Y}{\partial \delta r}\delta r}{\frac{\partial C_Y}{\partial \beta}} \quad [6]$$

The derivatives $\partial C_Y / \partial \beta$ and $\partial C_Y / \partial \delta r$ are aerodynamic characteristics of the airplane.
The side force Y can be calculated using

$$Y = (W)(n_y) \quad [7]$$

Where W is the weight of the airplane and n_y is the lateral load factor recorded by the FDR.

In this case, both n_y (when corrected for accelerometer bias; see Figure 20) and δr (Figure 21) are very small during the final approach, and so the β that would result from Equation [6] would also be very small. Consequently, for this *Study*, a β of zero is assumed during the approach.

Once γ and β are obtained, they can be used along with the pitch angle (θ) and roll angle (ϕ) recorded by the FDR to compute the angle of attack, α:

$$\alpha = \tan^{-1}\left(\frac{\tan\theta}{\cos\phi}\right) - \sin^{-1}\left(\frac{\sin\gamma + \sin\beta\cos\theta\sin\phi}{\cos\beta\sqrt{1-\cos^2\theta\sin^2\phi}}\right) \quad [8]$$

Note that when $\beta = \phi = 0$, Equation [8] simplifies to the well-known result that $\alpha = \theta - \gamma$. The α resulting from Equation [8] is shown in Figure 16 as the gray line labeled "α based on pressure altitude and airspeed." The α resulting from the components of airspeed along each of the airplane's axes, as determined from integrated accelerometer data and smoothed winds, is shown in Figure 16 as the red line labeled "α based on accelerometer integration and winds" (the accelerometer integration method is described below). The θ and ϕ recorded by the FDR are also shown in Figure 16.

The angles of attack based on the left and right α-vane measurements recorded on the FDR are also shown in Figure 16. There is a difference of about 0.35° between the FDR *AOA-1* and *AOA-2* parameters. The FDR *AOA-1* parameter agrees well with the α computed from the accelerometer integration and computed winds. The resolution of the FDR angle of attack parameters is 0.35°, so it appears that *AOA-1* and *AOA-2* differ by 1 "count" of the sensors.

Accelerometer data corrections and integration

The accuracy of the calculations that use the FDR altitude and airspeed data as inputs are limited by the accuracy and sample rate of that data. In particular, the rate of climb – and consequently, the γ and α – that are computed using the pressure-based altitude data will be "noisy" (see the "Rate of climb based on pressure altitude" result in Figure 12, and the resulting γ and α in Figure 16).

A more accurate calculation of the flight path of the airplane during relatively short intervals (about 100 seconds) can be obtained by integrating the accelerations recorded at the CG of the airplane. However, the accelerometers are generally not located exactly on the CG, and so the accelerations at the CG must be computed by adjusting the FDR-recorded load factors for the effects of angular rates and accelerations. Furthermore, accelerometers generally contain small offsets, or "biases," that produce large errors in speed and position if not removed prior to integration.[14] In addition, the initial values of speed, rate of climb, and track angle are required during the integration process (these are essentially the "constants of integration" when integrating acceleration to get speeds). The constants of integration and the values of the accelerometer biases can be estimated by selecting them such that the aircraft position that results from the integration agrees with known positions determined from another source. In this *Study*, the "target" positions are those defined by an integration of the groundspeed and drift angle data recorded by the FDR, and the "FDR altitude corrected for non-standard temperature & pressure" shown in Figures 8 & 9.

Accelerations at the CG

The accelerations at the CG can be computed from the load factors recorded by the FDR as follows. The acceleration at any point P on the airplane, $\vec{a}_P$, is given by

$$\vec{a}_P = \begin{Bmatrix} \dot{u} + wQ - vR \\ \dot{v} + uR - wP \\ \dot{w} + vP - uQ \end{Bmatrix} + \begin{Bmatrix} Q(yP - xQ) + R(zP - xR) + (z\dot{Q} - y\dot{R}) \\ R(zQ - yR) + P(xQ - yP) + (x\dot{R} - z\dot{P}) \\ P(xR - zP) + Q(yR - zQ) + (y\dot{P} - x\dot{Q}) \end{Bmatrix} = \vec{a}_{CG} + \Delta\vec{a} \qquad [9]$$

where:

$\{u, v, w\}$ = components of inertial velocity in the airplane body axes
$\{P, Q, R\}$ = components of angular velocity in the airplane body axes
$\{\dot{P}, \dot{Q}, \dot{R}\}$ = time derivatives of $\{P, Q, R\}$
$\{x, y, z\}$ = coordinates of point P in the airplane body axes

[14] For details about the equations to be integrated and the bias correction technique described in this Study, see Appendix A of Ref. 5.

(see Figure 17). Since by definition {x, y, z} at the CG = {0,0, 0}, the first term in brackets in Equation [9] is the acceleration of the CG ($\vec{a}_{CG}$), and the second term is the increment in acceleration due to the point P being away from the CG ($\Delta\vec{a}$).

A three axis accelerometer at point P will measure load factors as follows:

$$\vec{n}_P = \frac{\vec{a}_P - \vec{g}}{g} = \frac{\vec{a}_{CG} + \Delta\vec{a} - \vec{g}}{g} = \vec{n}_{CG} + \frac{\Delta\vec{a}}{g} \qquad [10]$$

Where $\vec{g}$ is the gravity vector, g is the acceleration due to gravity (32.17 ft/s^2), and Equation [9] has been used to substitute for $\vec{a}_P$. The components of $\vec{n}$ are {n_x, n_y, n_z}. The normal load factor (*nlf*) is

$$nlf = -n_z \qquad [11]$$

The FDR records n_x, n_y, and *nlf* as "Longitudinal Acceleration," "Lateral Acceleration," and "Vertical Accleration," respectively.[15] The values of {n_x, n_y, n_z} at the CG can be found using the FDR data and Equations [11], [10], and [9], with {x y, z} in [9] being the distance of the accelerometer unit from the CG.

The angular rates and accelerations used to evaluate Equation [9] are computed from the θ and ϕ angles recorded by the FDR, and true heading (ψ_T). The ψ_T is based on the magnetic heading (ψ_M) recorded by the FDR.[16] ψ_M and ψ_T are presented in Figure 16.

The angular rates and accelerations throughout flight 1354's approach were very small. This fact, together with the relatively close proximity of the accelerometers to the CG, make the $\Delta\vec{a}$ defined in Equation [9] negligibly small, and so in this case the {n_x, n_y, n_z} recorded by the accelerometers are good measures of the {n_x, n_y, n_z} at the CG. However, these data must still be corrected for accelerometer bias.

Accelerometer bias calculations

The accelerometer biases are not necessarily constant over an entire flight, but can drift over time. It is for this reason that integrating the accelerometers works best over relatively short intervals, during which the accelerometer biases are approximately constant. When the period of interest is lengthy, an integrated flight path for the entire length can be obtained by dividing it into shorter segments, and integrating the accelerometer data separately over each segment. In this case, however, the period of interest is only 92 seconds long, and a satisfactory integration can be obtained with a single segment.

The constants of integration and the accelerometer biases are chosen to minimize the difference between the integrated north and east position and the north and east position obtained from an integration of the FDR groundspeed and drift angle data, and the difference between the integrated altitude and the "FDR altitude corrected for non-standard temperature & pressure" data shown in Figures 8 & 9.

[15] In FDR parameters *AccelLong*, *AccelLat*, and *AccelVert*, respectively.
[16] True heading is computed assuming a magnetic variation of 3° west (i.e., $\psi_T = \psi_M - 3°$).

The constants of integration (the initial groundspeed, track angle, and rate of climb) are chosen to minimize the root-mean-square difference between the integrated flight path and the target flight path throughout the entire segment. The accelerometer biases are chosen to minimize the error between the integration and the target at the end point of the integration; i.e., the biases are chosen so that the integrated flight path and target flight path coincide at the end of the segment. The beginning and end times, constants of integration, and accelerometer biases for the segment are shown in Table 4. The constants of integration are expressed as increments, or biases, on the initial groundspeed, track, and rate of climb that would be computed using the target trajectory.

The integration of the FDR groundspeed and drift angle data, which serves as the "target" for the integration of the accelerometer data, also requires some correction. This is because the track produced by integrating the FDR groundspeed and drift angle (without adjustment) differs slightly from the track recorded in the FDR GPS position data.[17]

To ensure that the integration of groundspeed and drift angle match the GPS track over the length of each segment, a time-weighted velocity vector is added to the north and east velocities defined by the FDR groundspeed and drift angle. This vector then forces the integration of the north and east velocities to match the GPS position at a point near the end of the segment. The vector can be thought of as a "wind," with a velocity and direction, that "blows" the airplane onto the GPS position at the specified time.

The time-weighted "shape" of the velocity vector is shown in Figure 18. The magnitude of the vector is multiplied by the factor k in this Figure, which changes over the length of the integration. At the beginning and end of the integration, the value of k is 0.0, and so the corrected east and north velocities match those defined by the FDR groundspeed and drift angle data at these points. The k factor ramps up to 1.0 over the first third of the segment, remains at 1.0 over the second third, and ramps back to 0.0 over the last third.

The values of the velocity vectors for the integration segment, expressed as wind velocities and directions, are listed in Table 4.

The north and east positions, and MSL altitude, resulting from the accelerometer integrations (not the groundspeed/drift angle integration) are shown in Figures 6, 8, 9, and 24.

The load factors recorded on the FDR, and the load factors corrected with the biases listed in Table 4, are plotted in Figure 20. Plots of the flight control and throttle inputs (which result in changes in the load factors) are presented in Figure 21. Interestingly, it appears that the column force parameter senses inputs by the autopilot (e.g., non-zero forces while the autopilot is engaged), and so does not necessarily indicate a (human) pilot input; the parameter may simply reflect the force required to displace the column, from whatever source. The FO column input parameter on the FDR appears to be erroneous, and so is not presented here.

[17] The GPS provides a reliable measure of the absolute position of the airplane throughout the flight; however, speeds and track angles computed from the GPS data are more "noisy" than the inertial groundspeed and drift angle recorded by the FDR. To obtain a smooth "target" track for the accelerometer integration, the integrated groundspeed and drift angle track is preferred to the GPS track. However, since the GPS track, while noisier, provides a better measure of the "absolute" position of the airplane over long periods, the groundspeed / drift angle integration must be adjusted to prevent it from diverging from the GPS track over time.

Item	Value
Start time	04:46:01.92
End time	04:47:33.42
Speed bias, knots	-1.26
Track bias, degrees	0.92
Rate of climb bias, feet/minute	-239.99
n_x bias, G's	-0.010396
n_y bias, G's	0.008720
nlf bias, G's	0.023841
Groundspeed/drift correction vector magnitude, knots	6.09
Groundspeed/drift correction vector direction, degrees	66.2

Table 4. Biases and constants of integration for accelerometer integration segment.

Wind calculations

Airspeed, groundspeed, and wind are related as follows:

$$\vec{V}_W = \vec{V}_G - \vec{V} \qquad [12]$$

where $\vec{V}$ is the airspeed vector, $\vec{V}_G$ is the groundspeed vector and $\vec{V}_W$ is the wind vector (see Figure 19). The components of $\vec{V}_G$ in body axes result from the integration of the accelerometer data described above. The components of the airspeed $\vec{V}$ in body axes, as indicated by Figure 17, are related to α and β as follows:

$$u = V\cos(\beta)\cos(\alpha) \qquad [13a]$$
$$v = V\sin(\beta) \qquad [13b]$$
$$w = V\cos(\beta)\sin(\alpha) \qquad [13c]$$

where β and α are computed using Equations [6] and [8], respectively.[18] Once the components of $\vec{V}_W$ in the airplane body axes are computed using Equation [12], they can be transformed into Earth axes using the known θ, ϕ, and ψ_T. The results of the wind calculations are shown in Figure 13 as a function of time, and in Figure 22 as a function of altitude. The "Fit to computed winds" lines shown in Figure 22 provide a "smoothed" wind profile as a function of altitude, which can be used to compute inertial α, β, and γ values.

Inertial γ, α, and β calculations

A second method of calculating α and β involves computing the airplane's airspeed components along each of the body coordinate axes, using the known inertial speed components resulting from the accelerometer integration, the "smoothed" winds shown in Figure 22, and Equation [12]. This method assumes that the winds are not really as "noisy" as the computed winds shown in Figures 13 and 22. Furthermore, the method assumes zero vertical wind. Since the integrated inertial velocities are smooth, and the winds are smooth, the α and β computed from these quantities are also relatively smooth (compare the inertial α and β calculations with the other α and β calculations in Figure 16).

[18] As mentioned above, in this case β is assumed to be zero.

From Figure 17 (and Equation [13]), we see that

$$\alpha = \tan^{-1}\left(\frac{w}{u}\right) \quad [14]$$

$$\beta = \sin^{-1}\left(\frac{v}{V}\right) \quad [15]$$

where V is total airspeed, and {u, v, w} are the components of airspeed in body axes. Per Equation [12], the airspeed and its components in the body axes can be computed if the components of both the groundspeed and wind speed are known. The components of $\vec{V}_G$ in body axes result from the integration of the accelerometer data described above. The components of $\vec{V}_W$ can be calculated by transforming the components of the smoothed wind in Earth axes into body axis using the recorded Euler angles (θ, ϕ, and ψ_T). The resulting V is shown in Figure 12 as the red line labeled "True airspeed from accelerometer integration & smoothed winds."

The results of the inertial α and β calculations are shown in Figure 16 as the red lines. Note that the inertial α agrees well with the α computed using Equation [8], but is much smoother. The γ relative to Earth in Figure 16 is computed from Equation [4], using V as the total inertial speed relative to Earth (not airspeed). The γ relative to the airmass is computed using V as the "True airspeed from accelerometer integration & smoothed winds" in Figure 12.

VI. Estimate of cloud bases based on security video analysis

Description of security video

Figures 8, 9, and 24 depict a heavy dotted line labeled "Estimated cloud height." This line represents an estimate of the MSL altitude at which the airplane landing lights first become visible on a security video (hereafter, called "the video") from a camera located on a private hangar at the airport.[19] It should be noted that:

- The cloud bases are not defined by a sharp discontinuity, on either side of which visibility changes from zero to something much greater. Instead, the bases of the clouds are characterized by a gradual "thinning" of the cloud with altitude. Visibility through the cloud increases as the cloud thins. This characteristic (familiar to anyone who has looked out the window of an airplane) is reflected in the video as a gradual increase in the brightness and sharpness of the airplane's landing light over time. In Figures 8, 9, and 24, the gradual thinning of the clouds is depicted as the graduated gray shading extending downward from the "Estimated cloud height" line.

[19] Two security cameras located on the airport terminal building (cameras 293 and 817) also captured portions of the sequence of events recorded by the camera on the private hangar. However, it appears that the airplane enters the frame of the cameras on these videos after the landing light had already become visible, whereas the video from the private hangar clearly shows the landing light emerging from the clouds. Since the video from the private hangar shows a more complete sequence of events, it was used for the analysis described in this *Study*.

- While the “Estimated cloud height” line in the Figures runs across the length of each plot, it is not intended to imply that the ceiling was constant over the entire area stretching from the BASKN FAF to the airport. Instead, the line represents the estimate of the altitude of the appearance of the airplane landing lights (and cloud bases) at that point on the approach. The ceiling over the airport itself was likely higher than that over the approach to runway 18, per the ASOS observations current at the time (see Table 5). In fact, the METAR observation for 03:53:00 CDT included the following remark: “CLG 006V013,” indicating a variable ceiling between 600 and 1300 ft. AGL.

Time (CDT)	Wind speed (kts.)	Wind direction (deg. true)	Visibility (statute miles)	Clouds (feet MSL)	Temperature (°C)	Dew point (°C)	Altimeter setting (“Hg)
04:35:31	Calm	Calm	9	BKN 7500 BKN 10000	23	22	29.97
04:40:31	Calm	Calm	10	FEW 1100 BKN 7500	23	22	29.97
04:45:31	Calm	Calm	10	FEW 1100 OVC 7500	23	22	29.97
04:50:31	3	340	10	FEW 1100 SCT 3500 OVC 7500	23	22	29.97

Table 5. Automated Surface Observing System (ASOS) 5-minute observations near the time of the accident.

For additional information about the meteorological conditions at KBHM at the time of the accident, see Ref. 7.

The copy of the video that its owner provided to the NTSB is 36.83 seconds long, containing 1105 frames (30 frames / second).

The sequence of events depicted on the video is summarized in Table 6. The video depicts the appearance of the landing lights, their growth in brightness and clarity, a decrease in the brightness of the lights (dimming) followed by a much more rapid dimming, and the disappearance of the lights. About 4.6 seconds after the lights disappear, a bright, brief flash appears, likely corresponding to the airplane’s impact with a power transformer located near Tree 10 (point 14 in Table 2 and Figure 2). About 5 seconds after this flash, light from the explosion of the aircraft, likely corresponding to its contact with terrain near point 26 in Table 2 and Figure 2, becomes visible.

Event	Video Frame	Video Time, seconds	ΔT, seconds	CDT Time
Lights first appear	183	6.07	0.00	04:47:24.03
Peak of brightness	307	10.20	4.13	04:47:28.17
Lights start to dim	357	11.87	5.80	04:47:29.83
Sudden dimming	425	14.13	8.07	04:47:32.10
Lights totally out	433	14.40	8.33	04:47:32.37
Transformer flash	545	18.13	12.07	04:47:36.10
Impact explosion	683	22.73	16.67	04:47:40.70

Table 6. Sequence of events depicted on the security video from a private hangar at KBHM. Video time is from the start of the video. ΔT times are from the time that the lights first appear.

The video frames corresponding to the events in Table 6 are presented here in Figure 23, except for frame 357, which looks very similar to frame 307.

Correlation of video times to CDT

The elements shown in Table 6, except for the CDT Time, can be determined from the contents of the video itself. The correlation of the video time to CDT time depends on identifying the CDT time of at least one event in the video. Since the events listed in Table 6 correspond to points along flight 1354's flight path, the video can be time-correlated if the location of the airplane during one of the events can be identified.

Clearly, the airplane was at the (known) location of the power transformer at the time the transformer flash occurred. Unfortunately, the FDR ends shortly before the airplane reached the transformer,[20] so the flight path integration depicted in Figures 8 and 9 cannot be used to identify the CDT time of the transformer flash rigorously. However, a good estimate of this time can be made by observing that the distance between the point where the FDR ends (at about 1.012 nmi north of the KBHM runway threshold) and the location of the transformer (0.904 nmi north of the threshold) is only 0.108 nmi. Assuming that the airplane's groundspeed over this 0.108 nmi was approximately equal to its groundspeed at the point the FDR data ended, then the time of the transformer flash can be computed as

$$t_{flash} = t_{FDR\_end} + \frac{north_{FDR\_end} - north_{flash}}{V_{G\_FDR\_end}} \quad [16]$$

Where:

t_{flash} = time of transformer flash;
t_{FDR_end} = time of the end of the FDR data (04:47:33.42 CDT);
$north_{FDR\_end}$ = north coordinate at the time the FDR data ends (1.012 nmi);
$north_{flash}$ = north coordinate of the transformer (0.904 nmi)
$V_{G\_FDR\_end}$ = groundspeed at the time the FDR data ends (145 kts. and decreasing)

Evaluating Equation [16] with these values yields t_{flash} = 04:47:36.10 CDT. This time defines the correlation between the video times and CDT times listed in Table 6.

Since the position of the airplane as a function of CDT time is known (see Figures 8 and 9), its position at the times of the video events listed in Table 6 can also be determined. Figure 24 presents the locations of these events as black triangles overlaid on the flight path obtained from the integration of the accelerometer data. As shown in this Figure, the "Lights first appear" event occurs when the airplane is at about 1000 ft. MSL, and this altitude is selected as the "estimated cloud height." However, as discussed above, this does not mean that the airplane is suddenly in the clear (with 10 smi visibility) once it descends below 1000 ft. MSL; rather, 1000 ft. is the highest altitude at which the illumination of the clouds enveloping the airplane becomes visible to the camera. As the airplane descends and the clouds thin, the visibility improves and the lights become brighter and clearer. It is interesting that the "Peak of brightness" event occurs at about the same time that the crew reported the runway in sight, suggesting that at this point (about 900 ft. MSL) the airplane was truly in the clear, with good visibility.

[20] See Figure 9b; the power transformer is located about 0.90 nmi north of the KBHM runway 18 threshold.

Note that at the time the FDR data ends, the groundspeed is decreasing rapidly. Consequently, the average groundspeed between the point where the FDR data ends and the location of the transformer may be lower than the 145 kts. assumed in this analysis. If this is the case, then per Equation [16], t_{flash} will occur later than 04:47:36.10, and the other times listed in Table 6 will be similarly delayed. This would place the altitude of the airplane at the time of the "Lights first appear" even lower than the 1000 ft. depicted in Figure 24. In any case, the evidence from the video indicates that the airplane was not below the clouds (and the runway would not have been visible from the cockpit) until well below the MDA of 1200 ft. MSL, consistent with the crew's reporting the airport in sight at about 900 ft. MSL.

Obscuration of the security camera's line of sight by terrain

Note in Figure 24 that, per the time correlation described in Table 6, the "Lights totally out" event (at 04:47:32.37) occurs about a second before the end of the FDR data (at 04:47:33.42). If the FDR stopped recording because power to the recorder was lost, the same power loss may have caused the airplane's landing light to go out (see Ref. 3 for more information about the end of the FDR recording). However, in this case the average groundspeed between the end of the FDR data and the transformer flash would be 0.108 nmi / (12.07 sec. – 8.33 sec.) = 0.0289 nmi / sec. = 104 kts., considerably below the 145 kts. corresponding to the end of the FDR data. The location of the impact explosion, corresponding to point 26 in Table 2, is 0.766 nmi north of the runway threshold; consequently, the average groundspeed between the transformer flash and the impact explosion is (0.904 nmi - 0.766 nmi) / (16.67 sec. – 12.07 sec.) = 0.0300 nmi / sec. = 108 kts., roughly the same as (or a bit higher than) the average speed between the end of the FDR data and the transformer in this scenario. It seems unlikely that the airplane would cease decelerating after the impact with the transformer, after having decelerated so precipitously from the 145 kts. at the end of the FDR data; consequently, it is more likely that the "Lights totally out" event occurred *before* the end of the FDR data (as indicated in the correlation in Table 6), and was not the result of a loss of power to the lights.

The "Lights start to dim" event following the "Peak of brightness" event on the video suggests that, after emerging from the clouds and having a clear line of sight to the security camera, the airplane once again became progressively more obscured from the camera. This progressive obscuration may have been the result of obstacles, such as trees, entering the line of sight between the camera and the airplane. Since the canopies of trees are not completely solid, some light can filter through them, resulting in a dimming of the light, rather than its total obscuration. However, once the airplane descends so low that solid ground (terrain) blocks the line of sight between the airplane and the camera, no light would reach the camera and the lights would appear to go out.

To evaluate whether the "Lights totally out" event on the video could have been the result of the obscuration of the camera's line of sight by terrain, the terrain profile between the camera and the airplane (assumed to be near tree M2 for this analysis) was examined. For this analysis, accurate elevation data for the terrain between the camera and tree M2 is required. Significantly, the SRTM elevation database for the hill on which the airplane came to rest is outdated; the SRTM data was collected during Space Shuttle flights in 1994, and since that time, the elevation contours of the hill have changed significantly as the result of construction

and demolition projects.[21] A daytime photograph taken from the site of the security camera towards tree M2 (Figure 25) indicates that it is precisely the terrain on this hill that would obscure the camera's view of the airplane's final descent into trees; consequently, up-to-date measurements of elevations on the hill are required for the line-of-sight analysis.

Two recent surveys provide current elevation information on the hill: one is a survey of the highest point on the hill commissioned by KBHM airport, and the second is the Total Station survey data collected by the FBI on-scene following the accident. These data are shown in Figure 24 as the point labeled "top of hill as surveyed by KBHM airport," and the area labeled "FBI survey terrain profile along camera line of sight," respectively. The line of sight from the camera to tree M2 passes over terrain about 5 feet lower than the top of the hill. Note that the FBI survey data shows significantly lower elevations between 0.6 and 0.7 nmi from the threshold than does the SRTM data. A photograph taken on-scene near the brow of the hill looking south towards the runway (Figure 26) shows that the location of the security camera is in view, indicating that no obstructions to the line of sight of the camera lie to the south (and so accurate elevation data for points south of the brow of the hill are not required). The location of the security camera on the airport is shown in Figure 27.

The blue triangle in Figure 24 shows the location of the security camera in a profile view. The dashed blue line from the camera, tangent to the top of the shaded terrain, shows the line-of-sight below which objects to the north of the hill would be obscured from the camera. Note that the blue line passes very close to (within 10 ft. of) the points where the airplane's lights on the video suddenly dim and then go totally out, per the analysis outlined above. Consequently, it is likely that these events are the result of the airplane becoming obscured by terrain in the line of sight of the camera.

VII. PAPI geometry and visibility

Runway 18 at KBHM is served by a localizer signal, providing lateral guidance to the runway, but not a glideslope signal, which would provide vertical guidance to the runway. Consequently, there is no full ILS approach to runway 18, only non-precision instrument approaches: the Localizer approach attempted by flight 1354, and an RNAV (GPS) approach. These non-precision approaches specify how the airplane is to descend on the final approach course to the Minimum Descent Altitude (MDA), which in this case is 1200 ft. MSL. To descend from the MDA, the crew must have the airport / runway environment in sight, and complete the descent and landing visually.

Visual vertical flight path guidance to runway 18 is available from a Precision Approach Path Indicator (PAPI) lighting system. The FAA *Aeronautical Information Manual* (AIM, Ref. 8) describes the PAPI system as follows:

> **Precision Approach Path Indicator (PAPI).** The precision approach path indicator (PAPI) uses light units … installed in a single row of either two or four light units. These lights are visible from about 5 miles during the day and up to 20 miles at night. The visual glide path of the PAPI typically provides safe obstruction clearance within plus or minus 10 degrees of the extended runway centerline and to 4 SM from the runway threshold. Descent, using the PAPI, should not be initiated until the aircraft is visually aligned with the runway. The row of light units is normally installed on the left side of the runway and the glide path indications are as depicted [in Figure 28]. Lateral course guidance is provided by the runway or runway lights. In certain circumstances,

[21] At one time there was a housing development on the hill, which was demolished after the property was acquired by the KBHM airport authority.

the safe obstruction clearance area may be reduced due to local limitations, or the PAPI may be offset from the extended runway centerline. This will be noted in the Airport/ Facility Directory (AIM paragraph 2-1-2 (b)).

Technical specifications for the design of the PAPI system, including the flight path angle ranges corresponding to each combination of light displays, are contained in FAA Advisory Circular (AC) 150/5340-30G, *Design and Installation Details for Airport Visual Aids* (Ref. 9). Section 7.5(d) of this AC addresses the design of the PAPI, and Table 7-2 of the AC (Figure 29 here) describes the aiming of Type L-880 (4 Box) PAPI relative to the pre-selected flight path angle.

"Height group 4 aircraft" are described in Table 7-1 of AC 150/5340-30G, included here as Figure 30.

The A300 is listed explicitly in Figure 30 as a height group 4 aircraft. However, the threshold crossing height (TCH) and the light aiming angles of the PAPI for runway 18 correspond to those for group 3 aircraft, as shown in Table 7. The TCH value, touchdown reference point, and pre-selected glide path angle shown in Table 7 are taken from the FAA online database of airport and navigation aid information at http://avnwww.jccbi.gov/datasheet/. The aiming angles ("angular elevations") shown in Table 7 are taken from an entry on the PAPI performance record (Ref. 10), dated August 14, 2013 (the day of the accident). For further information on the operation of height group 4 aircraft on a runway served by a height group 3 PAPI, see Ref. 11.

Item	Value
Commissioned glide path angle	3.20°
Threshold Crossing Height (TCH)	47.7 ft.
Reference point latitude	N 33° 34' 12.0300"
Reference point longitude	W 086° 44' 49.8900"
Reference point elevation	630.6 ft.
Distance from runway threshold to reference point	1166.0 ft.
PAPI Light Housing Assembly (LHA) 1 angular elevation	3° 43' (3.717°)
PAPI LHA 2 angular elevation	3° 23' (3.383°)
PAPI LHA 3 angular elevation	3° 02' (3.033°)
PAPI LHA 4 angular elevation	2° 42' (2.700°)
Average of LHA 2 and LHA 3 angular elevations ("actual" glide path angle)	3.208°
Angular elevation of LHA 1 above actual glide path angle	0.509° (30.5')
Angular elevation of LHA 2 above actual glide path angle	0.175° (10.5')
Angular elevation of LHA 3 below actual glide path angle	0.175° (10.5')
Angular elevation of LHA 4 below actual glide path angle	0.508° (30.5')

Table 7. PAPI information for KKBHM runway 18.

It is of interest to know whether the PAPI lights would have been visible to the crew of flight 1354 as it approached runway 18, and if so, what light pattern would have been perceived. This problem amounts to knowing the position of the airplane relative to each of the four PAPI light beams, and identifying whether any obstructions (such as terrain) penetrated the line of sight between the PAPI and the airplane. The angle of these beams relative to the runway are defined by the (actual) PAPI glide path angle, and the (actual) aiming angles of each of the beams relative to the glide path angle.

PAPI beam solutions for both the design value of the PAPI glide path angle (3.20°), and the nominal aiming angles for a height group 3 PAPI are depicted in Figure 9 (per Table 7, the actual aiming angles are all within 0.5 minutes of arc of the nominal values, so the beam

paths depicted in Figure 9 are representative). The altitudes of the beams depicted in Figure 9 take into account the curvature of the Earth, which will increase the height of the beams as the distance from the PAPI increases, compared to the height obtained assuming a flat Earth.

Figure 9 indicates that prior to IMTOY, flight 1354 was above the PAPI glide path, and crossed below it about 0.1 nmi north of IMTOY, though at IMTOY, the PAPI display to the crew would still have been 2 white and 2 red lights (indicating on the glide path). The display would have changed to 3 red lights and 1 white light about 0.05 nmi south of IMTOY, indicating that the airplane was deviating below the glide path. The PAPI display would have changed to 4 red lights (indicating a position well below the flight path) about 0.3 nmi south of IMTOY, or about 1.7 nmi north of the runway threshold. Of course, the video analysis described in Section D-VI indicates that at this point the runway (and PAPI) would still have been obscured by clouds, and would remain so at least until the airplane descended below 1000 ft. MSL, about 1.4 nmi north of the threshold.

When the crew reported the runway in sight at about 900 ft. MSL and about 1.24 nmi north of the threshold, Figures 9 and 24 suggest that the PAPI would have been visible for less than a second, becoming obscured by terrain almost immediately.

VIII. Go-around maneuvers in the A300-600 engineering simulator

As indicated in Table 3 and multiple Figures in this *Study*, the EGPWS "too low terrain" warning on the CVR came 1 second after the "first sound of impact," and so was not able to alert the crew in time for them to take action to avoid descending into the trees. The function and performance of the EGPWS system is described in the *System Group Chairman's Factual Report* (Ref. 6). Ref. 6 also presents information that indicates that an updated version of the EGPWS software (version -218) would have provided the "too low terrain" warning at about 04:47:27, or about 6.5 seconds earlier than that provided by the software version installed on the accident airplane (version -212). It is of interest to know whether this earlier alert would have been timely enough for the crew to have taken action to avoid the accident.

To address this question, three go-around responses were evaluated in an engineering simulator at Airbus facilities in Toulouse, France. In increasing order of aggressiveness, these responses are:

- Dialing the commanded vertical speed up from -1500 ft./min. to +500 ft./min.;
- Clicking the Takeoff / Go-Around (TOGA) switches on the throttles, thereby commanding an automatic go-around maneuver to be flown by the autopilot;
- Executing a manual terrain-avoidance maneuver by disengaging the autopilot, commanding full thrust, and pitching the airplane into a maximum-performance climb.

In order to ensure that the resulting runs were comparable, the initial conditions of each maneuver were matched by initiating the maneuver as the airplane passed through 1700 ft. MSL while the descending at 1500 ft./min. with the autopilot engaged in "vertical speed" mode.[22] The simulator pilots attempted to initiate the maneuver at exactly 1700 ft., using a countdown ("three-two-one-go") to time the maneuver as 1700 ft. was approached.

[22] The simulator weight, CG, configuration, airspeed, and wind profile were set to match the conditions of the accident flight.

Examination of the recorded data indicated that the actual pilot inputs to execute the maneuver occurred about 15 to 20 ft. below the target altitude of 1700 ft.. In this *Study*, this 15 to 20 ft. altitude loss is included in the altitude lost during the execution of the maneuver, and reflects the delay between the pilot's intent to act, and his actual movement of the controls. Consequently, the "allowable reaction time" described below and listed in Table 8 is the allowable time between the EGPWS "too low terrain" alert, and the pilot's intent to act.

The result of interest in each of the runs was the additional altitude lost (below 1700 ft. MSL) before the airplane started to climb. This altitude loss represents the minimum height above the trees at which each maneuver could be initiated in order to avoid impacting the trees.

The results of the simulations are shown in Table 8 and Figures 31 and 32. Figure 8 lists the minimum altitude reached during each maneuver, and the corresponding additional altitude loss after the maneuver was intended to be initiated at 1700 ft. MSL. If the go-around maneuvers were initiated with a vertical speed of -1500 ft./min. as in the simulations, then these altitude losses could be added to the altitude of tree M2 (822 ft. MSL), to yield the minimum altitudes during the accident flight at which each maneuver would have had to be initiated in order to avoid contact with that tree. However, during the accident flight, the selected vertical speed (V/S) was reduced from -1500 ft./min. to -600 ft./min. at 04:47:27 (the same time as the "too low terrain" alert corresponding to the EGPWS -218 software), and the airplane was starting to respond to this command and reduce the rate of descent. Hence, a go-around maneuver initiated after 04:47:27 would start from a rate of descent lower than -1500 ft./min., and the altitude loss would be less than that obtained in the simulator.

To account for this effect for the TOGA and manual terrain-avoidance maneuvers, simulator data was used to determine the altitude loss corresponding to initiating those maneuvers at lower rates of descent.[23] These simulator runs consisted of duplicating the UPS 1354 flight scenario as closely as possible using the selected vertical speed, and then initiating the TOGA or manual terrain-avoidance maneuver immediately upon the "too low terrain" alert corresponding to the EGPWS -218 software.

The top graph in Figure 31 shows the altitude loss corresponding to the TOGA and manual terrain-avoidance maneuvers, starting from two different initial vertical speeds. The red line on this graph plots the vertical speed of UPS flight 1354 against its height above tree M2, based on the integrated accelerometer data. When the red line intersects the lines plotting the altitude loss from the go-around maneuvers, then the airplane is at the altitude and vertical speed combination where any further delay in the execution of the maneuver will result in the airplane hitting the tree. The BHM ASR times at which the airplane is at these conditions can be read off the bottom graph in Figure 31. The corresponding times and altitudes are also listed in Table 8.

The positions of the airplane at the minimum "successful" altitudes listed in Table 8 are plotted in Figure 32.

The difference between the times that the airplane was at the minimum "successful" altitudes and the time of the "too low terrain" warning with the EGPWS -218 software is the "allowable reaction time" listed in Table 8. As noted above, these reaction times are the allowable times

[23] This additional consideration is not necessary for the vertical speed change maneuver, because to avoid the trees, that maneuver would have had to have been initiated *before* 04:47:27 and the reduction in the rate of descent (see Table 8).

between when the EGPWS “too low terrain” alert is activated, and when the pilot intends to act; the delay between the pilot’s intent to act, and his inputs on the controls, are accounted for in the altitude loss listed in Table 8.

In Figure 32, the latest point on the flight path at which each avoidance maneuver would have to be initiated to avoid contact with tree M2 is indicated by the blue triangles. The time of the “too low terrain” warning with the -218 software is indicated in Figure 32 by the vertical green line labeled “Too Low Terrain (EGPWS -218).”

Item	Selected vertical speed change	TOGA / automated go-around	Manual terrain-avoidance maneuver
Minimum altitude reached, feet MSL	1580	1610	1640
Altitude lost in maneuver, feet (V/S = -1500 ft./min.)	120	90	60
Altitude lost in maneuver, feet (V/S per Figure 31)	n/a	89	49
Minimum altitude for successful go-around, ft. MSL	942	911	871
Time at minimum altitude for successful go-around	04:47:26.3	04:47:27.6	04:47:29.4
Time at EGPWS “too low terrain” (-218 software)	04:47:27.0	04:47:27.0	04:47:27.0
Allowable reaction time, seconds	-0.7	0.6	2.4

Table 8. Results of three different go-around maneuvers in the A300-600 engineering simulator.

Table 8 and Figure 32 indicate that:

- Contact with tree M2 cannot be avoided using the vertical speed change maneuver, since this maneuver would have to be initiated 0.7 seconds *before* the “too low terrain” warning provided by the EGPWS -218 software.

- Contact with tree M2 can be avoided with the TOGA / automated go-around maneuver, if the TOGA switches are activated within 0.6 seconds of the “too low terrain” warning provided by the EGPWS -218 software.

- Contact with tree M2 can be avoided with the manual terrain-avoidance maneuver, if the maneuver is initiated within 2.4 seconds of the “too low terrain” warning provided by the EGPWS -218 software.

It is beyond the scope of this *Study* to consider whether reaction times of 0.6 to 2.4 seconds are feasible or reasonable, or whether TOGA activation or a manual terrain-avoidance maneuver are expected responses to a “too low terrain” warning.

E. CONCLUSIONS

The accident scene, radar, FDR, CVR, EGPWS, PAPI, and video data presented in this *Study* are consistent with the sequence of events summarized in Table 9, concerning the motion of UPS flight 1354 during its final approach to runway 18 at KBHM:

Event	Time (CDT)	Altitude, ft. MSL	FDR radio altitude, ft.	Distance north of threshold, nmi	FDR Calibrated airspeed, kts.
ATC clears flight for LOC 18 approach & descent to 2500 ft. MSL	04:43:24.3	6942[1]	n/a	15.20	250
Crew notes localizer alive	04:43:53.5	5100[1]	n/a	13.21	249
Airplane centered on localizer, crew activates final approach mode	04:44:13.1	3844[1]	n/a	11.78	250
Airplane level at 2500 ft. MSL	04:45:13	2500[1]	2054	7.58	210
Descent from 2500 ft. initiated (selected vertical speed set to -700 ft./min.)	04:46:04	2586	1942	4.8	146
Airplane at BASKN FAF	04:46:06.4	2588	1979	4.70	143
FO announces landing checklist complete	04:46:17.4	2491	1841	4.23	139
Selected vertical speed = -1000 ft./min.	04:46:21	2447	1797	4.08	138
Crew comments will do vertical speed mode	04:46:27.0	2359	1674	3.83	137
FO comments not in profile mode	04:46:29.6	2315	1640	3.72	137
Selected vertical speed = -1500 ft./min.	04:46:35	2220	1588	3.49	137
Crew comments high on approach	04:46:53.7	1762	1210	2.69	140
FO announces 1000 ft. no flags	04:47:02.9	1527	990	2.30	141
CA comments DA is 1200 ft.	04:47:05.4	1469	942	2.19	141
Airplane passes through PAPI centerline	04:47:07.4	1416	866	2.10	141
Airplane at IMTOY step-down fix	04:47:09.8	1357	816	2.00	141
CA comments “two miles”	04:47:10.9	1332	781	1.96	141
PAPI displays 3 red lights, 1 white light	04:47:11.1	1325	778	1.95	141
Airplane at MDA (1200 ft. MSL)	04:47:16.0	1200	405	1.74	141
PAPI displays 4 red lights	04:47:17.0	1176	420	1.70	141

Notes:
[1]Indicated altitude; other altitudes are based on accelerometer integration.
[2]Terrain elevation at transformer site; transformer pole ~35 ft. high.
[3]Last sample recorded on FDR; at 04:47:32.7 for radio altitude and calibrated airspeed.

Text color	Event association
Black	Aircraft position or FDR / CVR related event
Blue	CVR communication event
Gold	Security video event
Green	Autopilot-associated event
Red	EGPWS event
Purple	PAPI event

Table 9. Sequence of events during final approach to KBHM runway 18 (page 1 of 2).

Event	Time (CDT)	Altitude, ft. MSL	FDR radio altitude, ft.	Distance north of threshold, nmi	FDR Calibrated airspeed, kts.
Airplane landing lights first become visible on security video (estimated cloud height)	04:47:24.03	1000	272	1.40	142
EGPWS "sink rate" alert	04:47:24.47	989	247	1.38	142
Selected vertical speed = -600 ft./min.	04:47:27	925	154	1.28	141
Crew comments about runway	04:47:27.87	903	152	1.24	141
Landing lights on security video reach peak brightness / clarity	04:47:28.17	896	139	1.228	141
PAPI becomes obscured by terrain	04:47:28.22	895	136	1.226	141
Landing lights on security video start to dim (likely due to obstacles in camera line of sight)	04:47:29.83	862	104	1.16	140
Selected vertical speed = -500 ft./min.	04:47:30	859	96	1.15	140
Autopilot disconnect click on CVR	04:47:31.47	835	83	1.09	140
Sudden dimming of airplane landing lights on security video	04:47:32.10	827	60	1.07	139
Landing lights on security video totally out (likely due to obscuration by terrain in camera's line of sight)	04:47:32.37	823	39	1.055	139
First sound of impact on CVR (contact with tree M2)	04:47:32.47	822	32	1.050	139
End of FDR data (*AccelVert* parameter)	04:47:33.42	812	14[3]	1.012	139[3]
EGPWS "too low terrain" alert	04:47:33.47	812	n/a	1.01	n/a
Transformer flash on security video	04:47:36.10	802[2]	n/a	0.904	n/a
Impact explosion on security video	04:47:40.70	754	n/a	0.77	n/a
End of loudest noise on CVR	04:47:41.27	n/a	n/a	n/a	n/a

Notes:
[1]Indicated altitude; other altitudes are based on accelerometer integration.
[2]Terrain elevation at transformer site; transformer pole ~35 ft. high.
[3]Last sample recorded on FDR; at 04:47:32.7 for radio altitude and calibrated airspeed.

Text color	Event association
Black	Aircraft position or FDR / CVR related event
Blue	CVR communication event
Gold	Security video event
Green	Autopilot-associated event
Red	EGPWS event
Purple	PAPI event

Table 9. Sequence of events during final approach to KBHM runway 18 (page 2 of 2).

As noted in Section D-VII, non-precision approach procedures specify how the airplane is to descend on the final approach course to the Minimum Descent Altitude (MDA), which in this case is 1200 ft. MSL. To descend from the MDA, the crew must have the airport / runway environment in sight, and complete the descent and landing visually. However, the security video analysis described in Section D-VI indicates that the airplane was not below the clouds (and the runway would not have been visible from the cockpit) until about 1000 ft. MSL, 200 ft. below the MDA. This finding is consistent with the crew's reporting the airport in sight at about 900 ft. MSL.

Furthermore, the PAPI visibility analysis described in Section D-VII indicates that when the crew reported the runway in sight at about 900 ft. MSL and about 1.24 nmi north of the threshold, the PAPI would have been visible for less than a second, becoming obscured by terrain almost immediately. Consequently, it is likely that the crew never saw or recognized the PAPI lights, which could have alerted them to the airplane's dangerously low altitude.

The EGPWS "too low terrain" warning on the CVR came 1 second after the "first sound of impact," and so was not able to alert the crew in time for them to take action to avoid descending into the trees. An updated version of the EGPWS software (version -218) would have provided the "too low terrain" 6.5 seconds earlier than that provided by the software version installed on the accident airplane (version -212). Section D-VIII describes engineering simulator tests intended to determine whether this earlier alert would have been timely enough for the crew to have taken action to avoid the accident, considering three different responses to the terrain alert. The result of the simulator tests indicate that the first tree hit by flight 1354 could have been cleared using the following maneuvers:

- An automated go-around maneuver, initiated by activating the TOGA switches within 0.6 seconds of the "too low terrain" warning provided by the EGPWS -218 software;

- A manual terrain-avoidance maneuver, initiated within 2.4 seconds of the "too low terrain" warning provided by the EGPWS -218 software.

The simulator tests indicated that the tree could not have been cleared simply by changing the selected vertical speed from a 1500 ft./min. descent to a 500 ft./min. climb, since this action would have to be initiated 0.7 seconds *before* the "too low terrain" warning provided by the EGPWS -218 software.

It is beyond the scope of this *Study* to consider whether reaction times of 0.6 to 2.4 seconds are feasible or reasonable, or whether TOGA activation or a manual terrain-avoidance maneuver are expected responses to a "too low terrain" warning.

_____

John O'Callaghan
National Resource Specialist – Aircraft Performance
Office of Research and Engineering

F. REFERENCES

1. *A300-600 General Freighter, Data Basis for Design*, Airbus document # EGLCL1 D03001860, Issue 2.0, November 28, 2003, p. I-1. (Airbus Proprietary document).

2. National Transportation Safety Board, Office of Aviation Safety, *Operations Group Chairman's Factual Report,, Airbus A300-600, registration N155UP, Birmingham, AL, August 14, 2013.* NTSB Accident Number DCA13MA133, Docket Item 7 (Washington, DC: NTSB, January 31, 2014). (Contact NTSB at pubinq@ntsb.gov).

3. National Transportation Safety Board, Office of Research and Engineering, *Flight Data Recorder Group Chairman's Factual Report, Airbus A300-600, registration N155UP, Birmingham, AL, August 14, 2013.* NTSB Accident Number DCA13MA133, Docket Item 19 (Washington, DC: NTSB, January 29, 2014). (Contact NTSB at pubinq@ntsb.gov).

4. National Transportation Safety Board, Office of Research and Engineering, *Cockpit Voice Recorder Group Chairman's Factual Report, Airbus A300-600, registration N155UP, Birmingham, AL, August 14, 2013.* NTSB Accident Number DCA13MA133, Docket Item 70 (Washington, DC: NTSB, January 28, 2014). (Contact NTSB at pubinq@ntsb.gov).

5. National Transportation Safety Board, Office of Research and Engineering, *Group Chairman's Aircraft Performance Study, American Airlines Flight 587, Airbus A300B4-605R, Belle Harbor, New York, November 12, 2001*, NTSB Accident Number DCA02MA001, Docket Item 188 (Washington, DC: NTSB, October 10, 2002). (Contact NTSB at pubinq@ntsb.gov).

6. National Transportation Safety Board, Office of Aviation Safety, *Systems Group Chairman's Factual Report, Airbus A300-600, registration N155UP, Birmingham, AL, August 14, 2013.* NTSB Accident Number DCA13MA133, Docket Item 92 (Washington, DC: NTSB, February 5, 2014). (Contact NTSB at pubinq@ntsb.gov).

7. National Transportation Safety Board, Office of Aviation Safety, *Meteorology Group Chairman's Factual Report, Airbus A300-600, registration N155UP, Birmingham, AL, August 14, 2013.* NTSB Accident Number DCA13MA133, Docket Item 79 (Washington, DC: NTSB, February 6, 2014). (Contact NTSB at pubinq@ntsb.gov).

8. Federal Aviation Administration, *Aeronautical Information Manual*, February 9, 2012. Available at http://www.faa.gov/air_traffic/publications/ATpubs/AIM/index.htm.

9. Federal Aviation Administration, *Advisory Circular 150/5340-30G: Design and Installation Details for Airport Visual Aids*, September 21, 2012. Available at http://www.faa.gov/regulations_policies/advisory_circulars/index.cfm/go/document.information/documentID/1020353

10. Federal Aviation Administration, *Technical Performance Record: Precision Approach Path Indicator (PAPI), ID: BXO PAPI, Birmingham AL.* Obtained from KBHM airport authorities.

11. National Transportation Safety Board, Office of Aviation Safety, *Survival Factors Group Chairman's Factual Report, Airbus A300-600, registration N155UP, Birmingham, AL, August 14, 2013.* NTSB Accident Number DCA13MA133, Docket Item 45 (Washington, DC: NTSB, January 23, 2014). (Contact NTSB at pubinq@ntsb.gov).

G. GLOSSARY OF SYMBOLS AND ACRONYMS

English characters

$\vec{a}$	Acceleration vector
AGL	Above Ground Level
ASR	Airport Surveillance Radar
BHM	Birmingham ASR
CA	Captain
CDT	Central Daylight Time
CG	Center of Gravity
CVR	Cockpit Voice Recorder
C_Y	Side-force coefficient
EGPWS	Enhanced Ground Proximity Warning System
FAA	Federal Aviation Administration
FAF	Final Approach Fix
FBI	Federal Bureau of Investigation
FDR	Flight Data Recorder
FO	First Officer
g	Acceleration due to gravity (32.17 ft/s^2)
GPS	Global Positioning System
h	Altitude or height above the ground
KBHM	Birmingham-Shuttlesworth International Airport, Birmingham, Alabama
MAC	Mean Aerodynamic Chord
MDA	Minimum Descent Altitude
MSL	Mean Sea Level
$\vec{n}$	Load factor vector
nlf	Normal load factor = $-n_z$
NTSB	National Transportation Safety Board
P	Body-axis roll rate
Q	Body-axis pitch rate
R	Body-axis yaw rate or rolling moment (dependent on context)
S	Wing area
SRN	Subframe Reference Number
SRTM	Shuttle Radar Topography Mission
t	Time
u	Velocity component along x-body axis
USGS	United States Geological Survey
UTC	Universal Coordinated Time
v	Velocity component along y-body axis
V	Total velocity (inertial speed or airspeed dependent on context)
$\vec{V}$	Velocity vector (inertial speed or airspeed dependent on context)
V/S	Vertical speed (rate of climb)
w	Velocity component along z-body axis
W	Airplane weight = mg
x	x-coordinate (axis system dependent on context)
y	y-coordinate (axis system dependent on context)
Y	Side-force
z	z-coordinate (axis system dependent on context)

Greek characters

α	Angle of attack
β	Sideslip angle
γ	Flight path angle
θ	Pitch angle
ϕ	Roll angle
ψ	Heading or track angle (magnetic or true dependent on context)
ρ	Air density

FIGURES

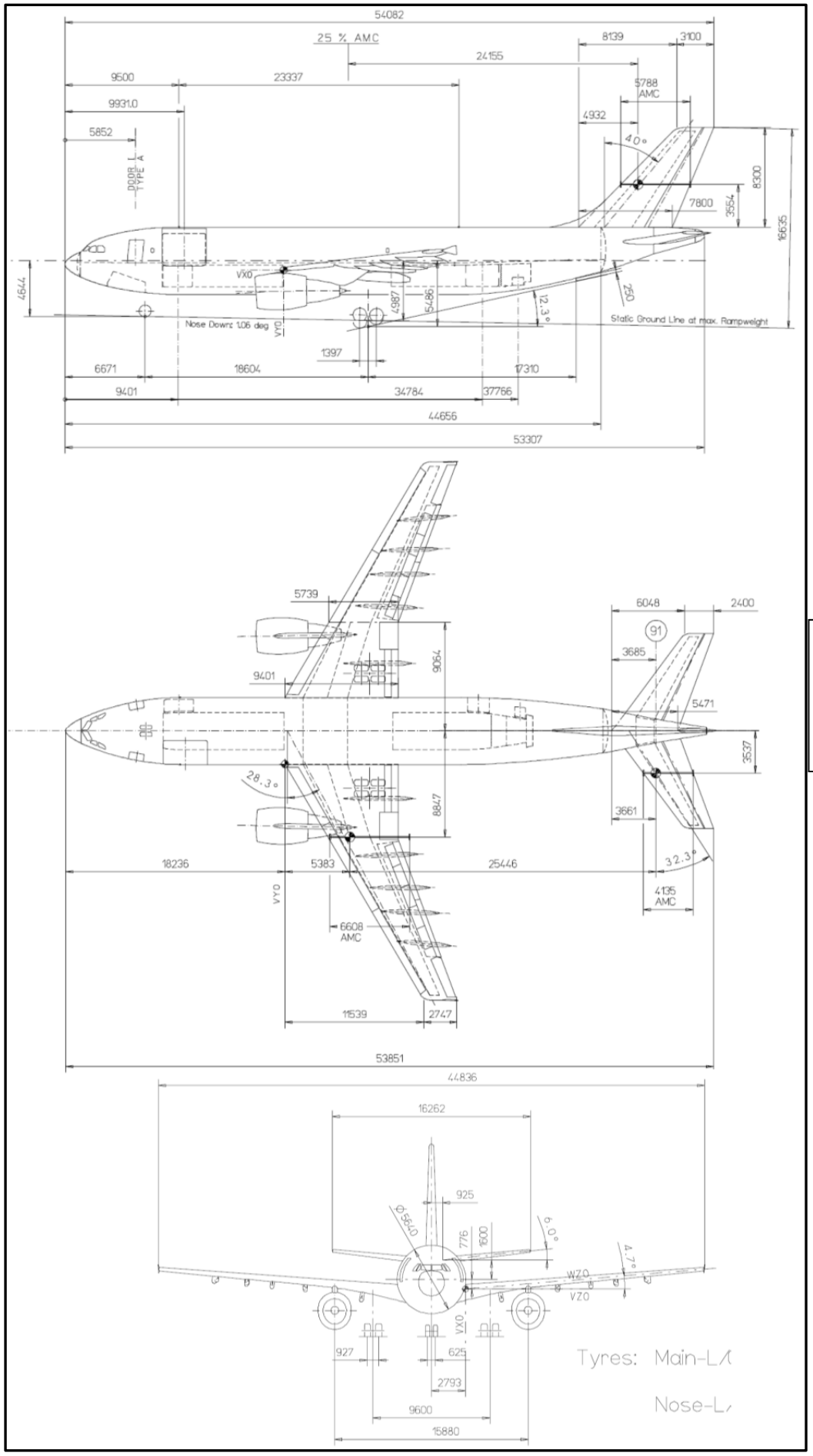

Figure 1:
3-view of the A300 F4-622R airplane (from Ref. 1). Dimensions in mm.

DCA13MA133: UPS flight 1354, Airbus A300-600, KBHM 08/14/2013

Plan view of accident scene items surveyed by ACPG

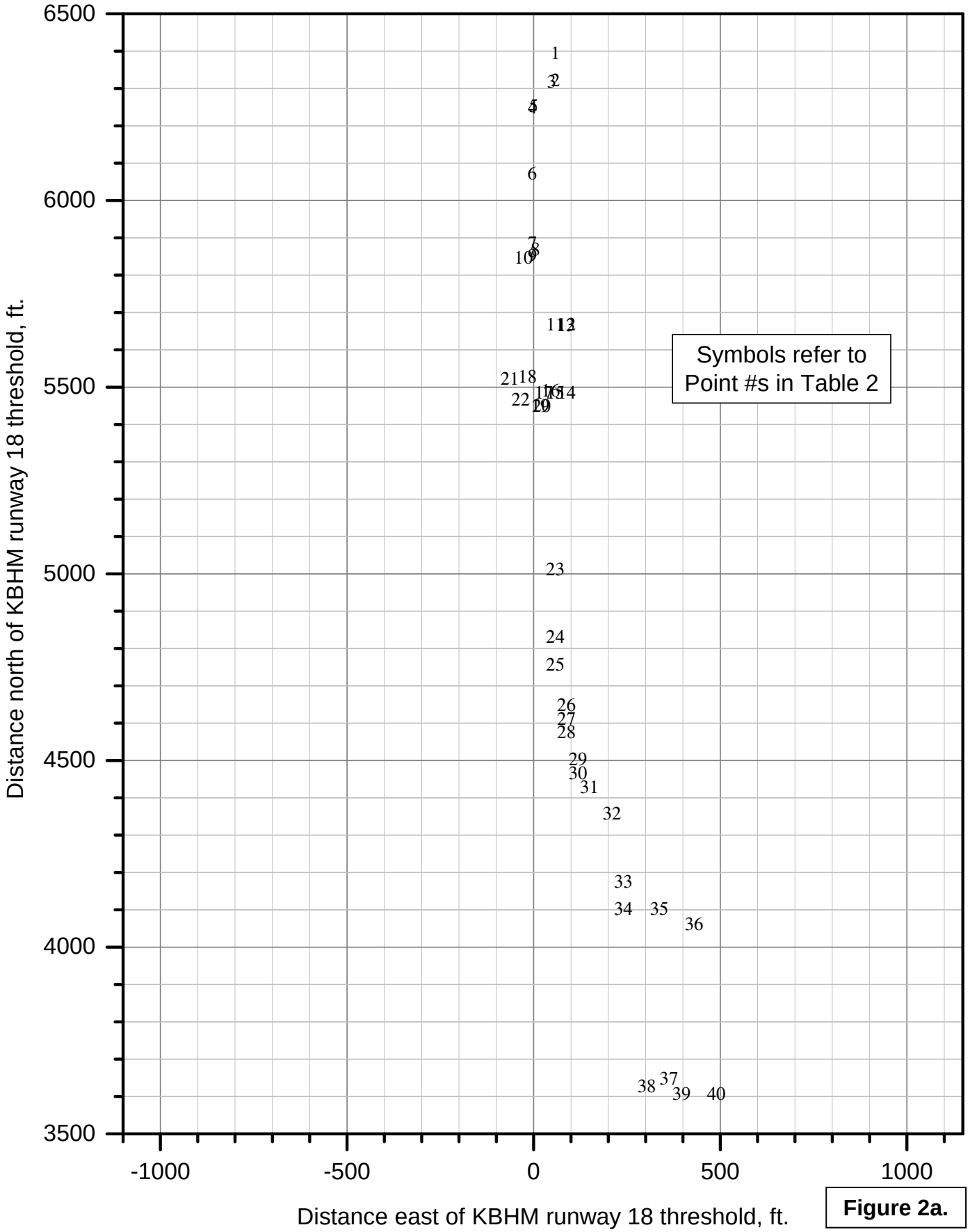

Figure 2a.

DCA13MA133: UPS flight 1354, Airbus A300-600, KBHM 08/14/2013
Plan view of accident scene items surveyed by ACPG

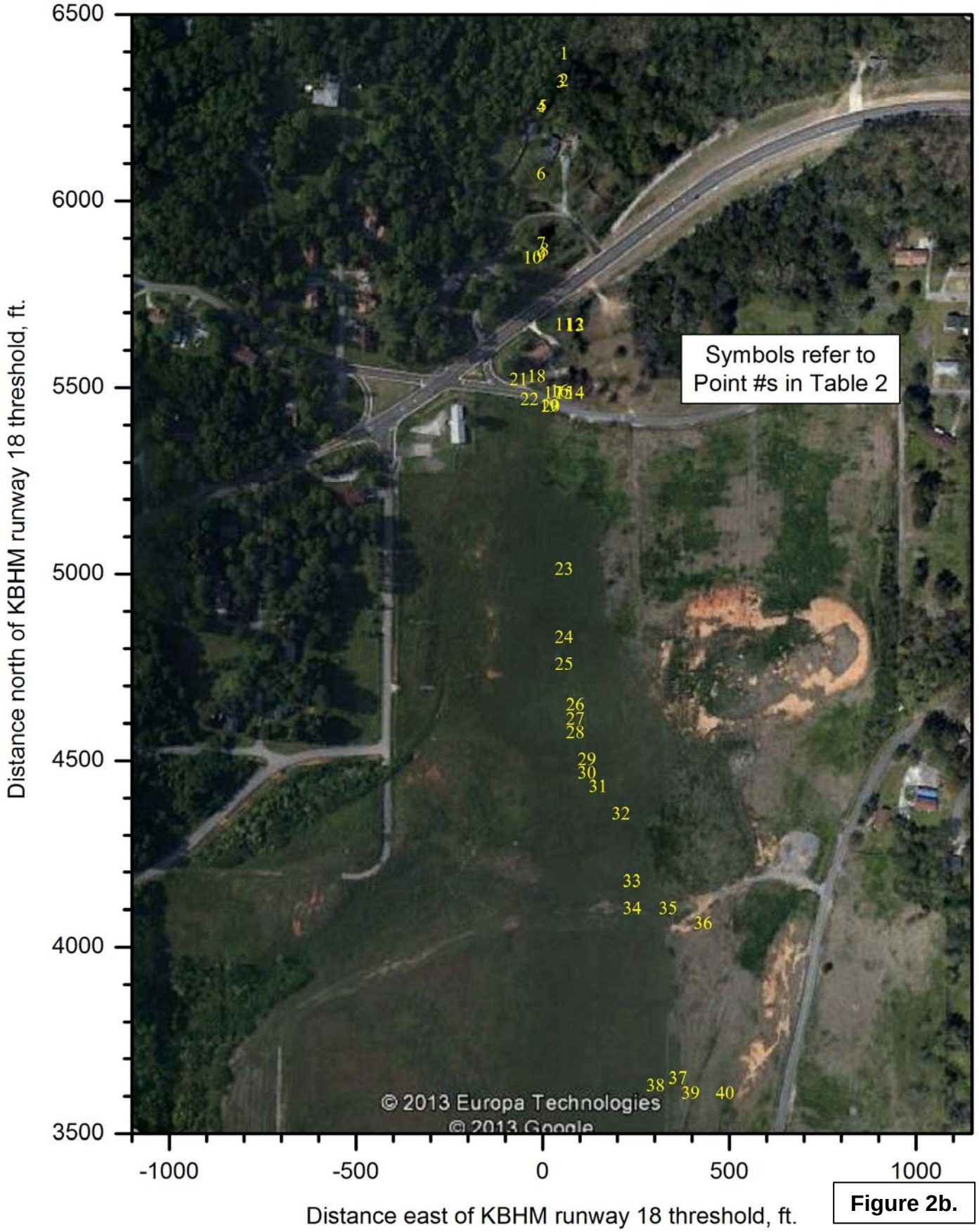

Figure 2b.

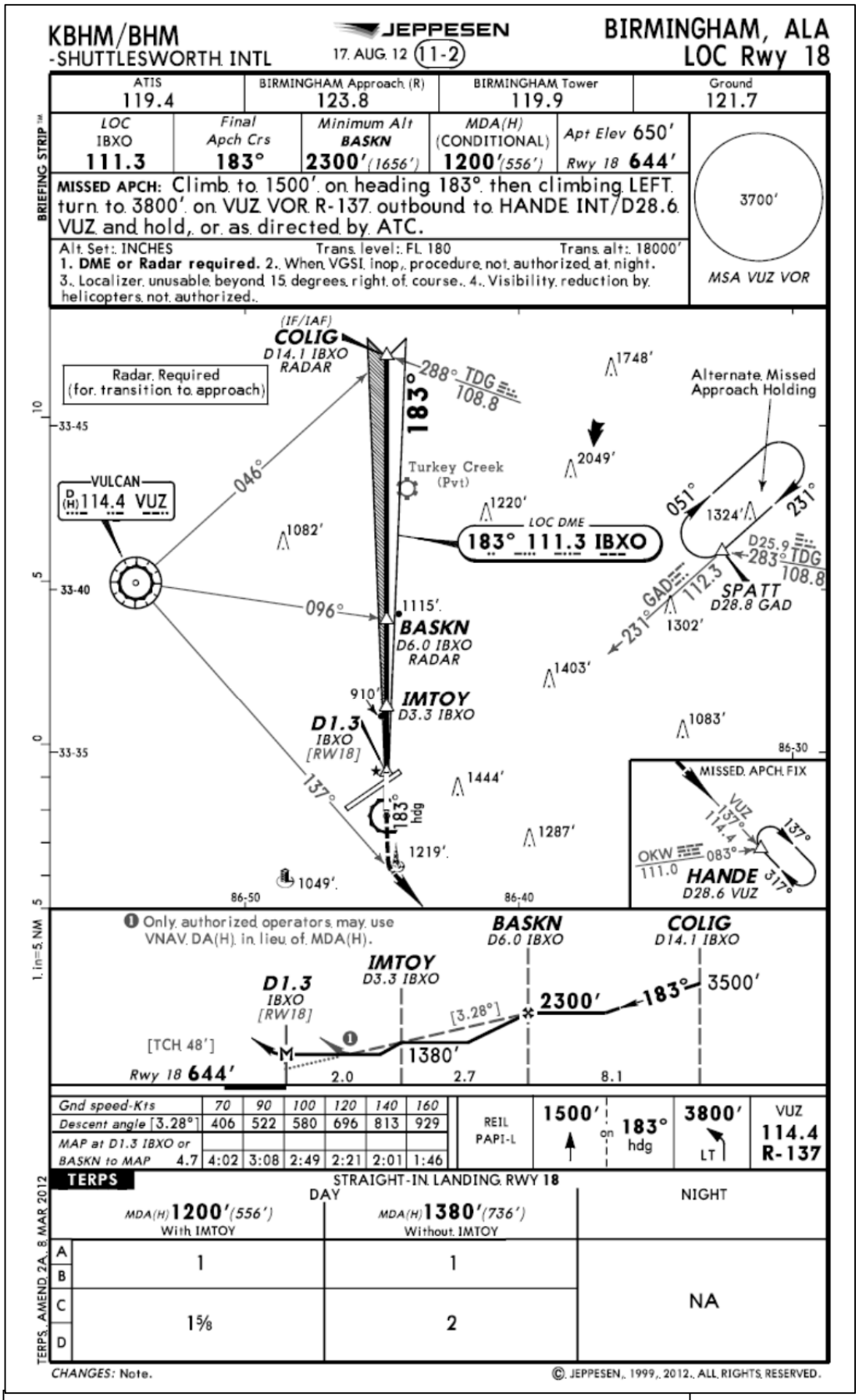

Figure 3. Approach plate for KBHM LOC RWY 18.

DCA13MA133: UPS flight 1354, Airbus A300-600, KBHM 08/14/2013

Plan view of approach to KBHM runway 18

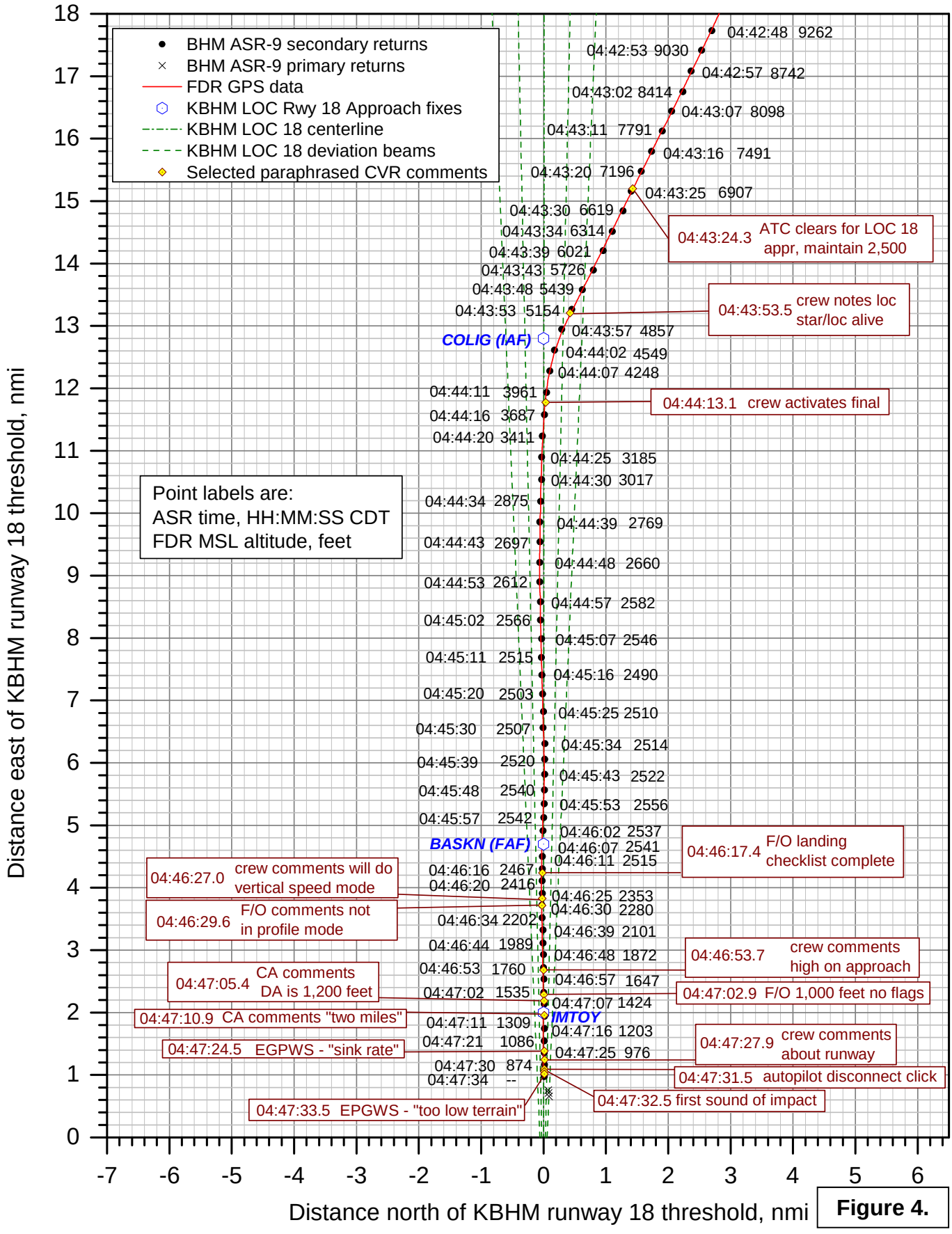

Figure 4.

DCA13MA133: UPS flight 1354, Airbus A300-600, KBHM 08/14/2013
MSL altitude vs. time during approach to KBHM runway 18

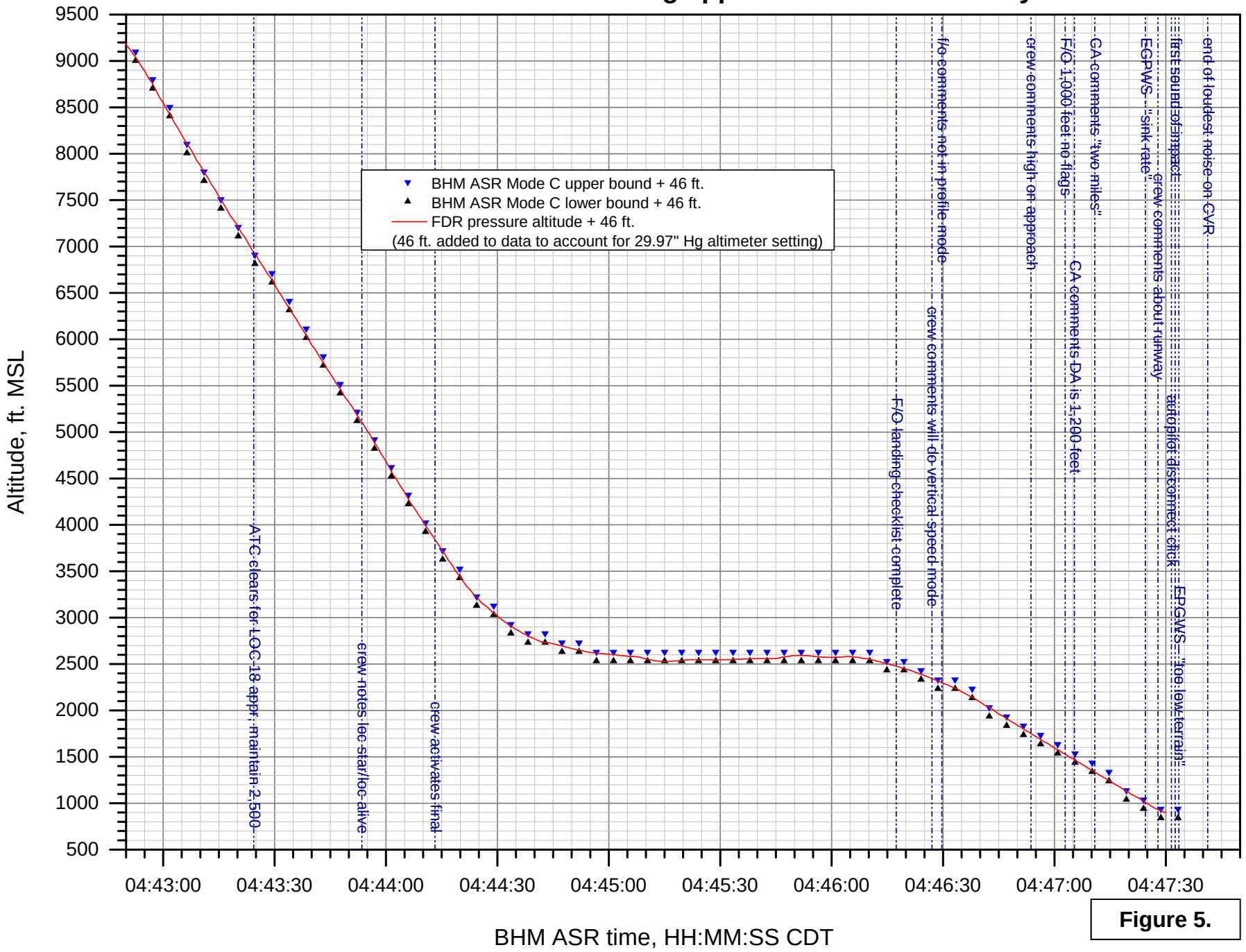

Figure 5.

DCA13MA133: UPS flight 1354, Airbus A300-600, KBHM 08/14/2013
Distance north of threshold vs. time during approach to KBHM runway 18

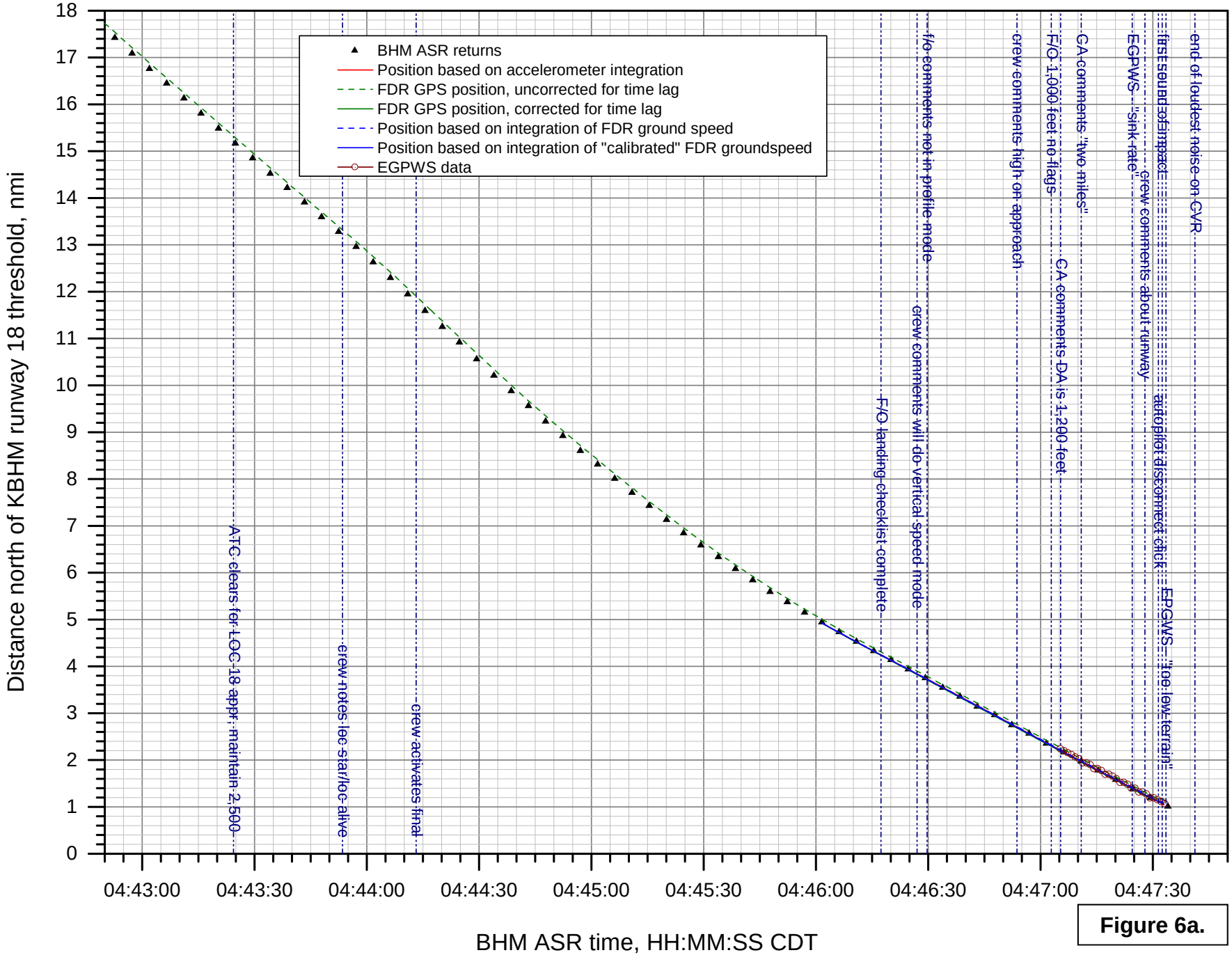

Figure 6a.

DCA13MA133: UPS flight 1354, Airbus A300-600, KBHM 08/14/2013
Distance north of threshold vs. time during approach to KBHM runway 18 (detail 1)

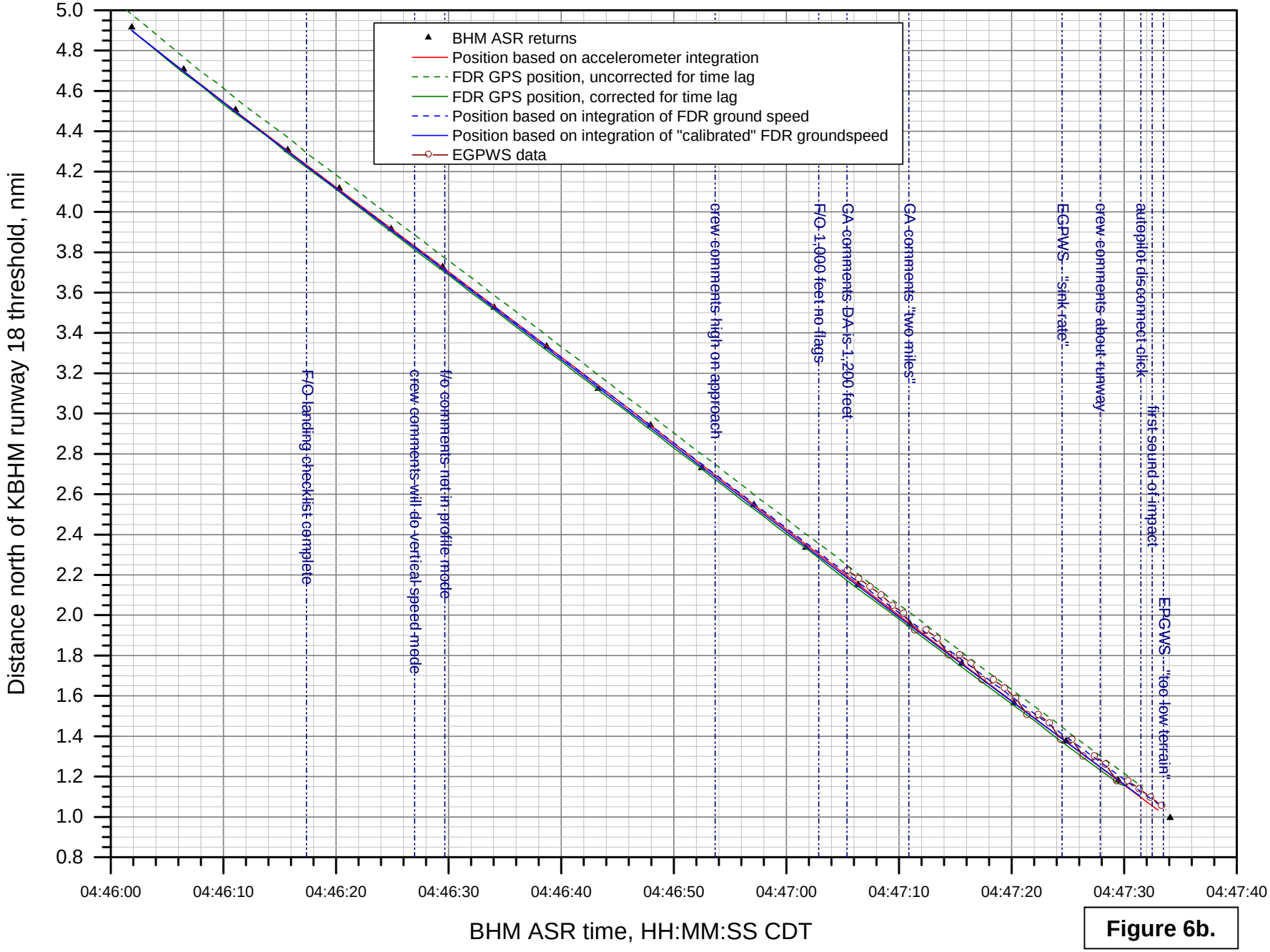

Figure 6b.

DCA13MA133: UPS flight 1354, Airbus A300-600, KBHM 08/14/2013
Distance north of threshold vs. time during approach to KBHM runway 18 (detail 2)

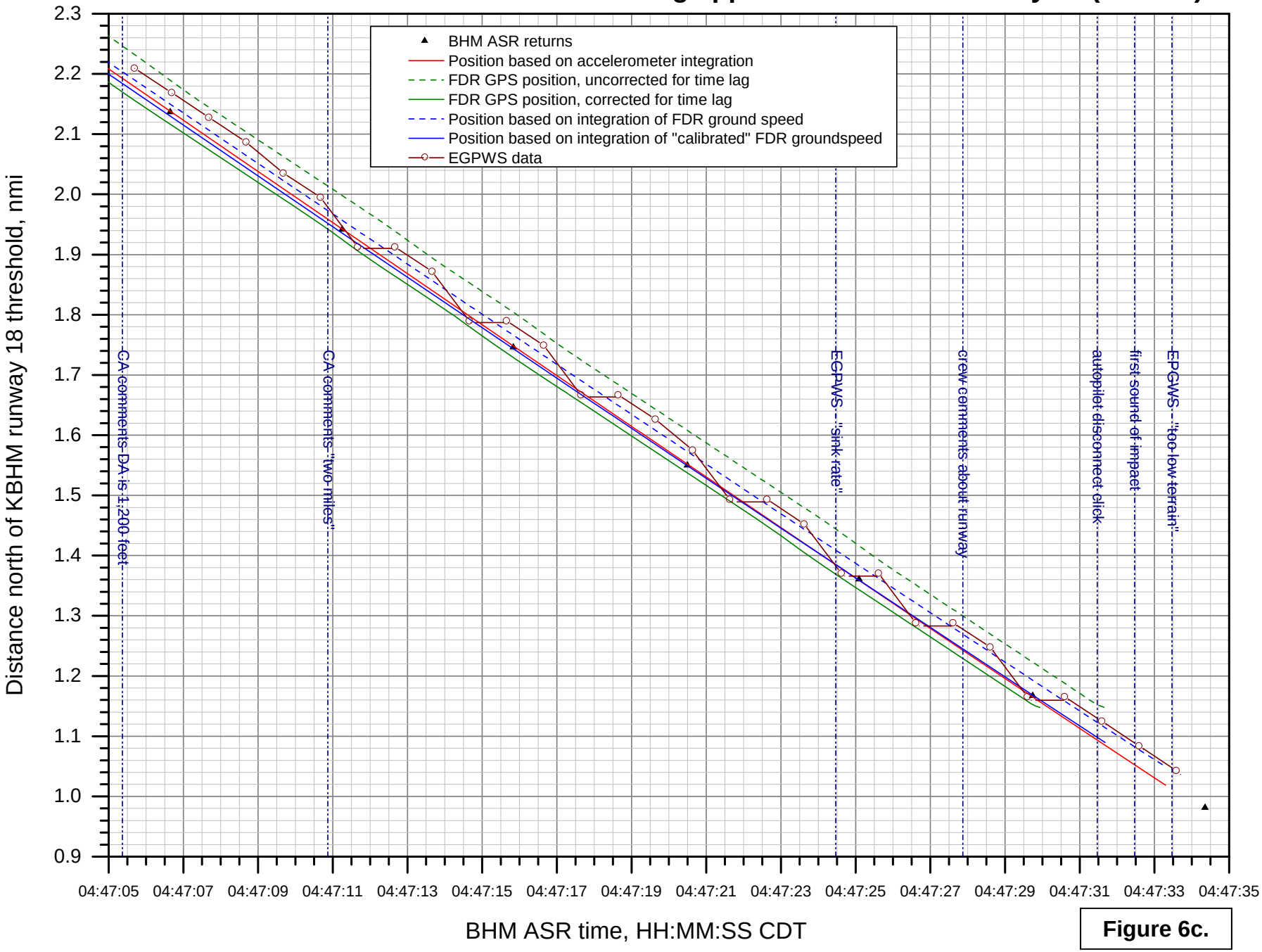

Figure 6c.

DCA13MA133: UPS flight 1354, Airbus A300-600, KBHM 08/14/2013
Profile view of approach to KBHM runway 18

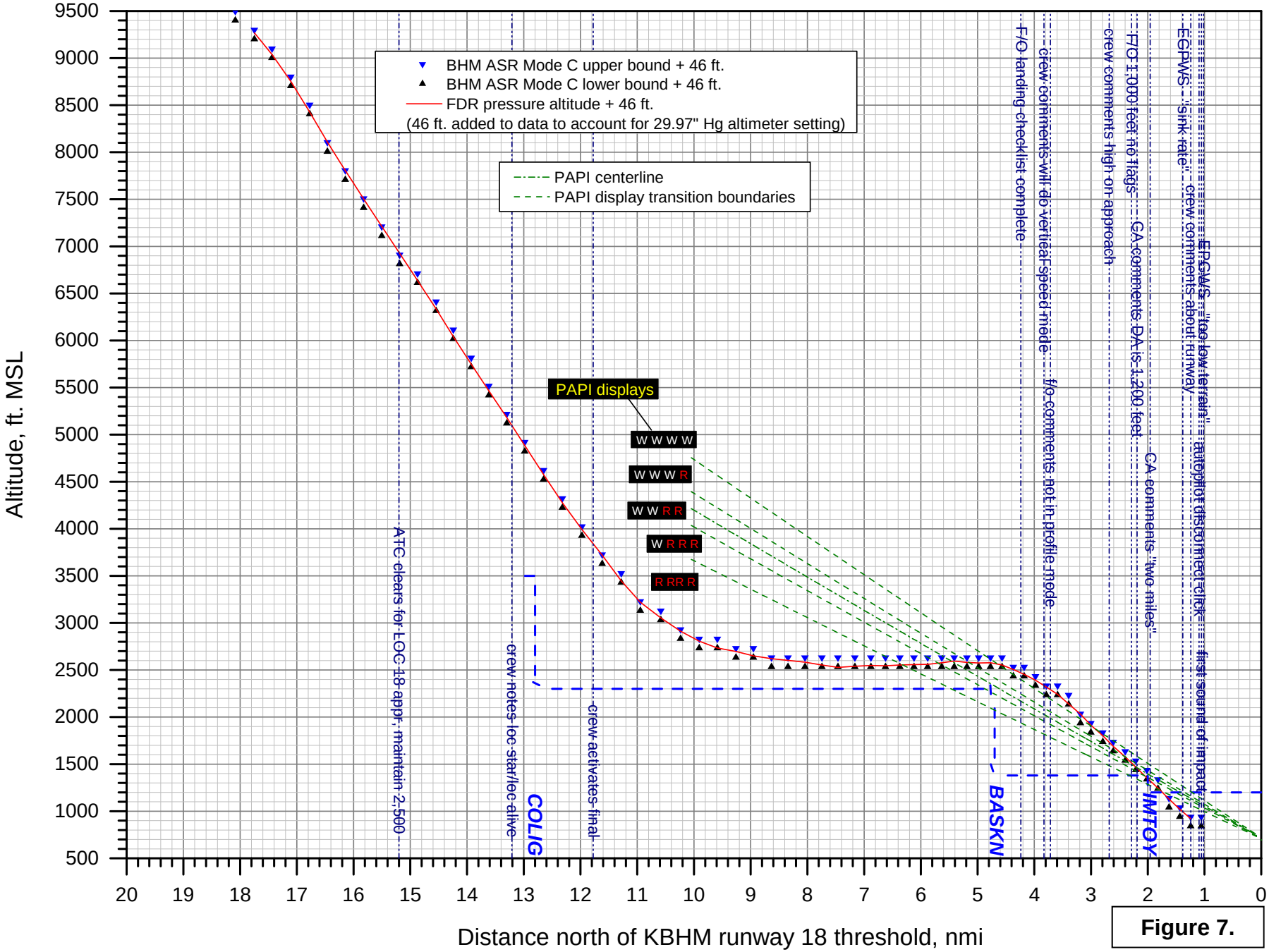

Figure 7.

DCA13MA133: UPS flight 1354, Airbus A300-600, KBHM 08/14/2013
MSL altitude vs. time

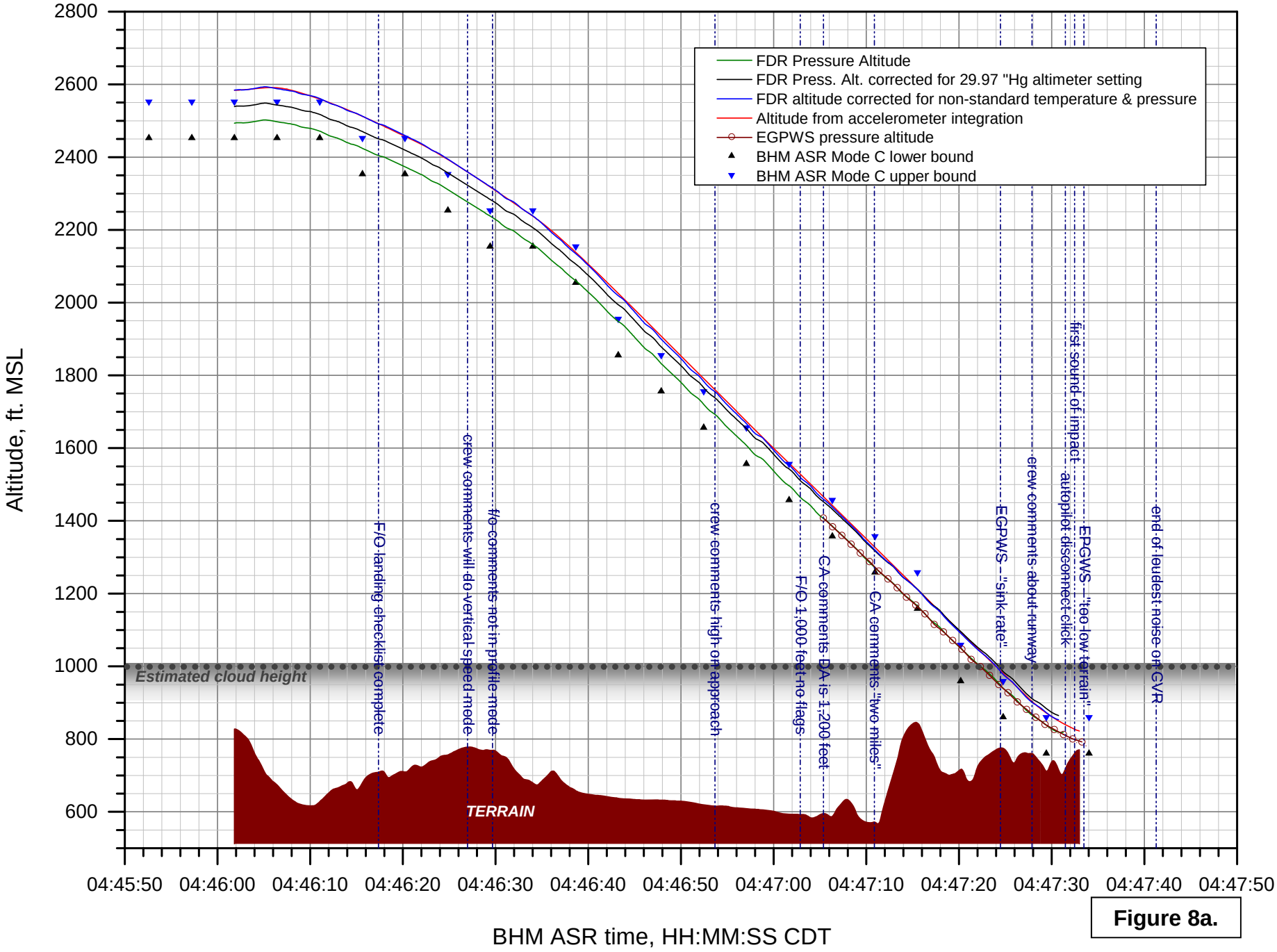

Figure 8a.

DCA13MA133: UPS flight 1354, Airbus A300-600, KBHM 08/14/2013
MSL altitude vs. time (detail)

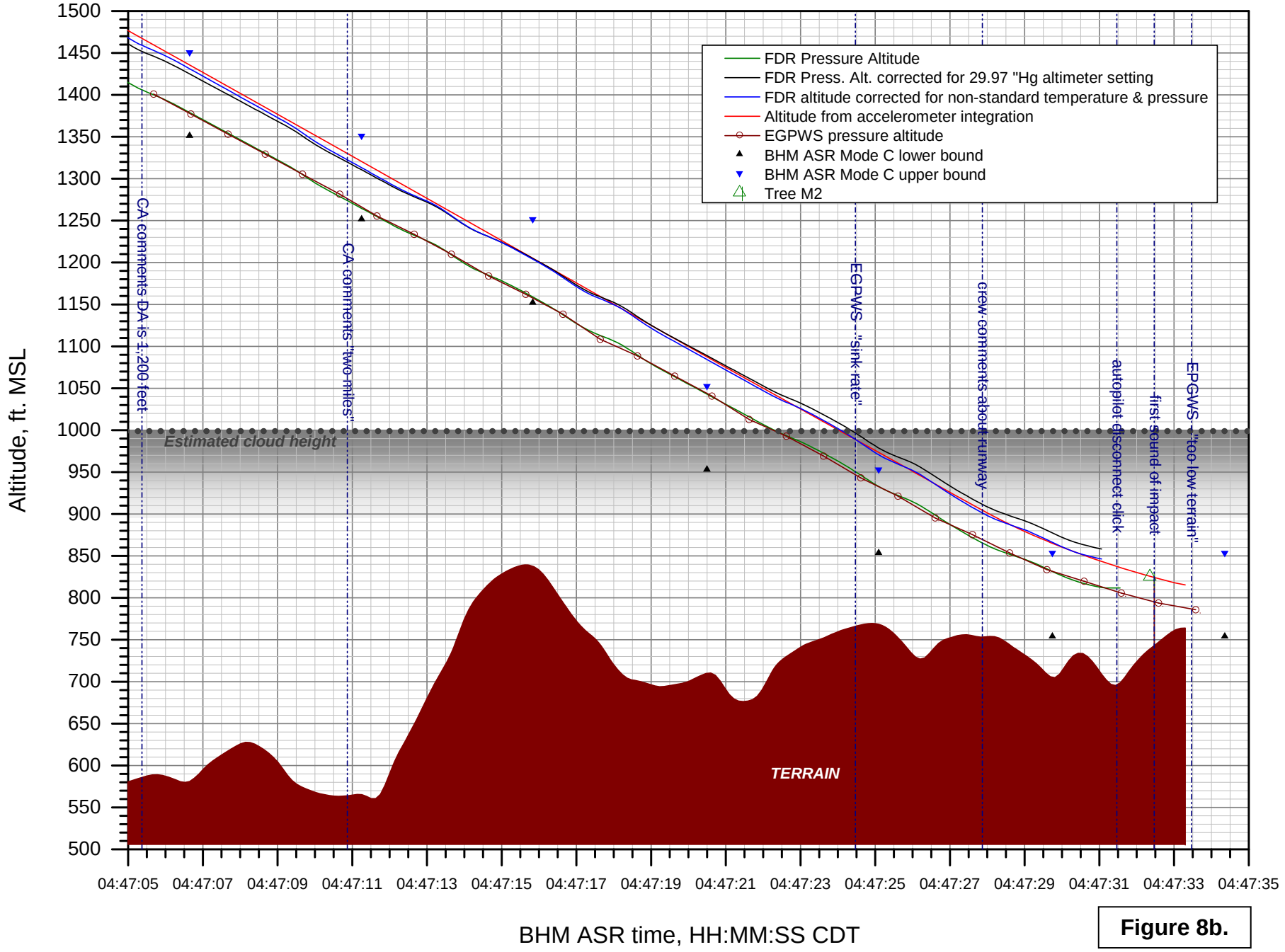

Figure 8b.

DCA13MA133: UPS flight 1354, Airbus A300-600, KBHM 08/14/2013
MSL altitude vs. distance north of threshold

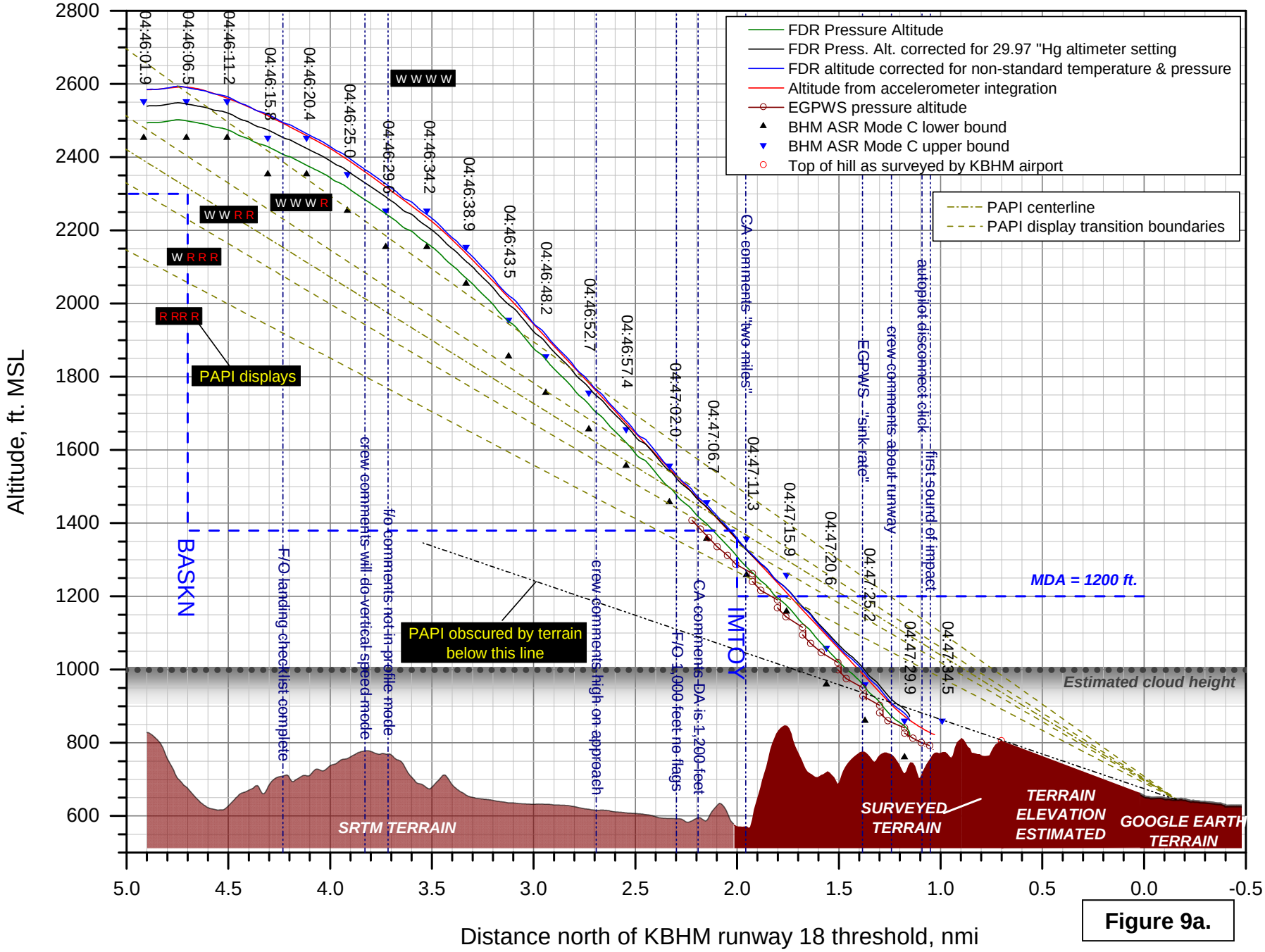

Figure 9a.

DCA13MA133: UPS flight 1354, Airbus A300-600, KBHM 08/14/2013
MSL altitude vs. distance north of threshold (detail)

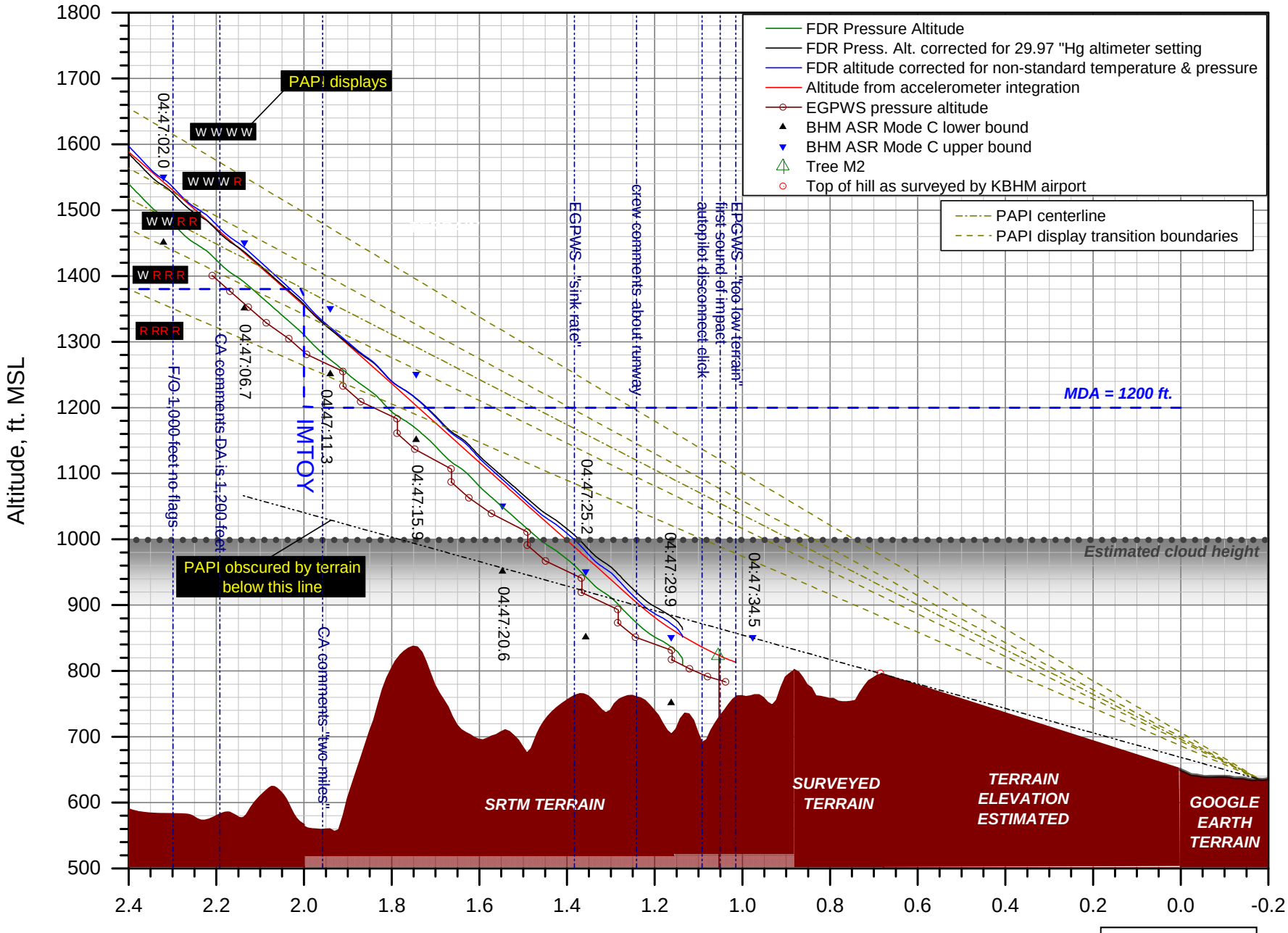

Figure 9b.

DCA13MA133: UPS flight 1354, Airbus A300-600, KBHM 08/14/2013
AGL altitude vs. time

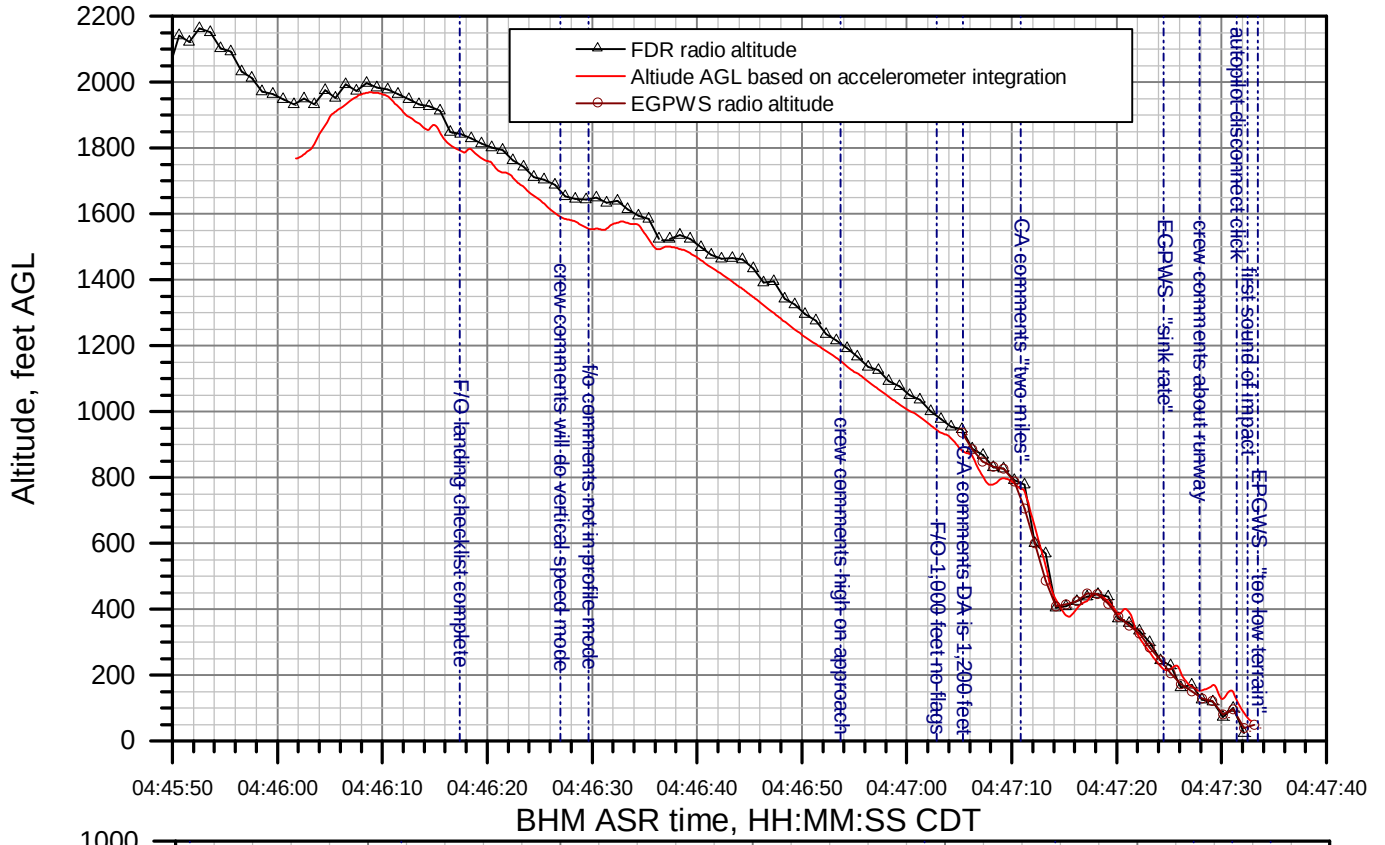

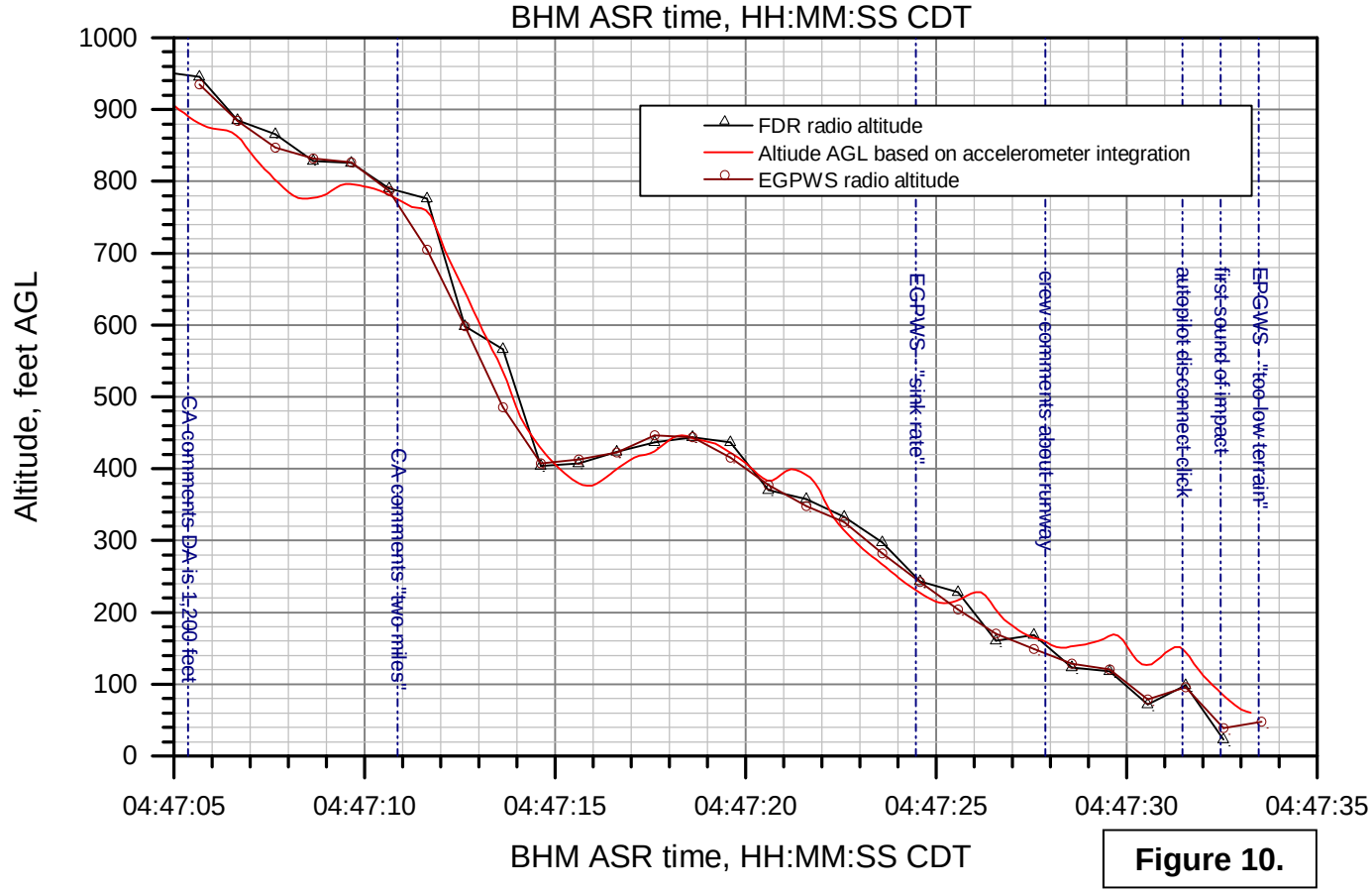

Figure 10.

DCA13MA133: UPS flight 1354, Airbus A300-600, KBHM 08/14/2013
AGL altitude vs. distance north of threshold

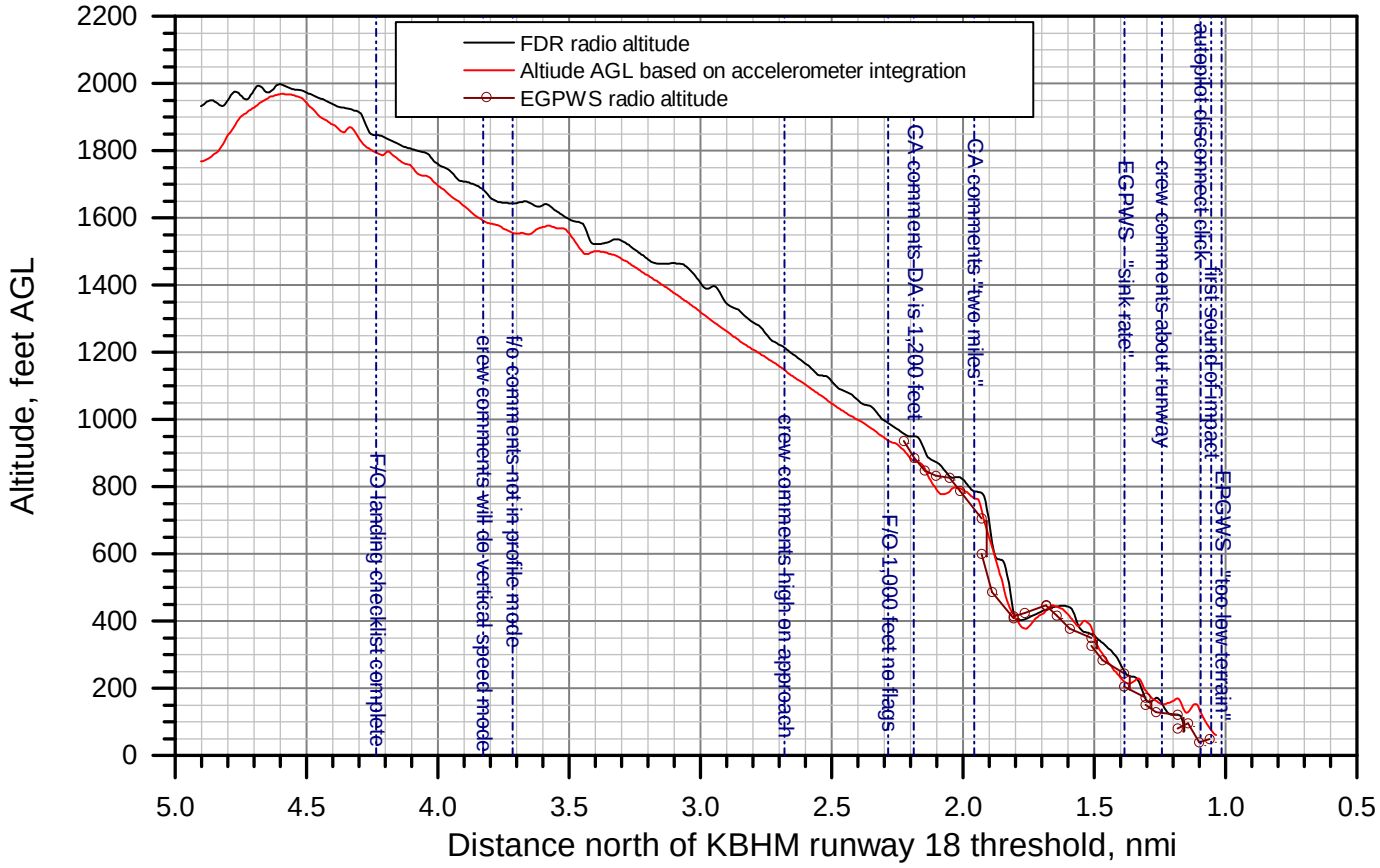

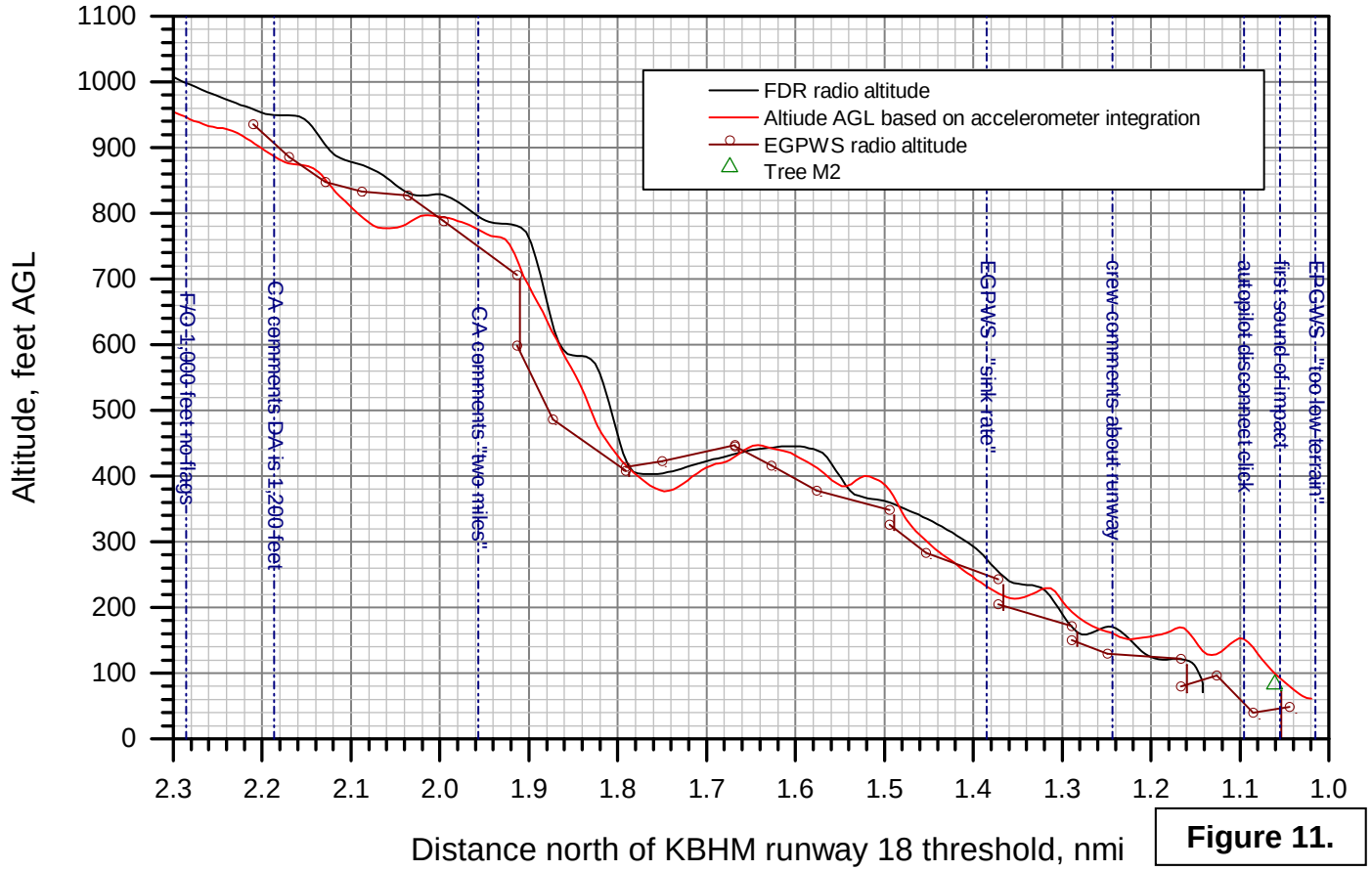

Figure 11.

DCA13MA133: UPS flight 1354, Airbus A300-600, KBHM 08/14/2013
Speed and rate of climb vs. time

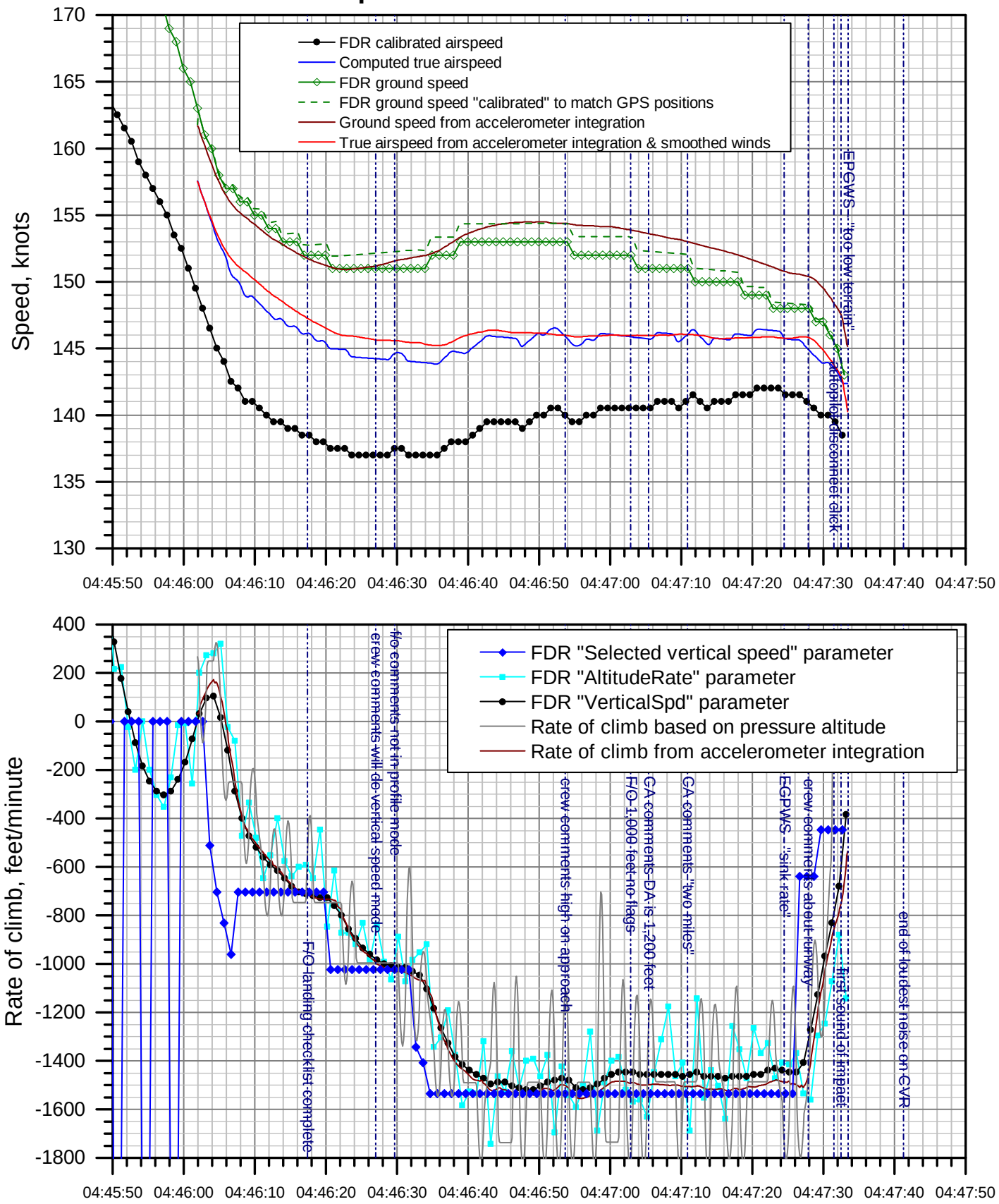

Figure 12a.

DCA13MA133: UPS flight 1354, Airbus A300-600, KBHM 08/14/2013

Speed and rate of climb vs. time (detail)

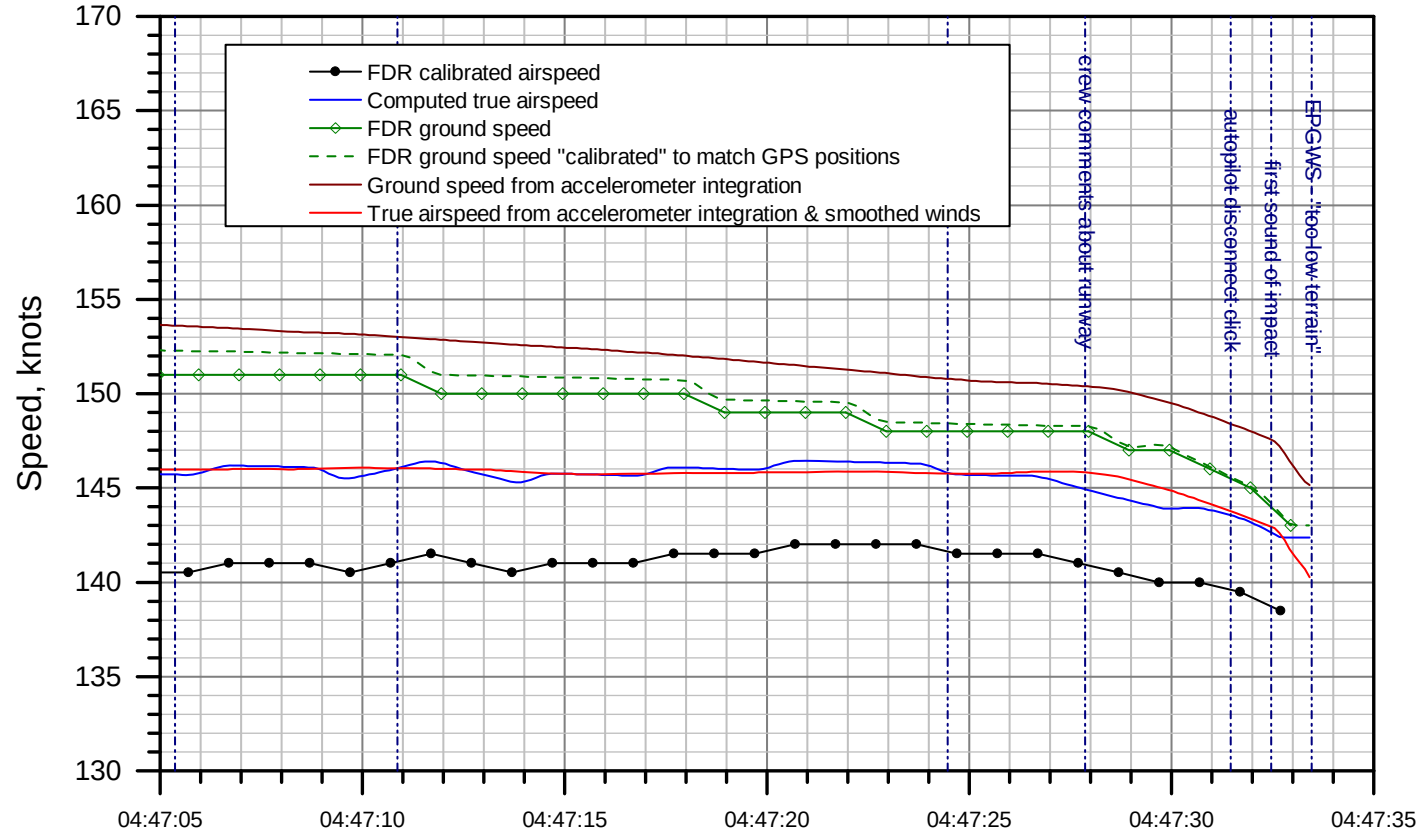

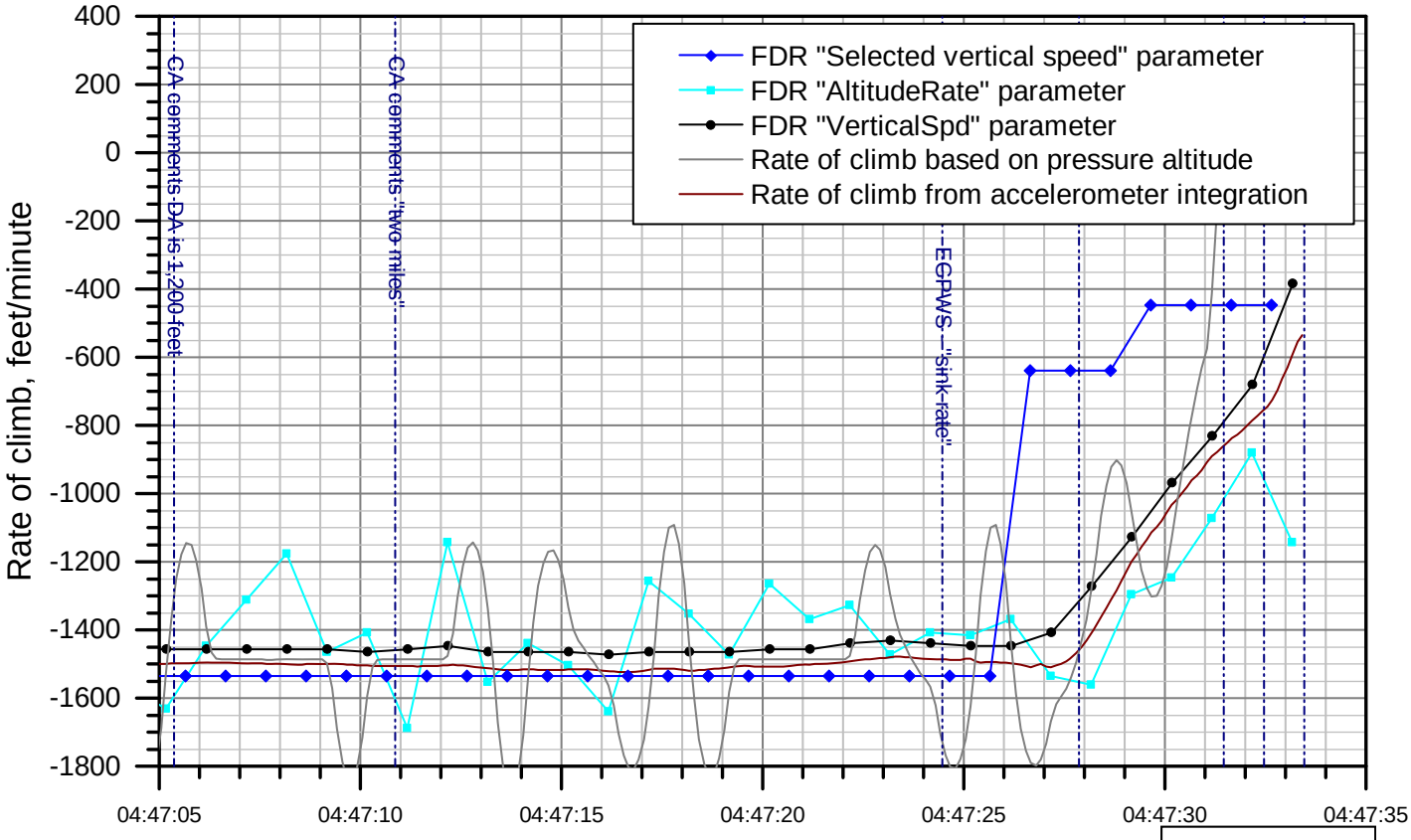

Figure 12b.

DCA13MA133: UPS flight 1354, Airbus A300-600, KBHM 08/14/2013
Winds and temperatures vs. time

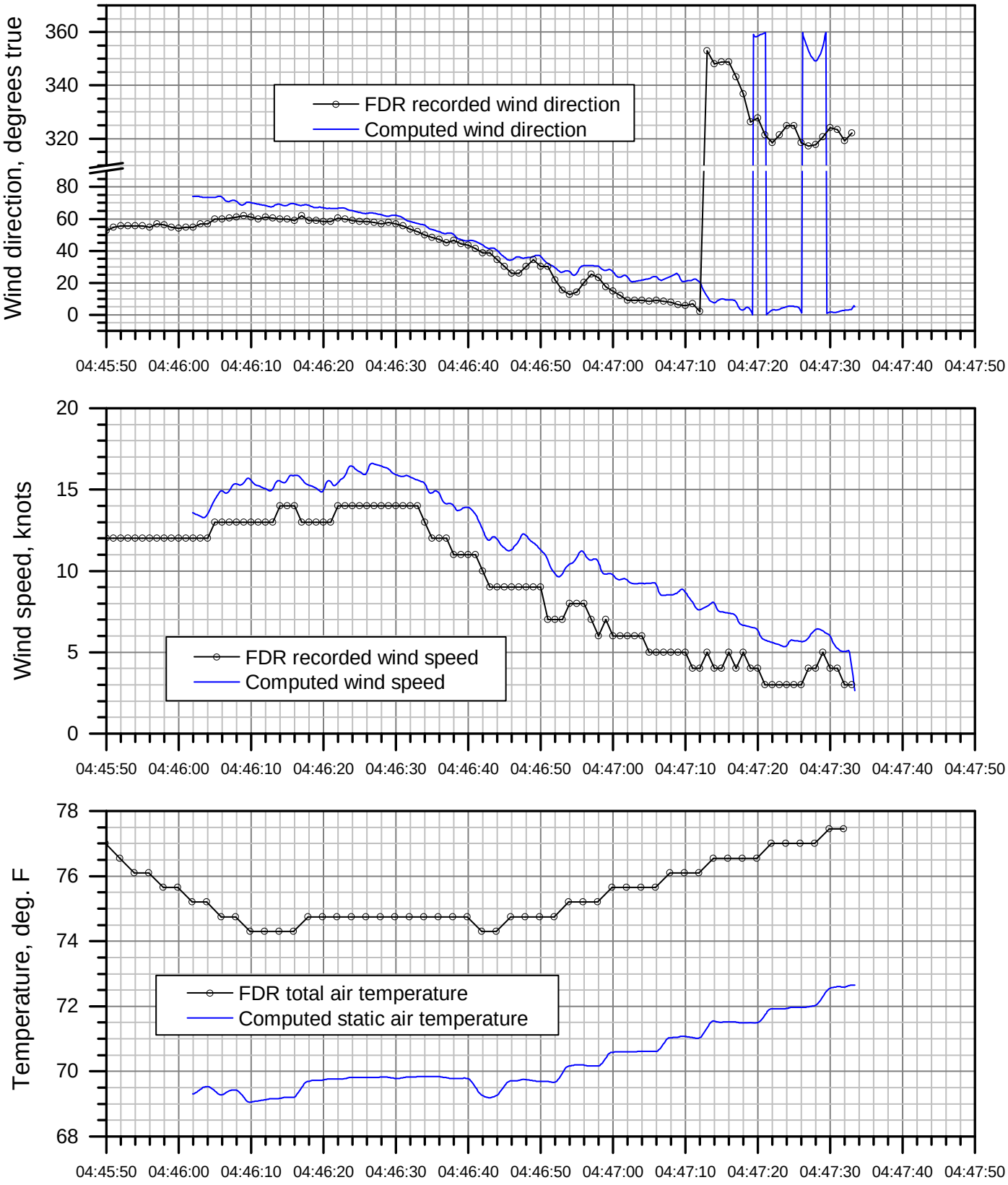

Figure 13.

DCA13MA133: UPS flight 1354, Airbus A300-600, KBHM 08/14/2013
Time-alignment of EGPWS and FDR parameters (p. 1 of 2)

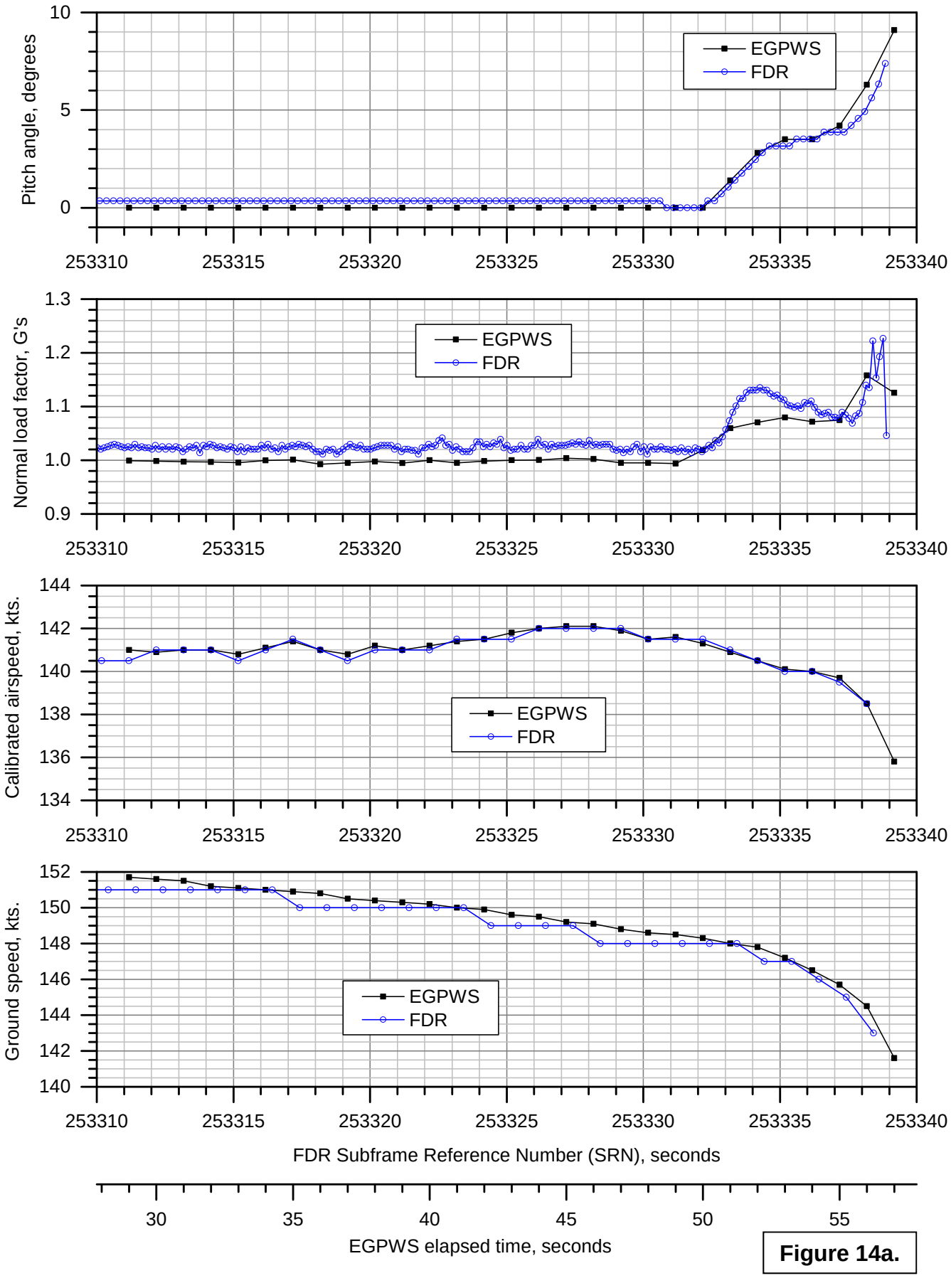

Figure 14a.

DCA13MA133: UPS flight 1354, Airbus A300-600, KBHM 08/14/2013
Time-alignment of EGPWS and FDR parameters (p. 2 of 2)

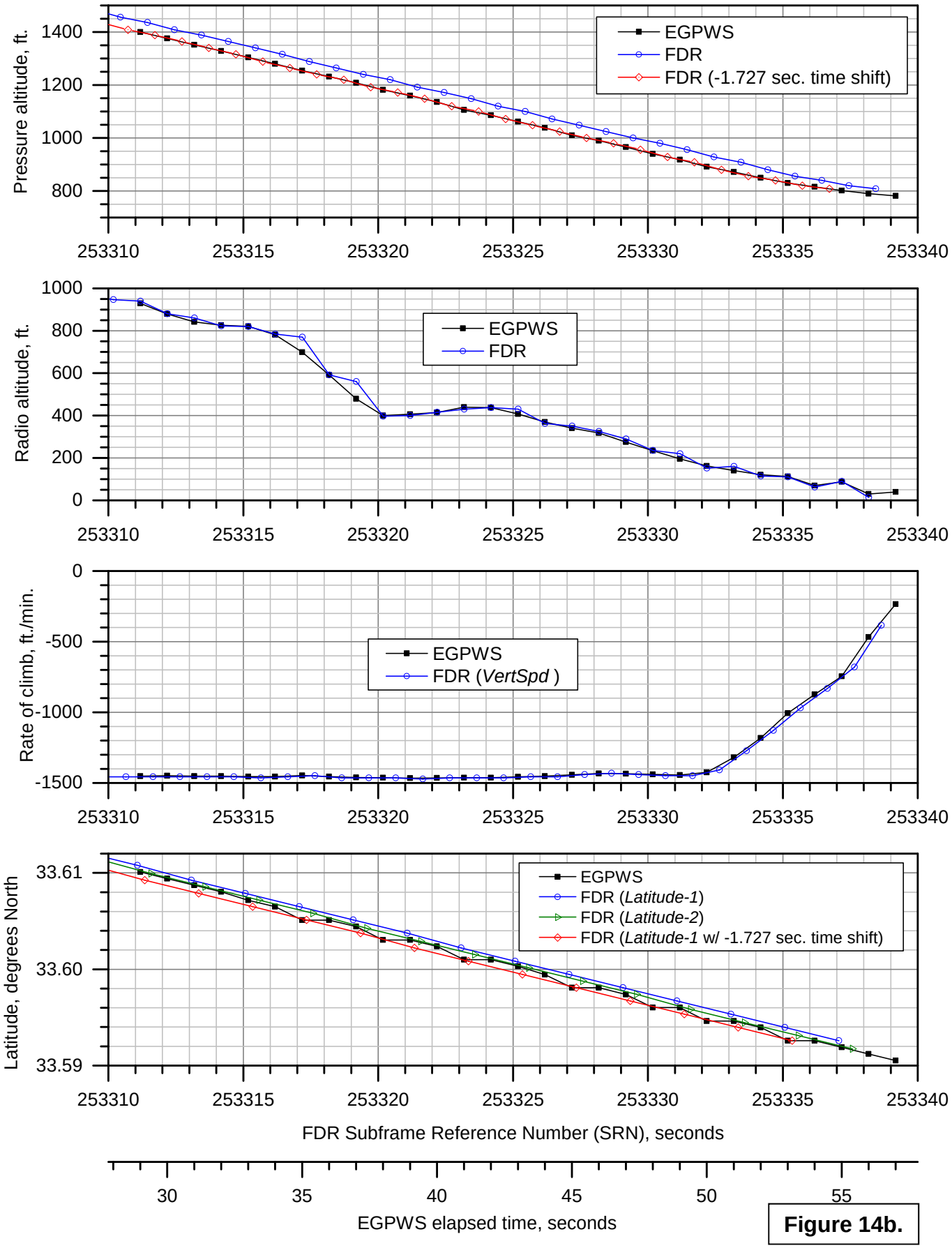

Figure 14b.

DCA13MA133: UPS flight 1354, Airbus A300-600, KBHM 08/14/2013
Computed and recorded AGL altitudes with two time alignments

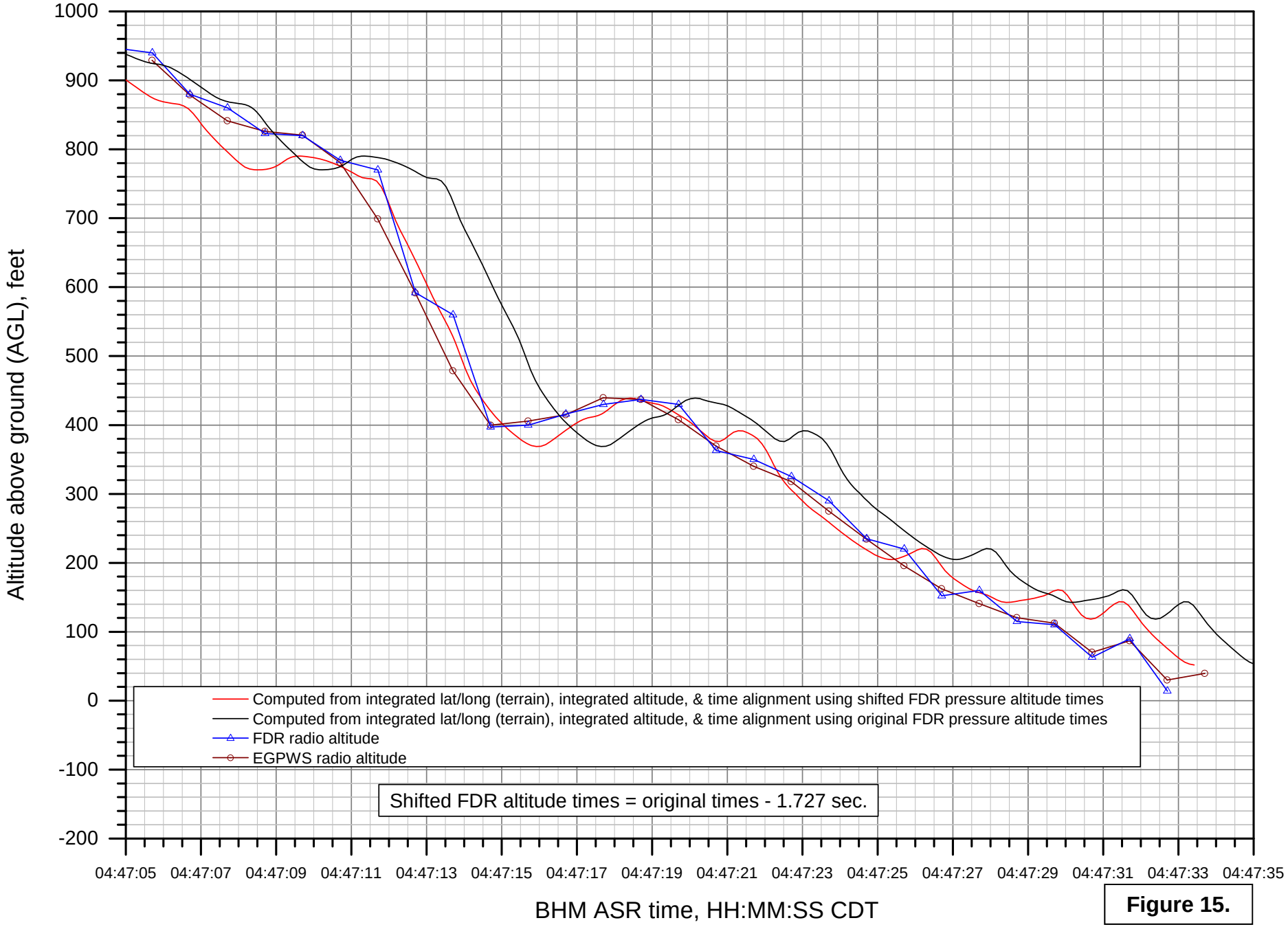

Figure 15.

DCA13MA133: UPS flight 1354, Airbus A300-600, KBHM 08/14/2013
Euler and aerodynamic angles vs. time

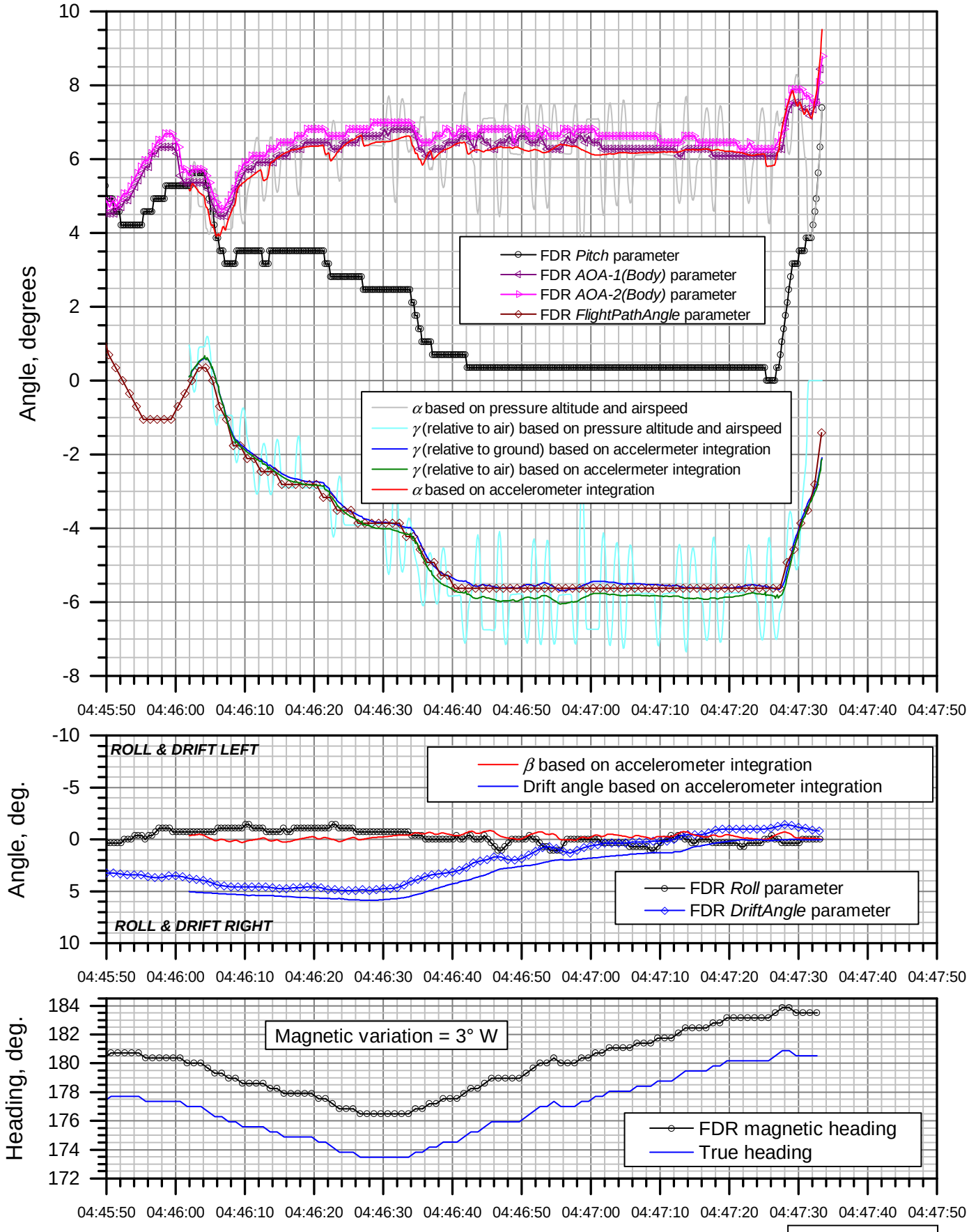

Figure 16a.

DCA13MA133: UPS flight 1354, Airbus A300-600, KBHM 08/14/2013
Euler and aerodynamic angles vs. time (detail)

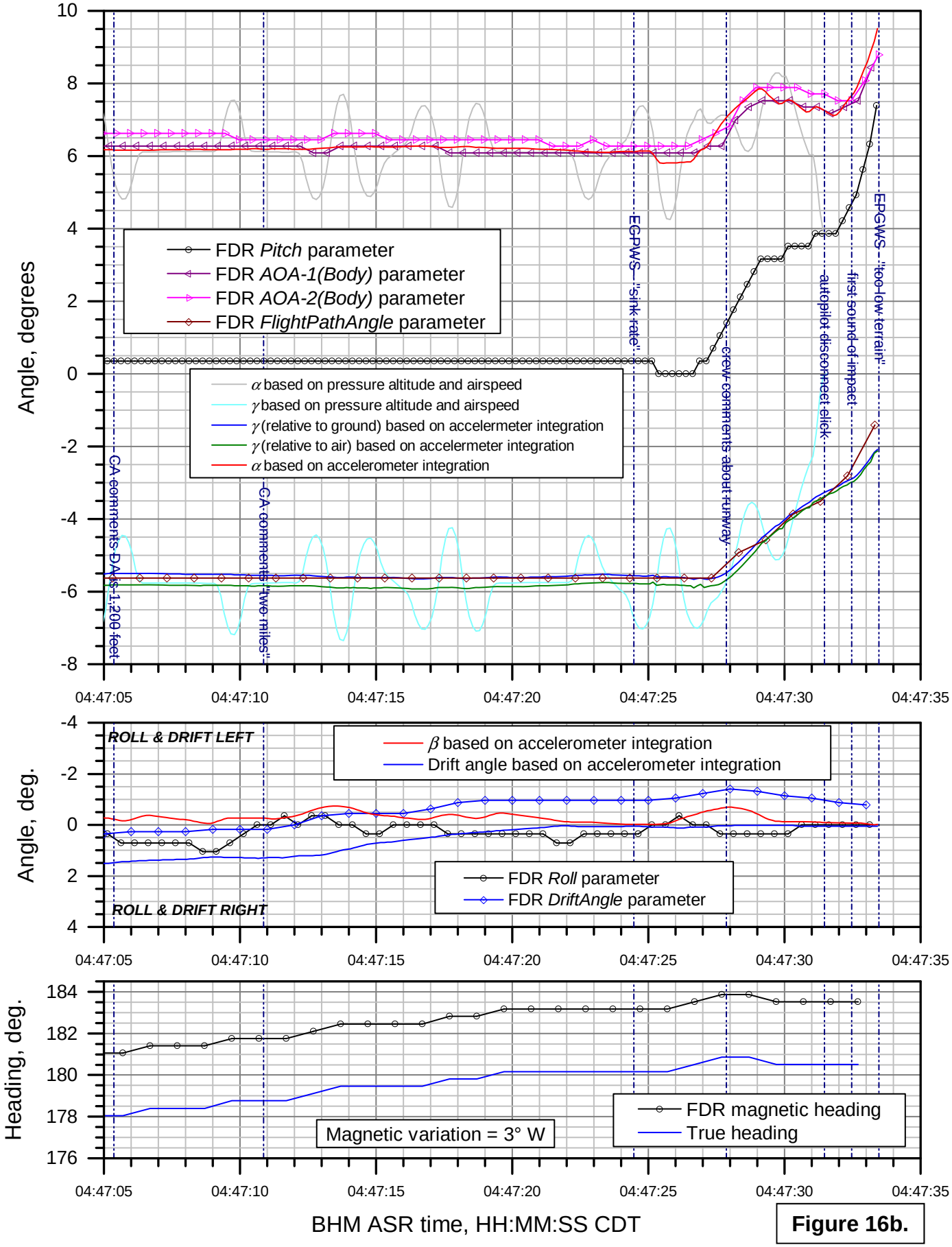

Figure 16b.

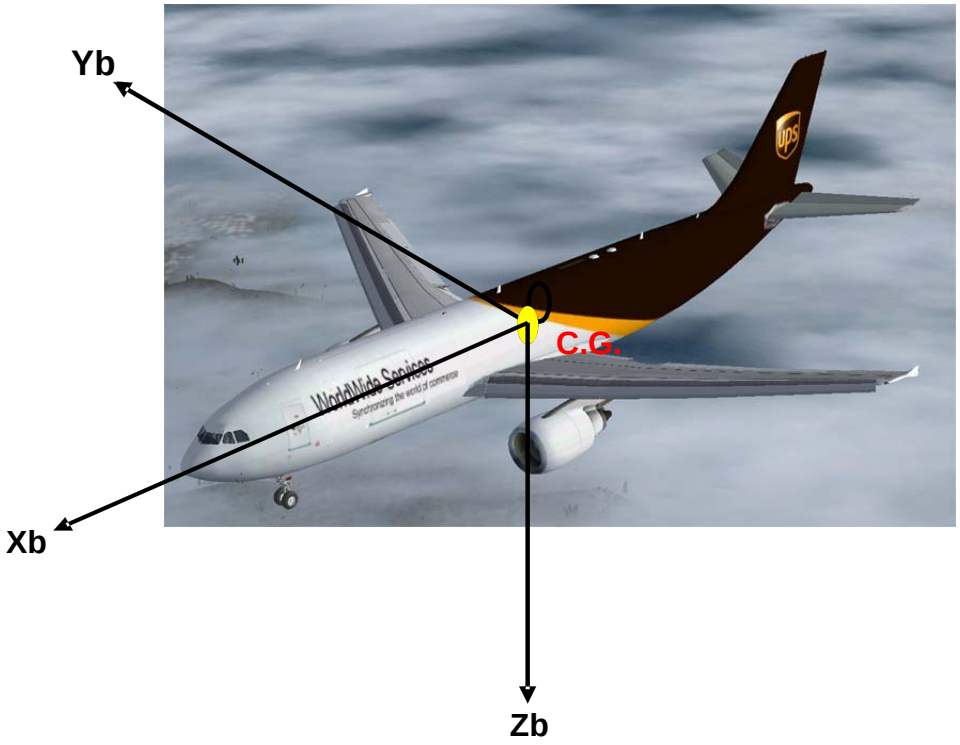

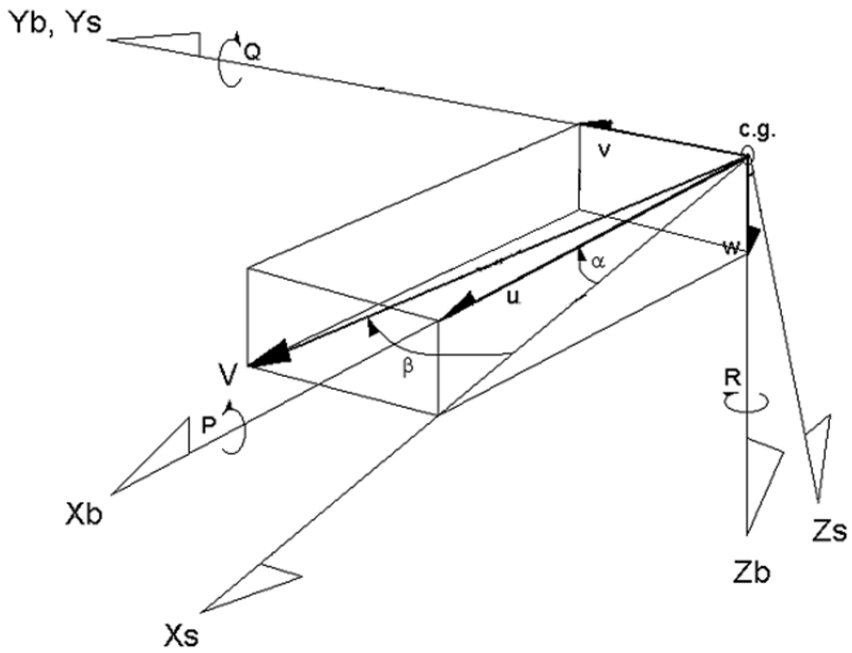

C.G. = center of gravity

{Xb, Yb, Zb} = body axis system

{Xs, Ys, Zs} = stability axis system

V = velocity vector

α = angle of attack

β = sideslip angle

P = body axis roll rate

Q = body axis pitch rate

R = body axis yaw rate

u = component of V along Xb

v = component of V along Yb

w = component of V along Zb

Figure 17.

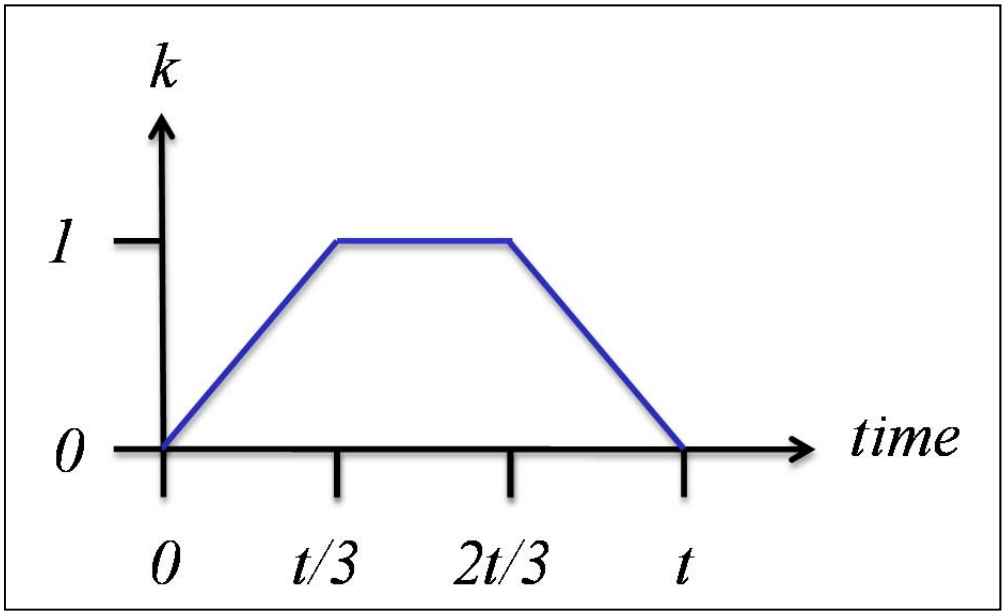

Figure 18. k – factor for velocity vector addition to velocity defined by FDR groundspeed and track angle.

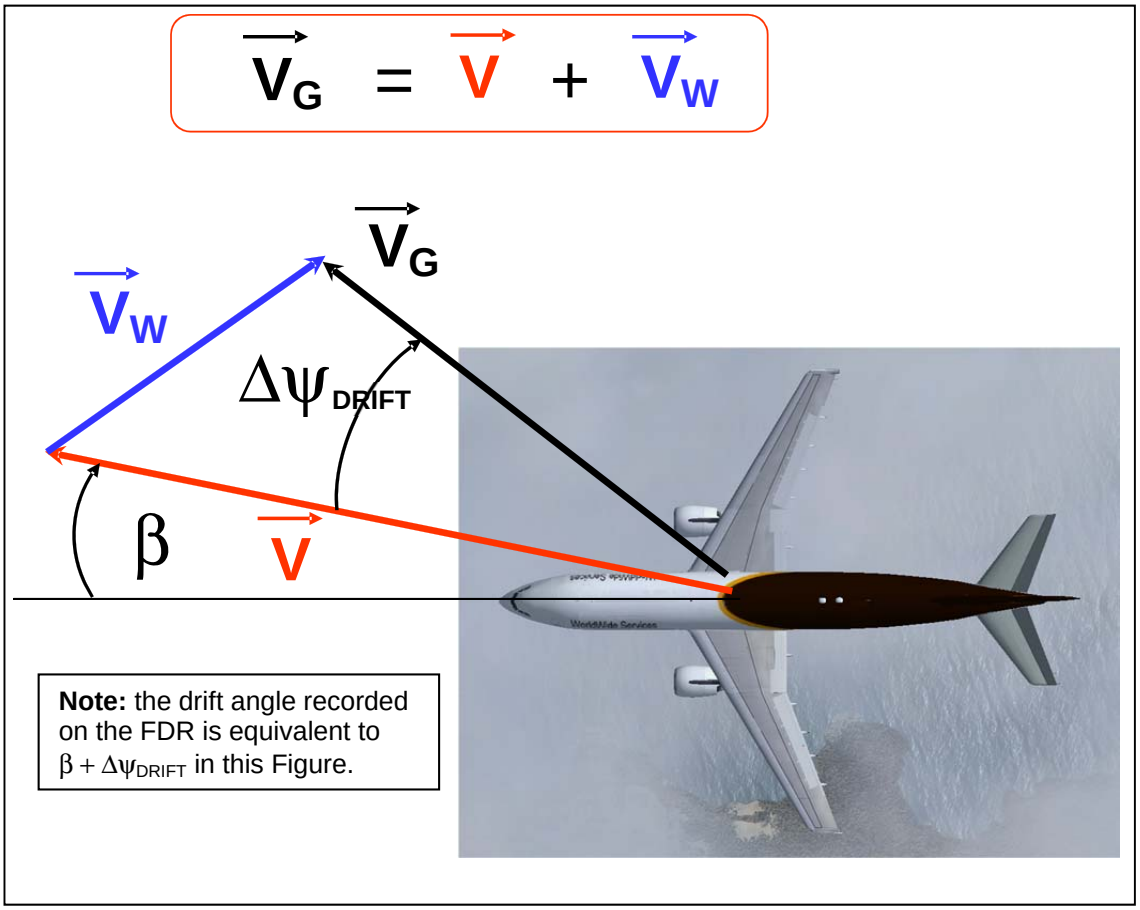

Figure 19. Wind triangle.

DCA13MA133: UPS flight 1354, Airbus A300-600, KBHM 08/14/2013

Load factors vs. time

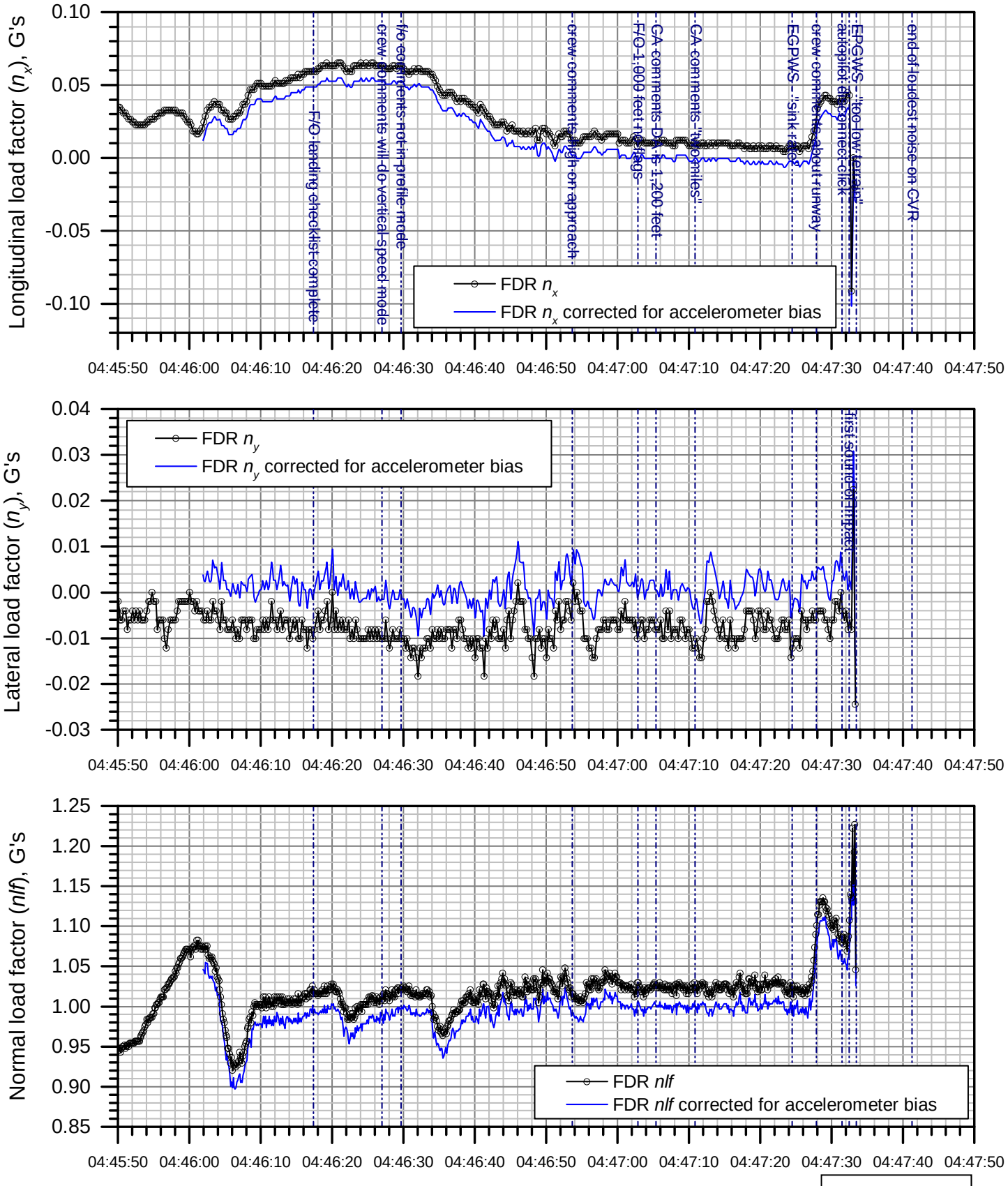

Figure 20a.

DCA13MA133: UPS flight 1354, Airbus A300-600, KBHM 08/14/2013
Load factors vs. time (detail)

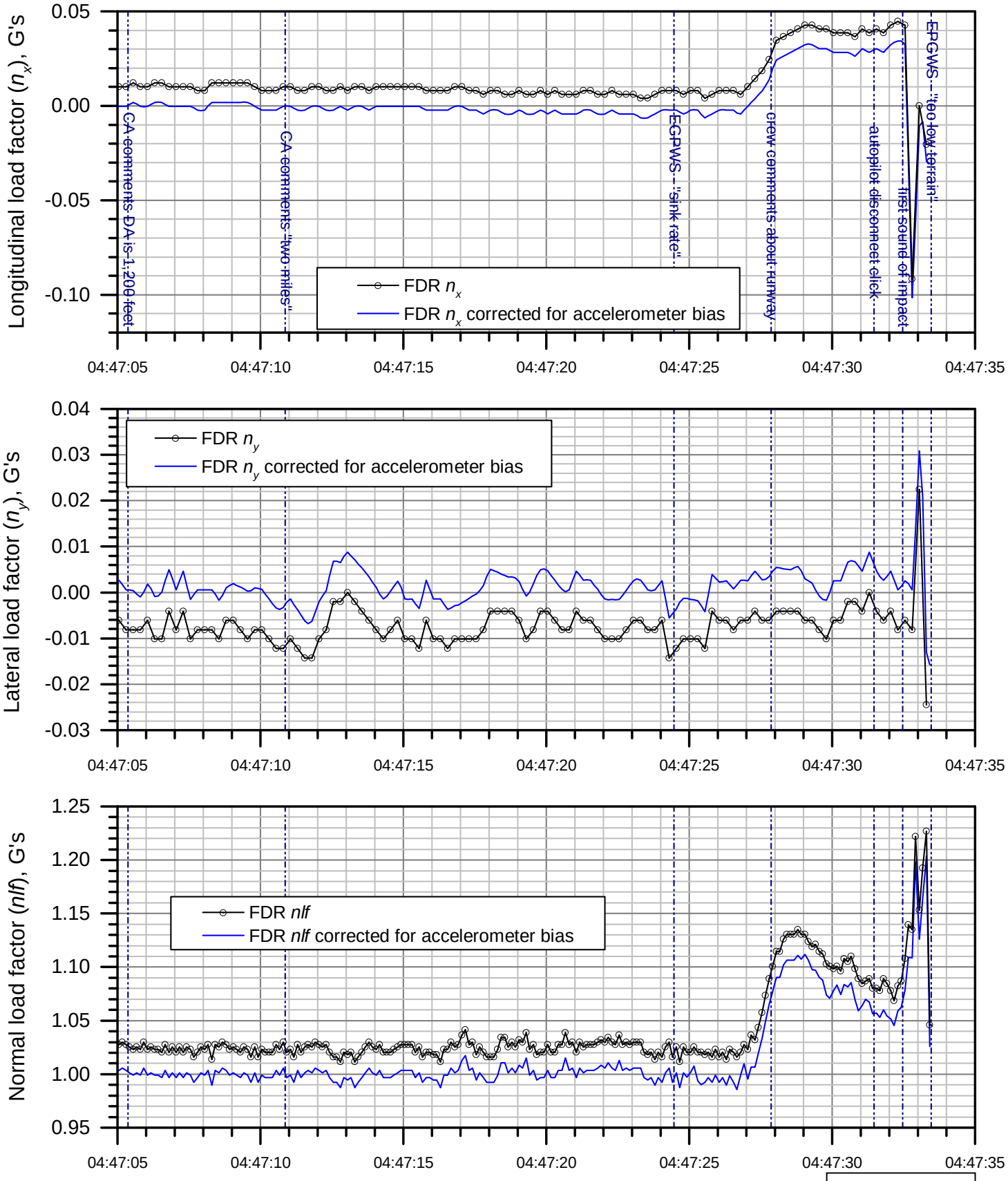

Figure 20b.

DCA13MA133: UPS flight 1354, Airbus A300-600, KBHM 08/14/2013
Control inputs vs. time

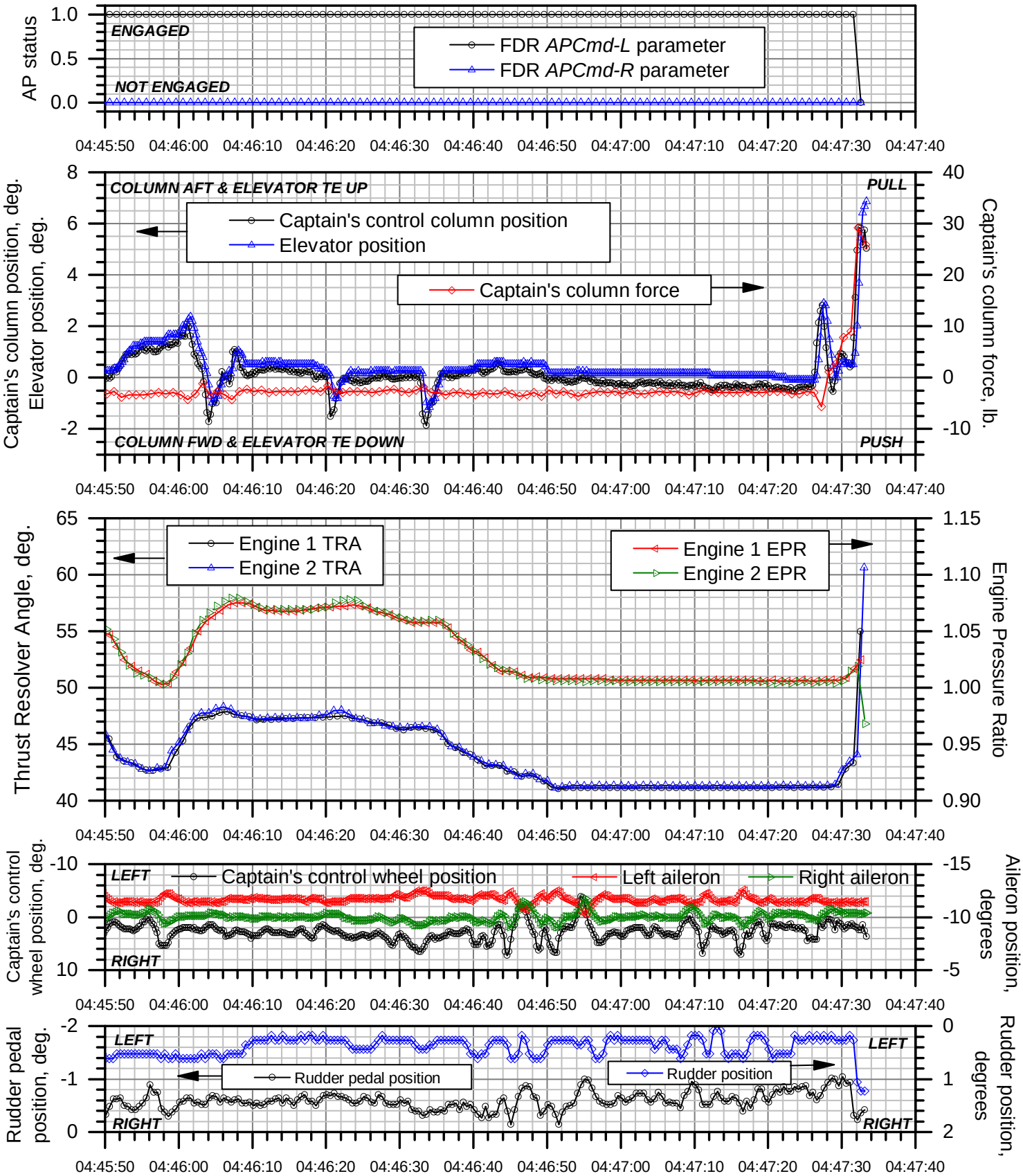

Figure 21a.

BHM ASR time, HH:MM:SS CDT

DCA13MA133: UPS flight 1354, Airbus A300-600, KBHM 08/14/2013
Control inputs vs. time (detail)

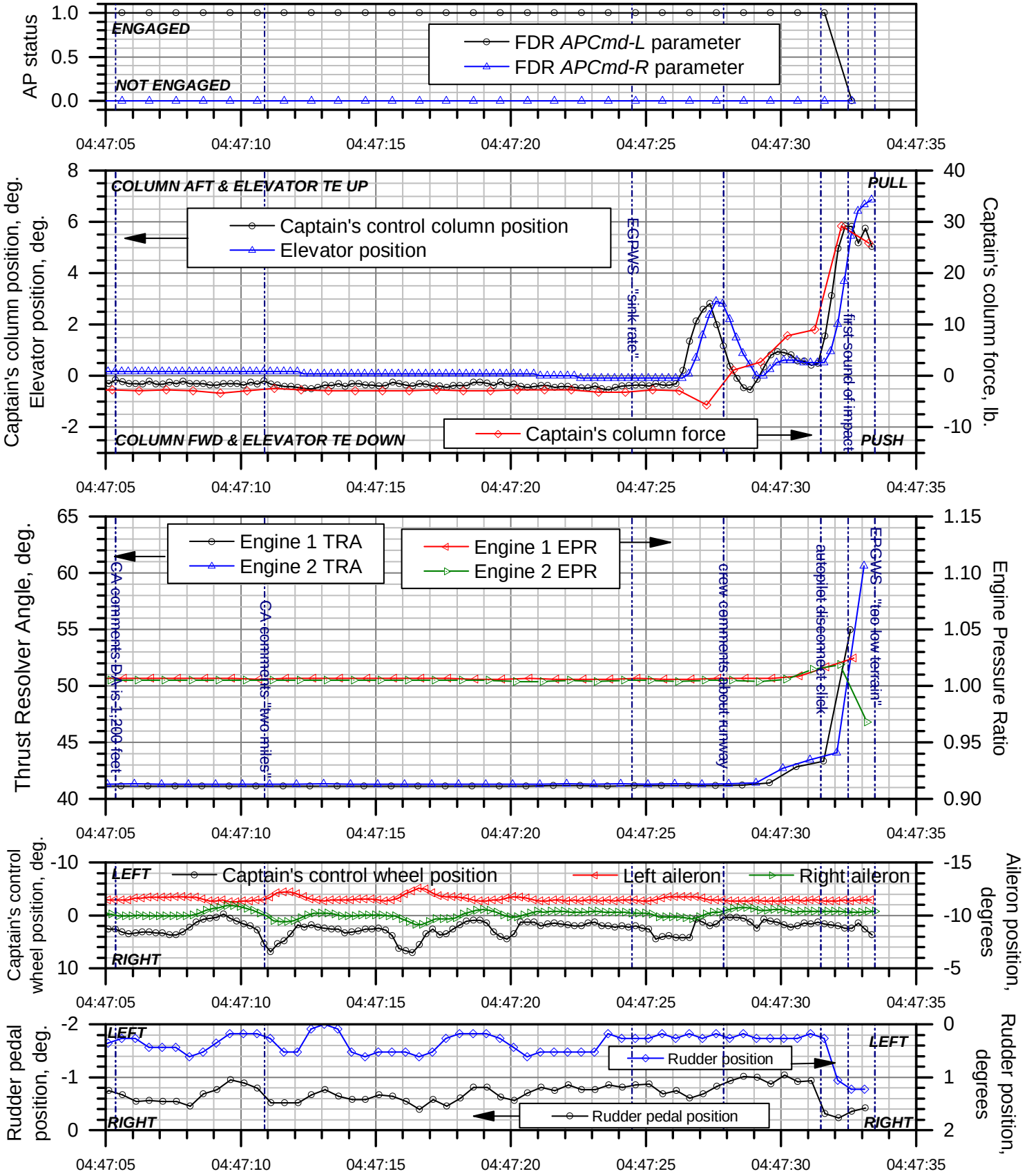

Figure 21b.

DCA13MA133: UPS flight 1354, Airbus A300-600, KBHM 08/14/2013
Computed winds vs. altitude

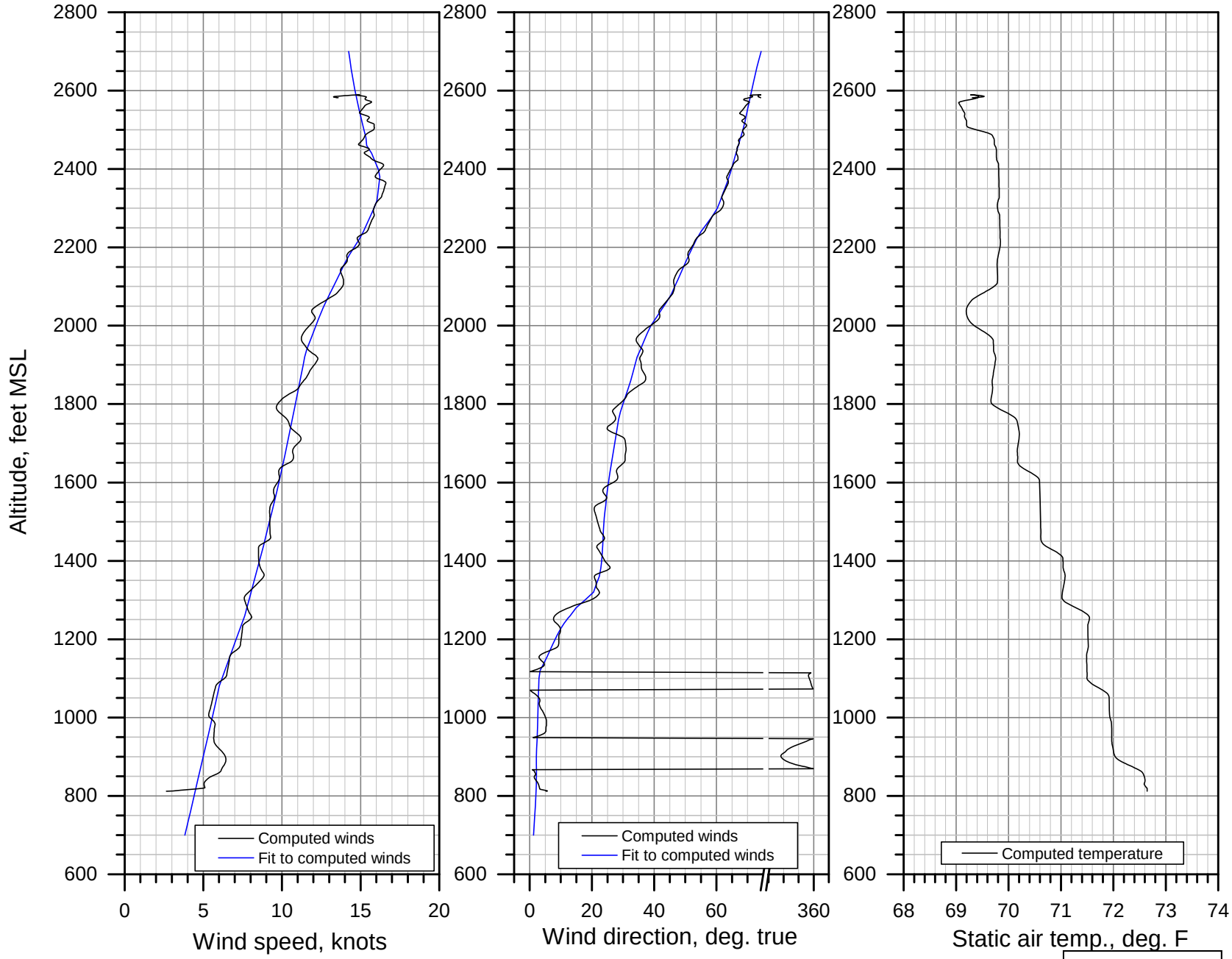

Figure 22.

a) Frame 183, 04:47:24.40: Lights first appear. Airplane lights indicated by yellow circle.

b) Frame 307, 04:47:28.17: Peak of brightness.

c) Frame 425, 04:47:32.10: Sudden dimming.

d) Frame 433, 04:47:32.37: Lights totally out.

e) Frame 545, 04:47:36.10: Transformer flash.

f) Frame 683, 04:47:40.70: Impact explosion.

Figure 23. Selected frames from the security camera video. The timestamp on the video lags the BHM ASR CDT time by approximately 3 seconds.

DCA13MA133: UPS flight 1354, Airbus A300-600, KBHM 08/14/2013
Visibility of security camera and runway along aircraft flight path

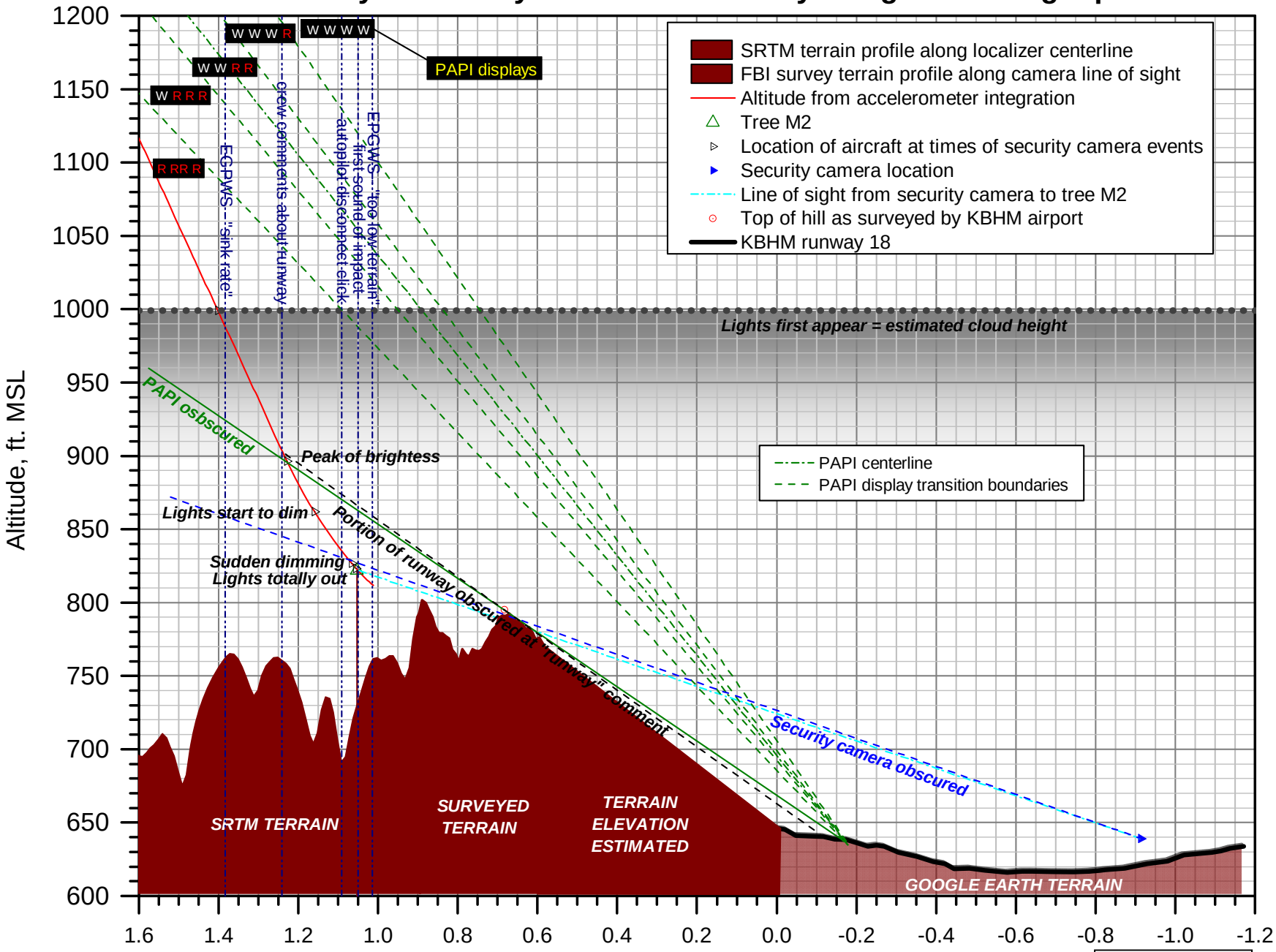

Figure 24.

a) Picture of security camera, and view north towards tree M2.

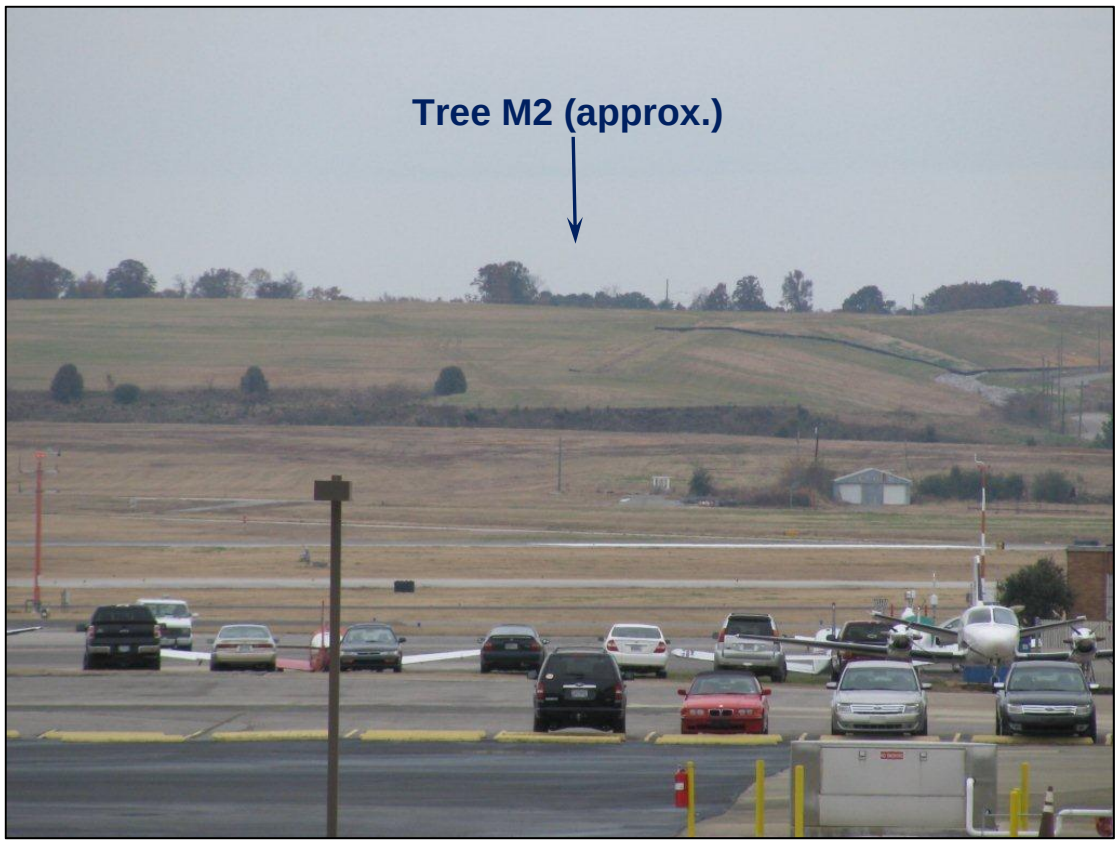

b) Zoomed-in photo of view to north.

Figure 25.

Figure 26. Photo from approximate brow of hill, looking south towards runway.

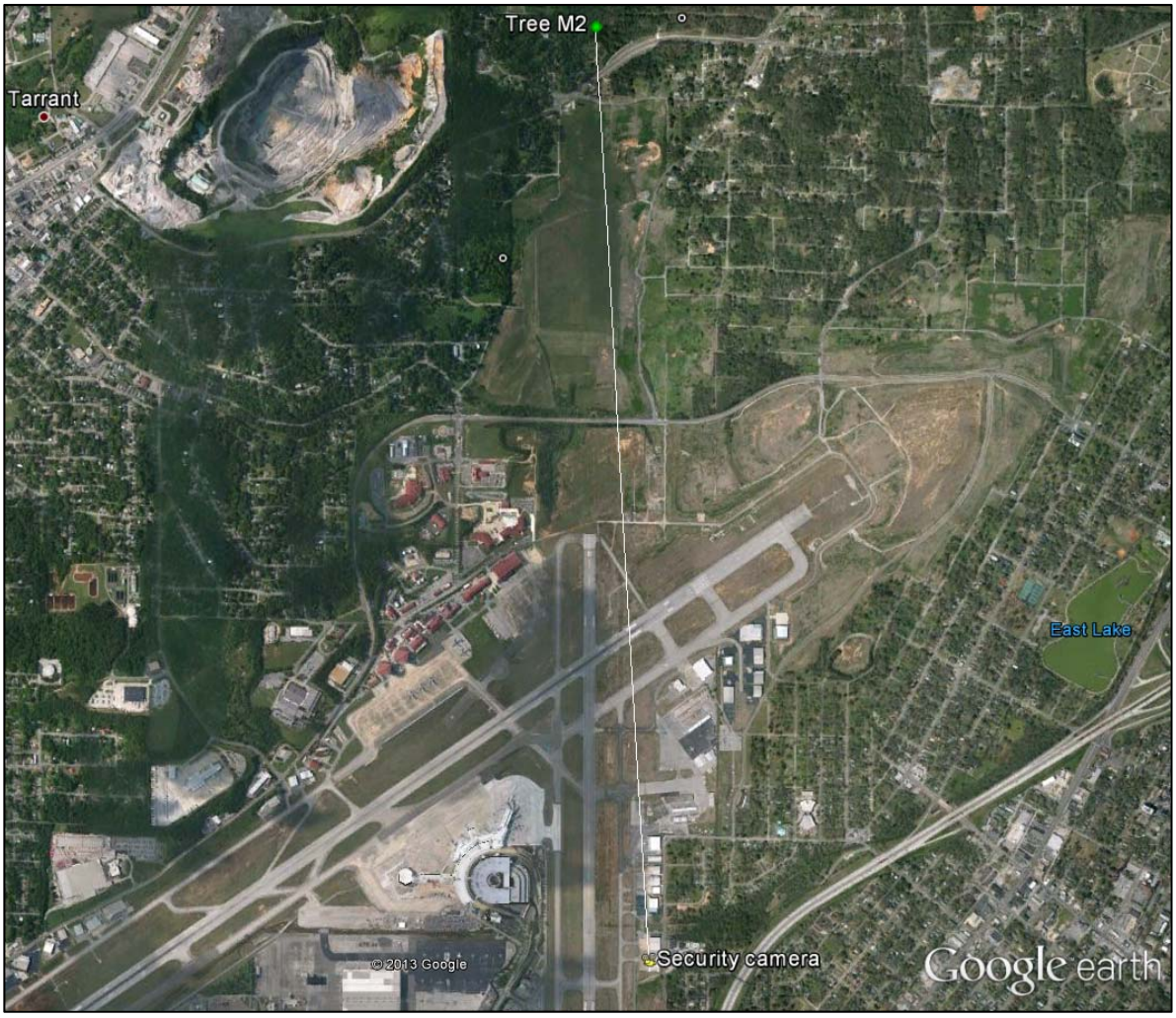

Figure 27. Plan view of line of sight from the security camera to tree M2.

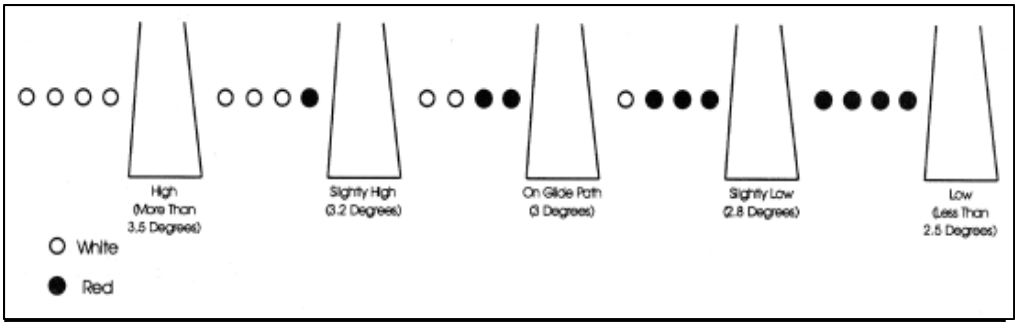

Figure 28. PAPI presentation (AIM Figure 2-1-5).

Table 7-2. Aiming of Type L-880 (4 Box) PAPI Relative to Pre-selected Glide Path.

Light Unit	Aiming Angle (in minutes of arc)	Height group 4 aircraft on runway with ILS
	Standard installation	
Unit nearest runway	30' above glide path	35' above glide path
Next adjacent unit	10' above glide path	15' above glide path
Next adjacent unit	10' below glide path	15' below glide path
Next adjacent Unit	30' below glide path	35' below glide path

Figure 29. Table 7-2 from AC 150/5340-30G.

Table 7-1. Threshold Crossing Heights.

Representative aircraft. Type	Approximate Cockpit-to-wheel height	Visual Threshold Crossing Height	Remarks
Height Group 1 General aviation Small commuters Corporate turbo jets	10 ft. (3 m) or less	40 ft. (+5, -20) 12 m (+2, -6)	Many runways less than 6,000 ft. (1829 m) long with reduced widths and/or restricted weight bearing that would normally prohibit landings by larger aircraft.
Height Group 2 F-28, CV-340/44O/580 B-737, DC-9, DC-8	15 ft. (4.5 m)	45 ft. (+5, -20) 14 m (+2, -6)	Regional airport with limited air carrier service
Height Group 3 B-727/707/720/757	20 ft. (6 m)	50 ft. (+5,-15) 15 m (+2, -6)	Primary runways not normally used by aircraft with ILS glide-path-to-wheel heights exceeding 20 ft. (6 m).
Height group 4 B-747/767, L-1011, DC-10 A-300	Over 25 ft. (7.6 m)	75 ft. (+5, -15) 23 m (+2, -4)	Most primary runways at major airports.

Figure 30. Table 7-1 from AC 150/5340-30G.

DCA13MA133: UPS flight 1354, Airbus A300-600, KBHM 08/14/2013

Effect of vertical speed on minimum altitudes for succesful climb maneuvers

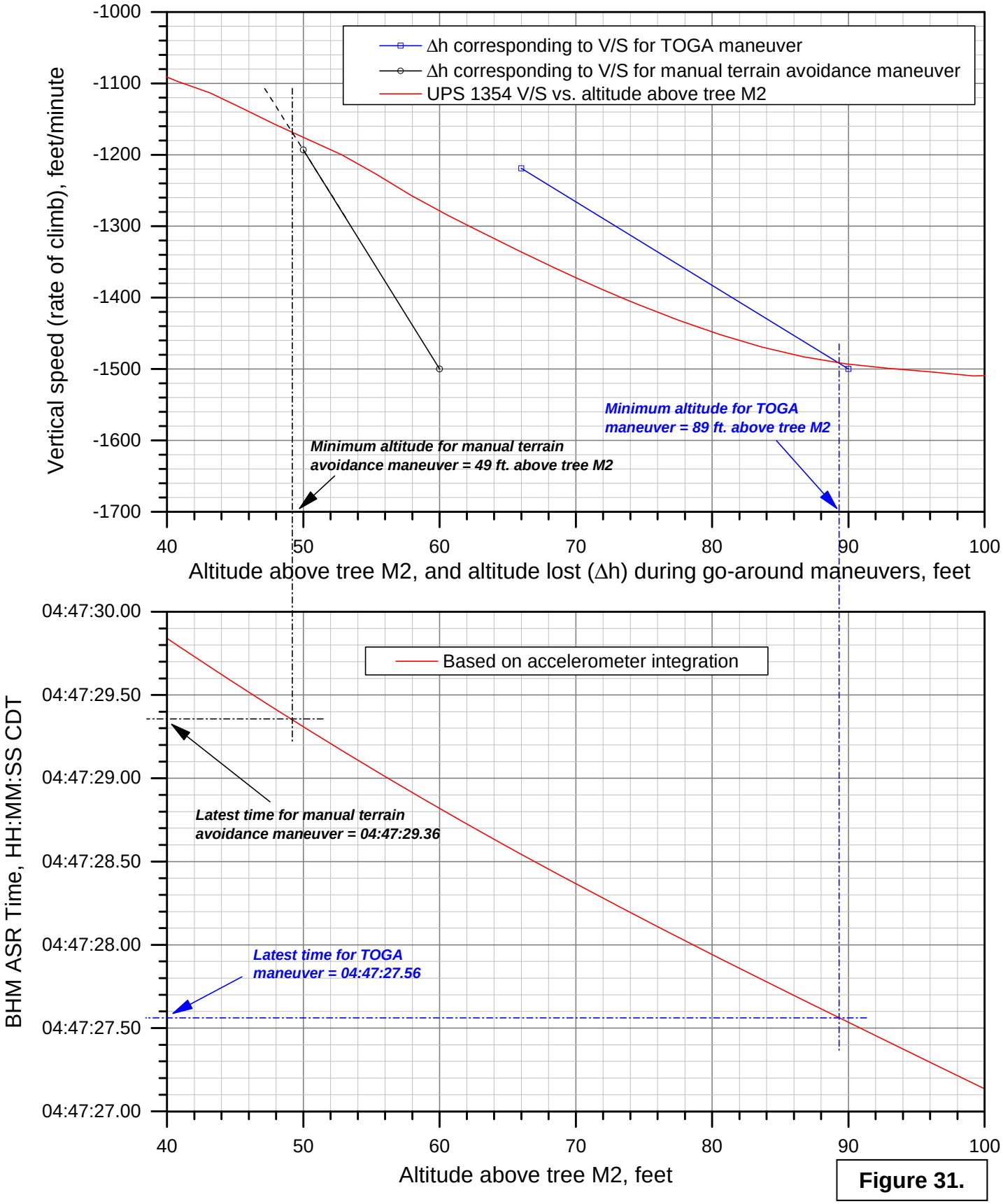

Figure 31.

DCA13MA133: UPS flight 1354, Airbus A300-600, KBHM 08/14/2013
Minimum altitudes for succesful climb maneuvers

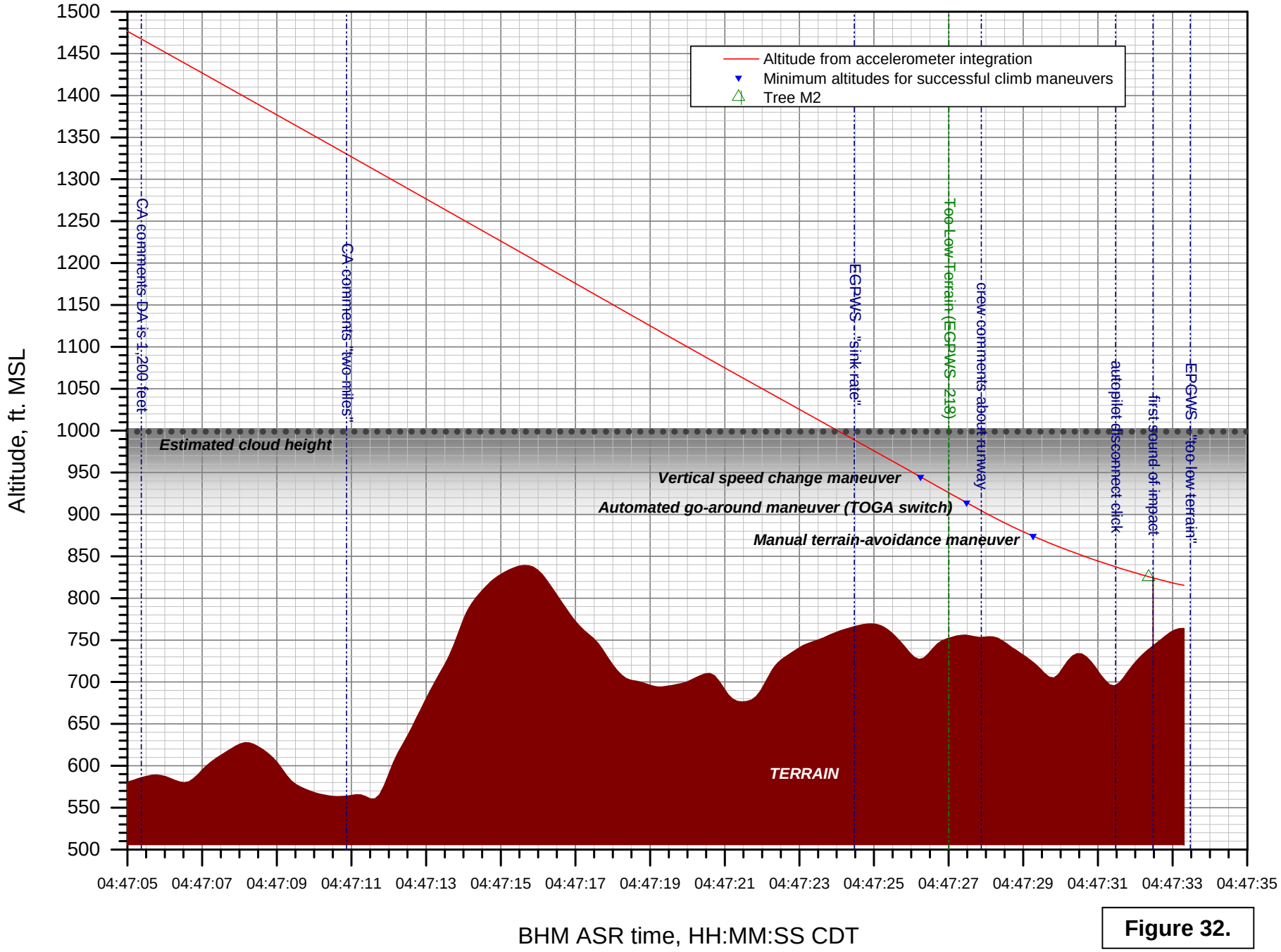

Figure 32.

THIS PAGE INTENTIONALLY LEFT BLANK